LEAPS MEETS QUANTUM TECHNOLOGY
1st Biennial LEAPS Conference at ELBA, Italy
MAY 15-20, 2022

Probing high-pressure superconductivity with diamond quantum sensing

Jean-François ROCH – ENS Paris-Saclay

jean-francois.roch@ens-paris-saclay.fr

Joint work with Paul Loubeyre's team
CEA-DAM, Bruyères-le-Châtel

High-pressure superconductivity
→ record of critical temperature T_C

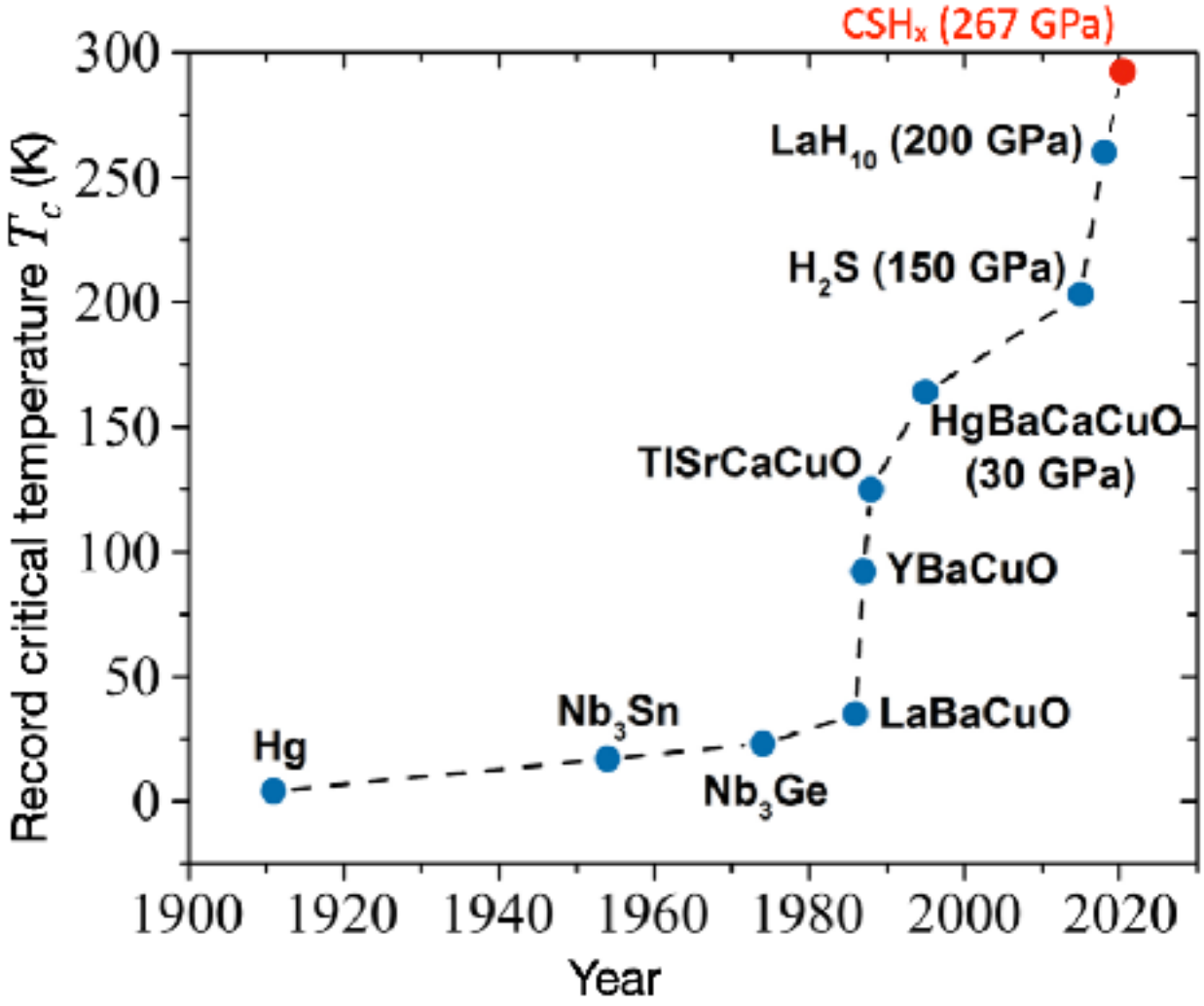

High-pressure superconductivity
→ record of critical temperature T_C

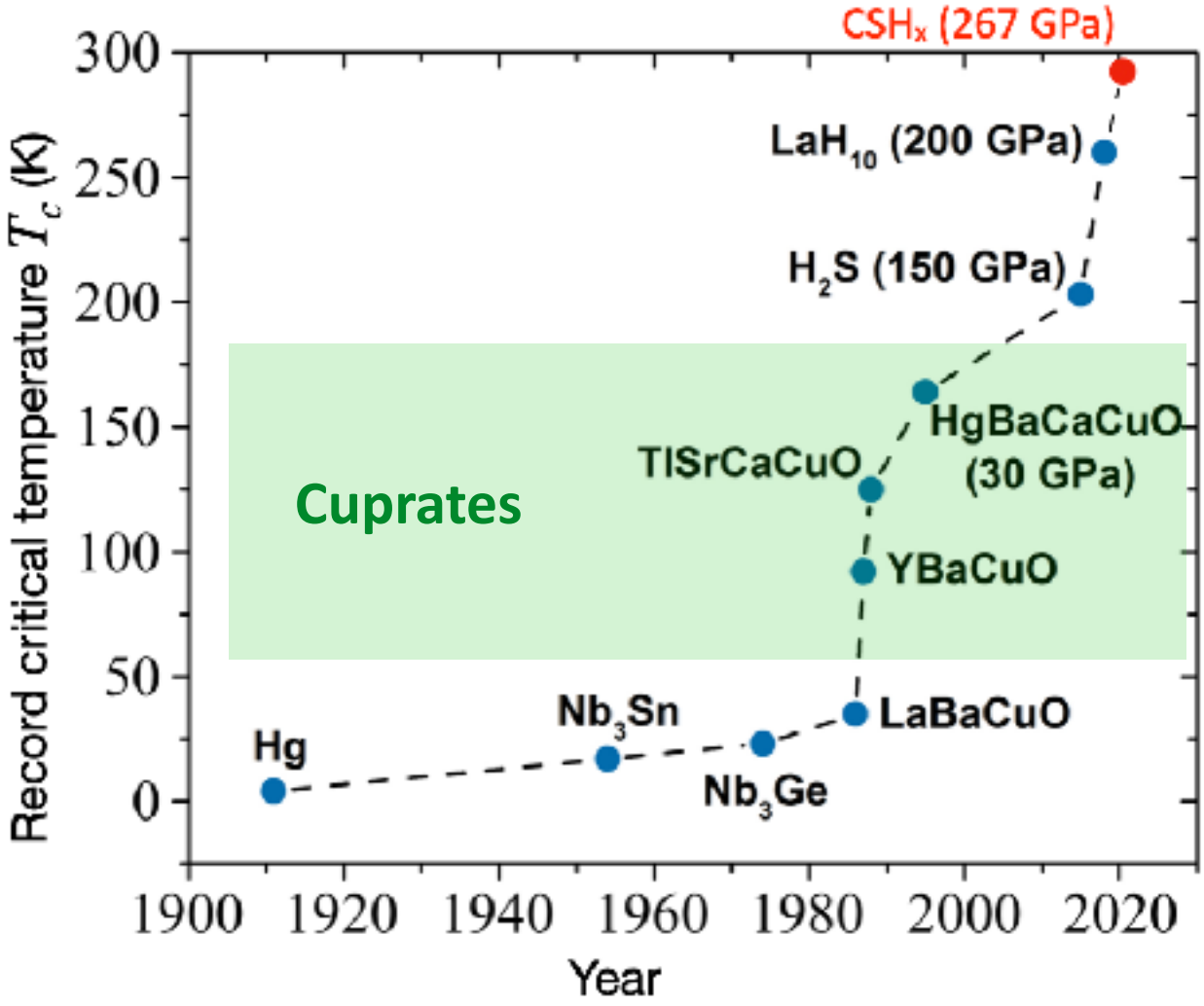

High-pressure superconductivity
→ record of critical temperature T_C

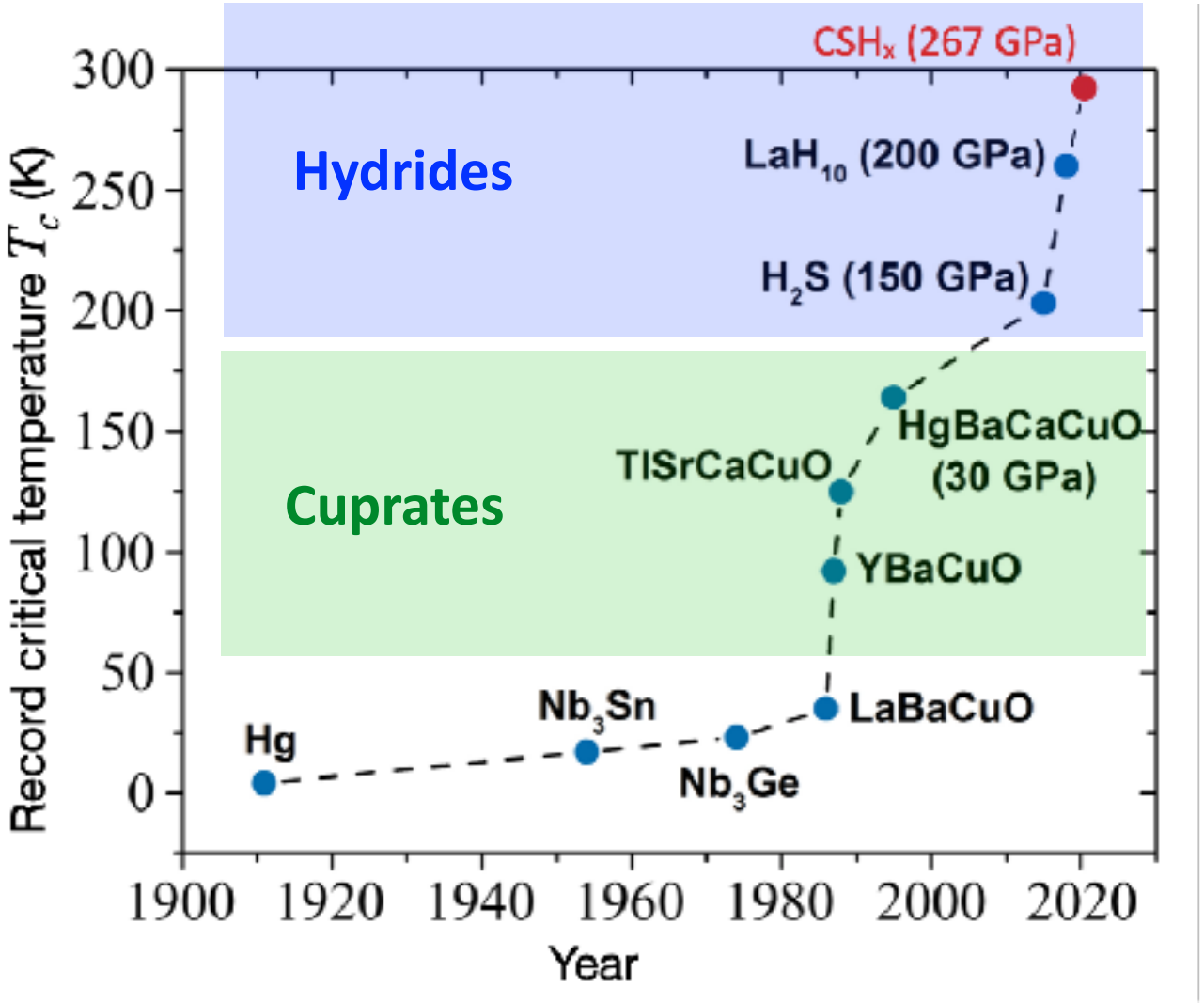

High-pressure superconductivity
→ record of critical temperature T_C

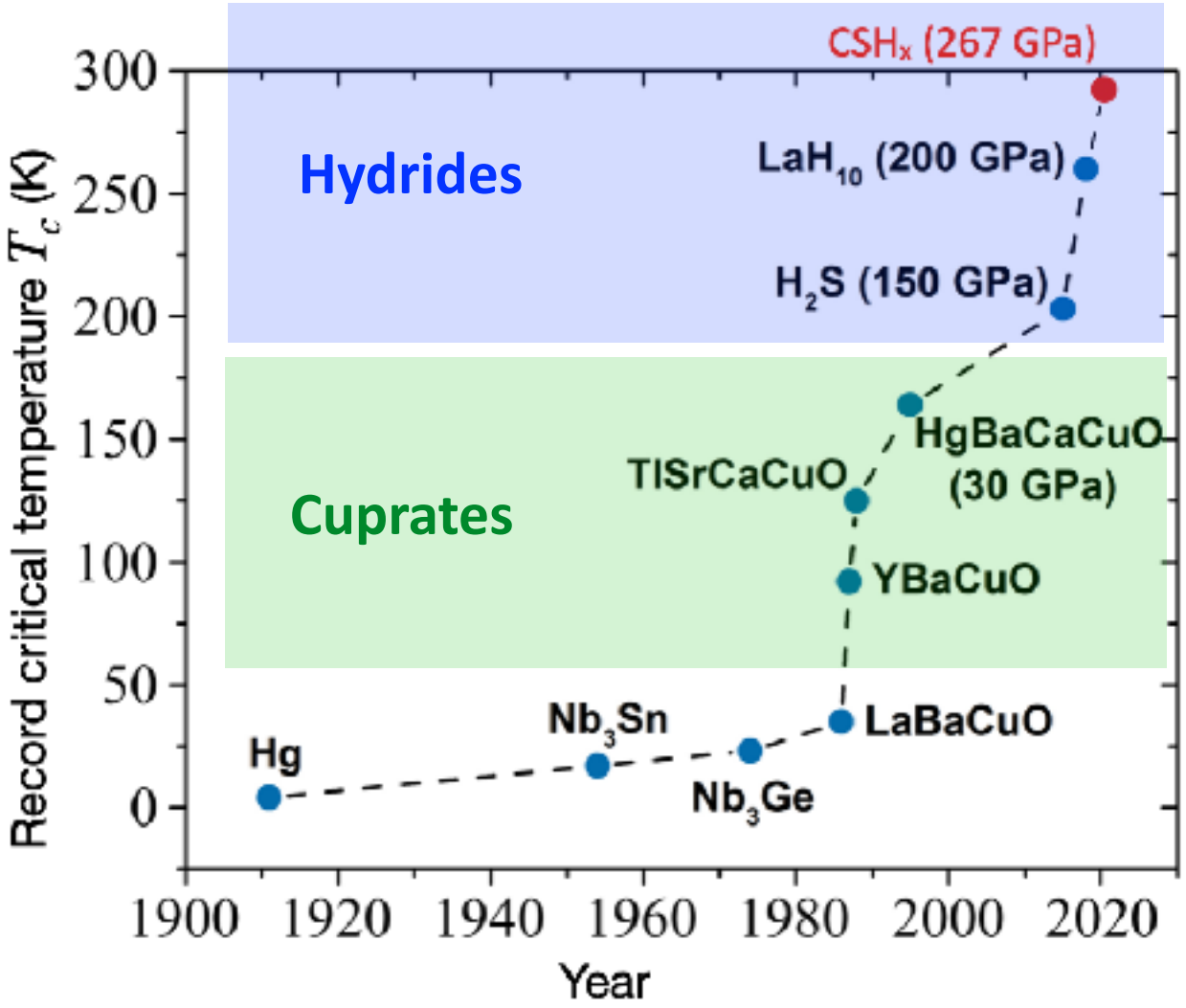

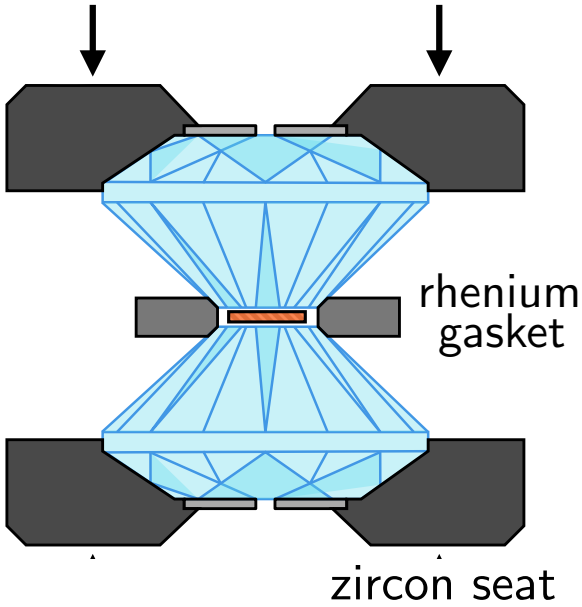

diamond anvil cell

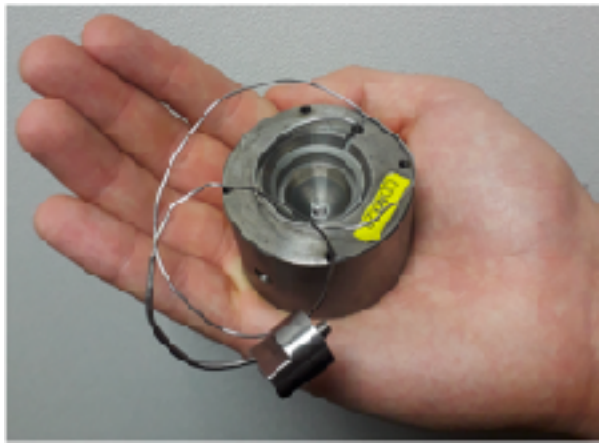

Superconductivity of hydrides

H_3S: A. P. Drozdov , M. I. Eremets et al., Nature **52** ,73 (2015)

CSH_x: group of R. Dias, Nature **586**, 373 (2020)

Isotope effect

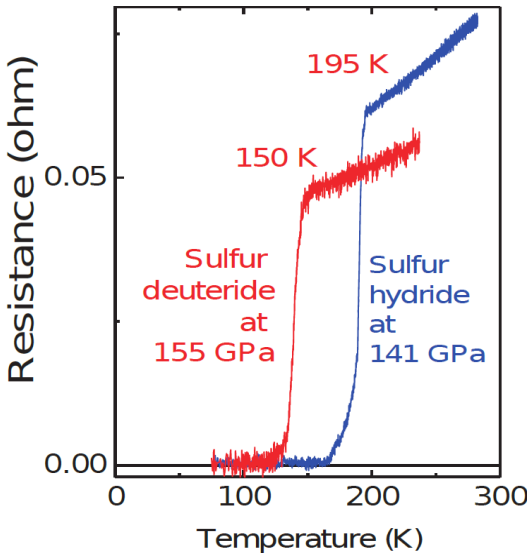

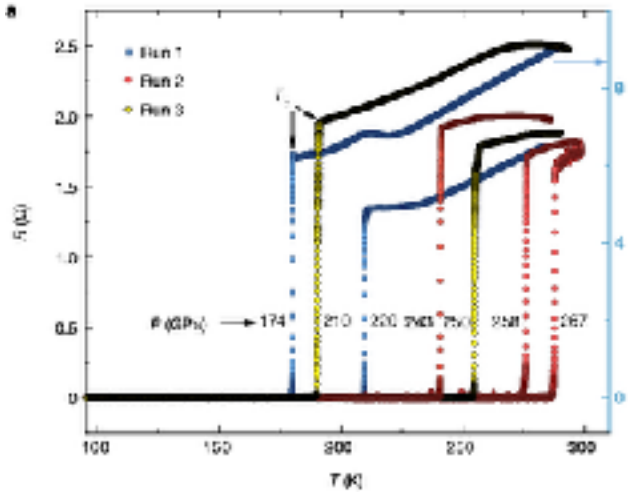

Superconductivity of hydrides

H_3S: A. P. Drozdov , M. I. Eremets et al., Nature **52** ,73 (2015)

CSH_x: group of R. Dias, Nature **586**, 373 (2020)

Isotope effect

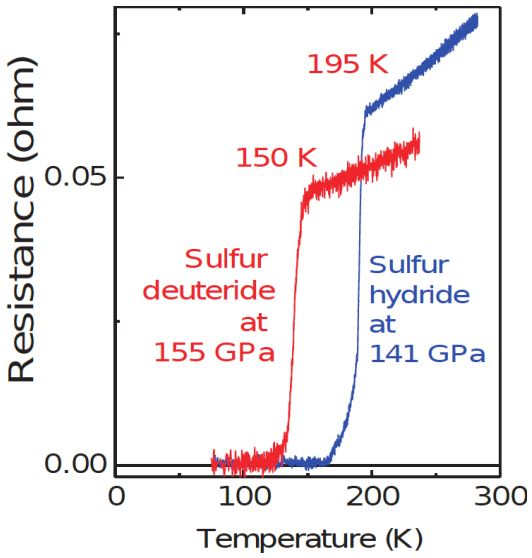

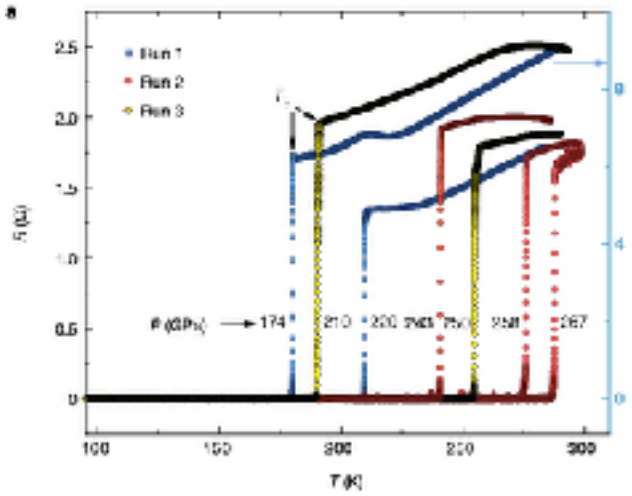

Absence of high temperature superconductivity in hydrides under pressure

J. E. Hirsch[a] and F. Marsiglio[b]
[a] Department of Physics, University of California, San Diego, La Jolla, CA 92093-0319
[b] Department of Physics, University of Alberta, Edmonton, Alberta, Canada T6G 2E1

arXiv:2010.10307 (2020)

Breakthrough or bust? Claim of room-temperature superconductivity draws fire, Science 22 Oct. 2021 (doi: 10.1126/science.acx9428)

Features of the experimental data indicate that the phenomenon observed in that material is *not* superconductivity. This observation calls into question earlier similar claims of high temperature conventional superconductivity in hydrides under high pressure based on similar or weaker evidence.

It even casts doubts on the previous experiments on H_3S and LaH_{10}!

Standard Superconductivity in Carbonaceous Sulfur Hydride

Ranga P. Dias[1,2] and Ashkan Salamat[3]

https://arxiv.org/abs/2111.15017 (29 Nov 2021)

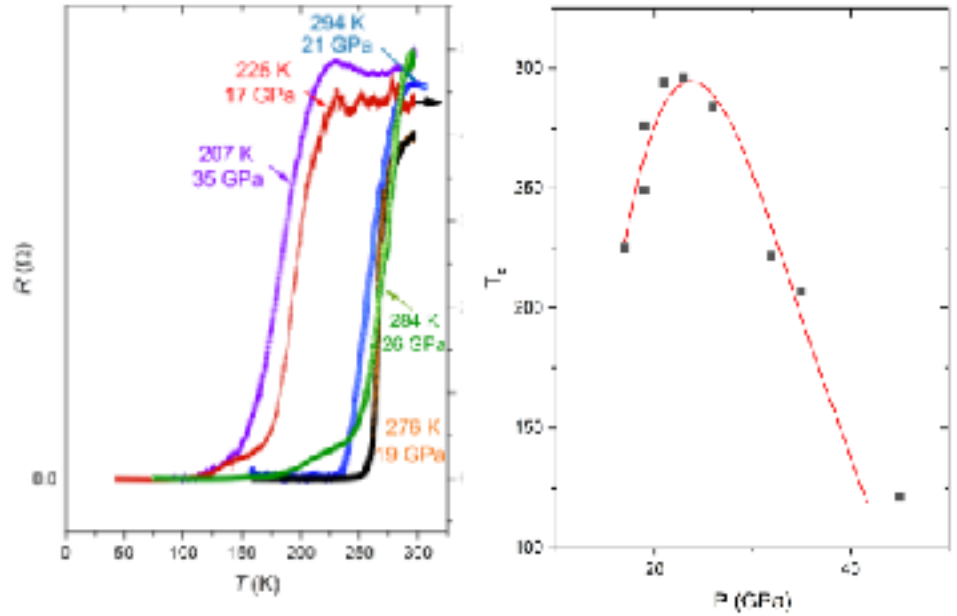

Figure 2. Showing room temperature conductivity in a new material at pressures an order of magnitude lower pressure than CSH.

Structure of the sample not revealed.
Reason invoqued: ongoing patenting

Standard Superconductivity in Carbonaceous Sulfur Hydride

Ranga P. Dias[1,2] and Ashkan Salamat[3]

https://arxiv.org/abs/2111.15017 (29 Nov 2021)

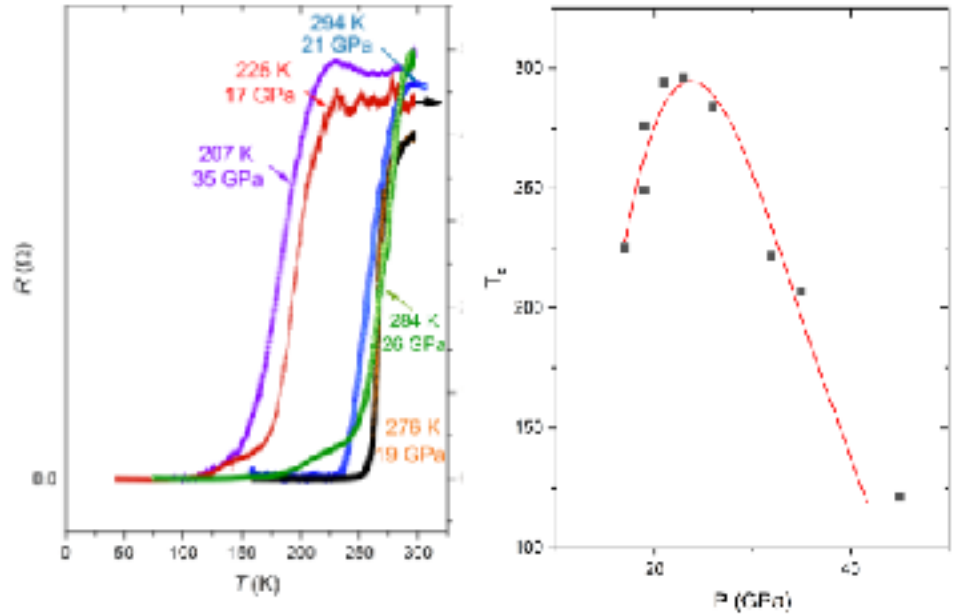

Figure 2. Showing room temperature conductivity in a new material at pressures an order of magnitude lower pressure than CSH.

Structure of the sample not revealed.
Reason invoqued: ongoing patenting

Preprint server removes 'inflammatory' papers in superconductor controversy

Some physicists worry about stifling debate, others commend arXiv's system of moderating papers

14 MAR 2022 · 10:20 AM · BY ROBERT F. SERVICE

High-pressure sensing methods

Electrical transport

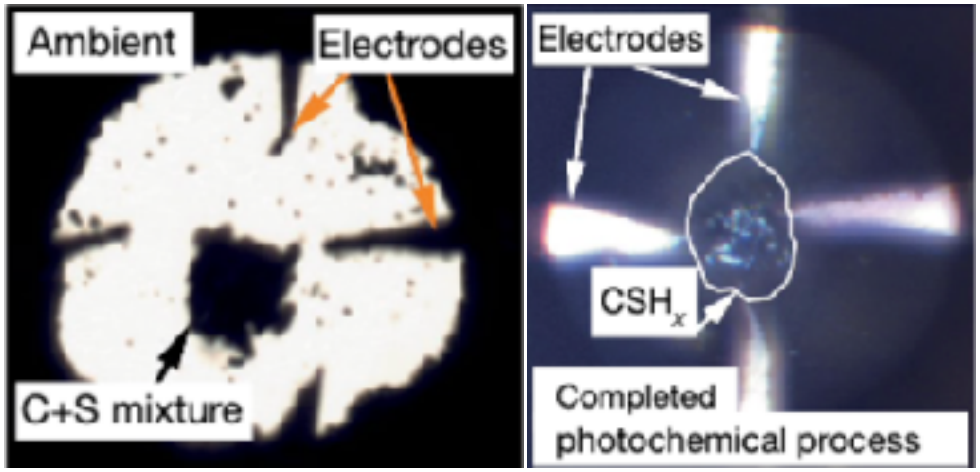

Snider et al, Nature 586, 373 (2021)

High-pressure sensing methods

Electrical transport

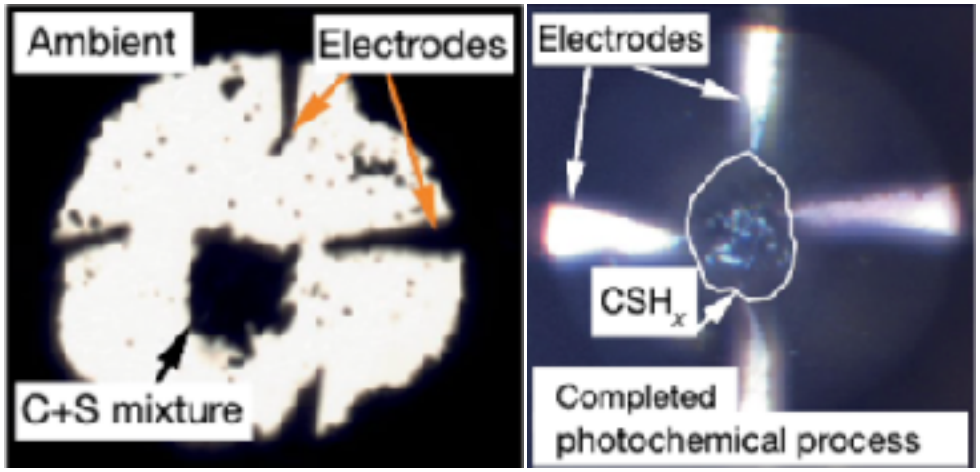

Snider et al, Nature 586, 373 (2021)

Diamagnetism

Inductively coupled coils

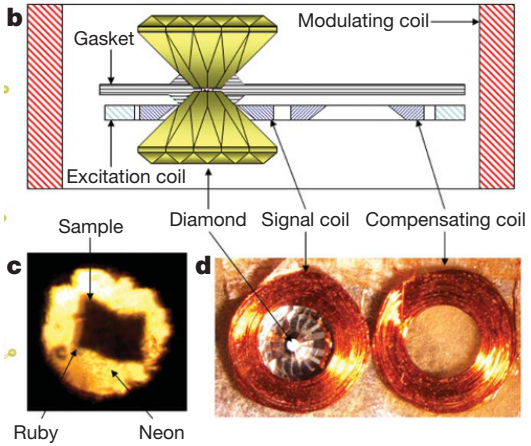

Chen et al, Nature 466, 950 (2010)

High-pressure sensing methods

Electrical transport

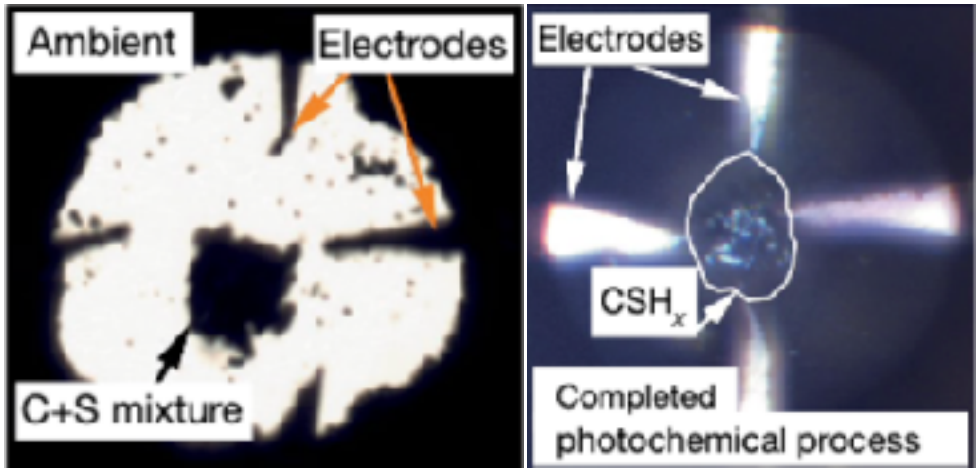

Snider et al, Nature 586, 373 (2021)

Diamagnetism

Inductively coupled coils

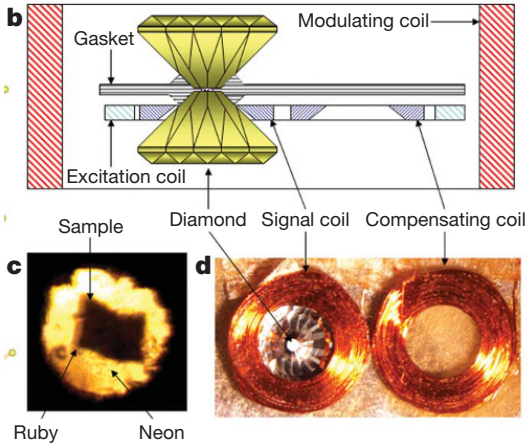

Chen et al, Nature 466, 950 (2010)

DAC compatible with SQUID

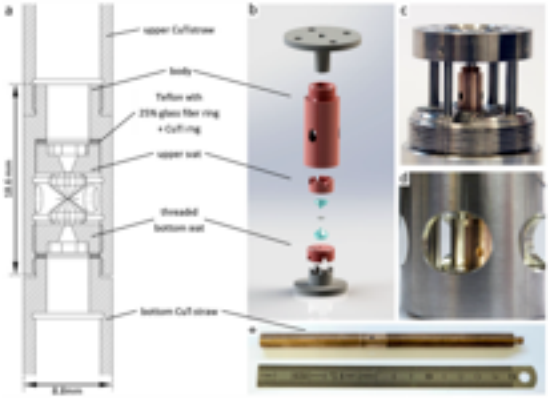

Marizy et al, High Pressure Research 37, 465 (2017)

High-pressure sensing methods

Electrical transport

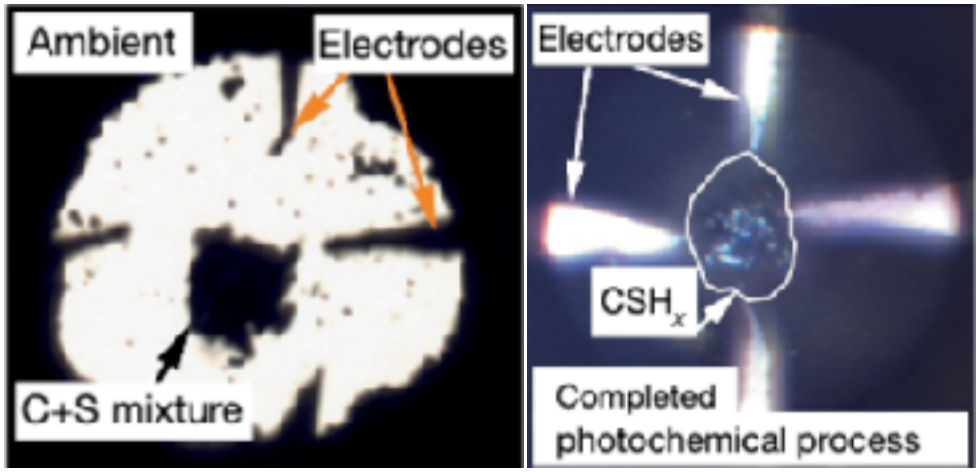

Snider et al, Nature 586, 373 (2021)

Problem : No spatial resolution, whole sample probing (+contamination from electrodes)

→ higher pressure

⇔ smaller samples ⇔ less signal

Technically challenging, hardly reproducible

Diamagnetism

Inductively coupled coils

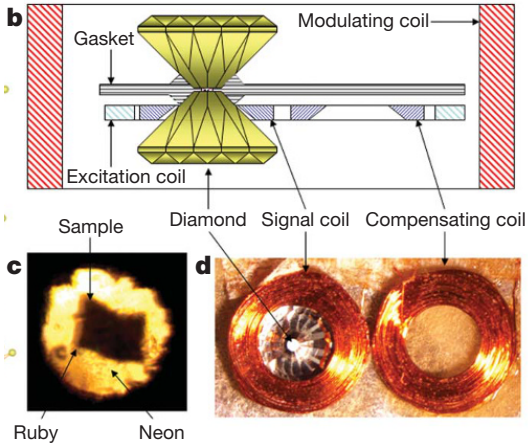

Chen et al, Nature 466, 950 (2010)

DAC compatible with SQUID

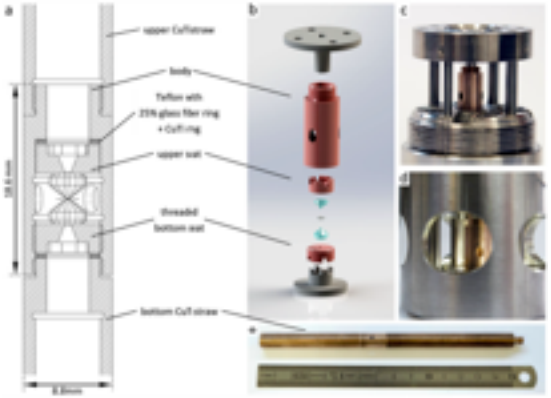

Marizy et al, High Pressure Research 37, 465 (2017)

In-situ observation of the Meissner effect

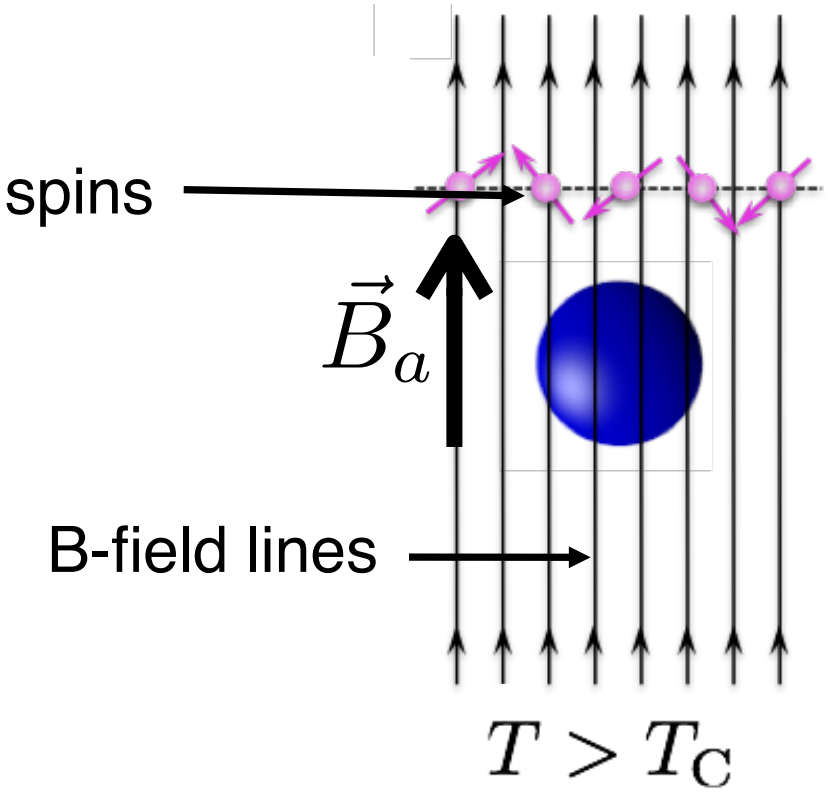

In-situ observation of the Meissner effect

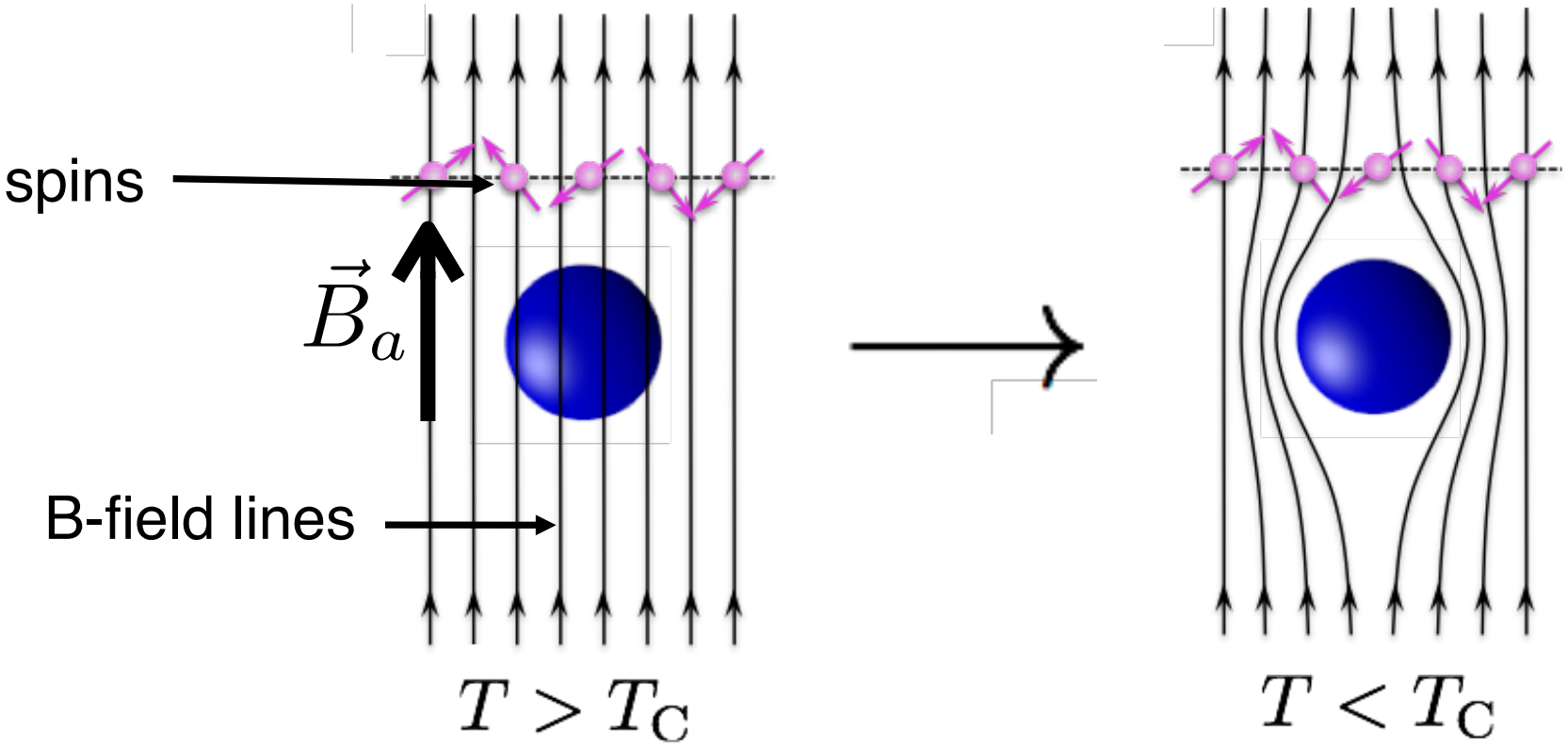

In-situ observation of the Meissner effect

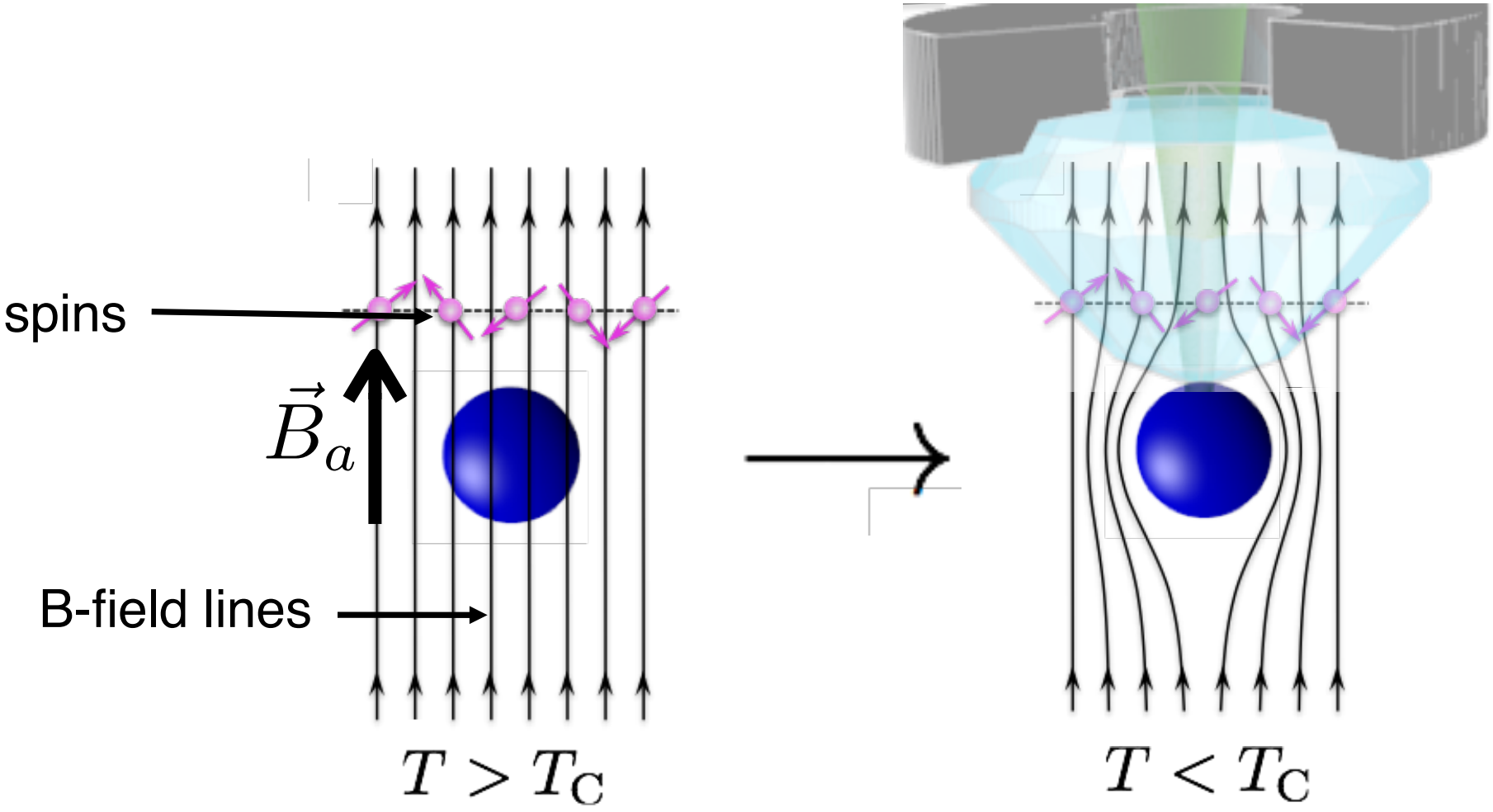

In-situ observation of the Meissner effect

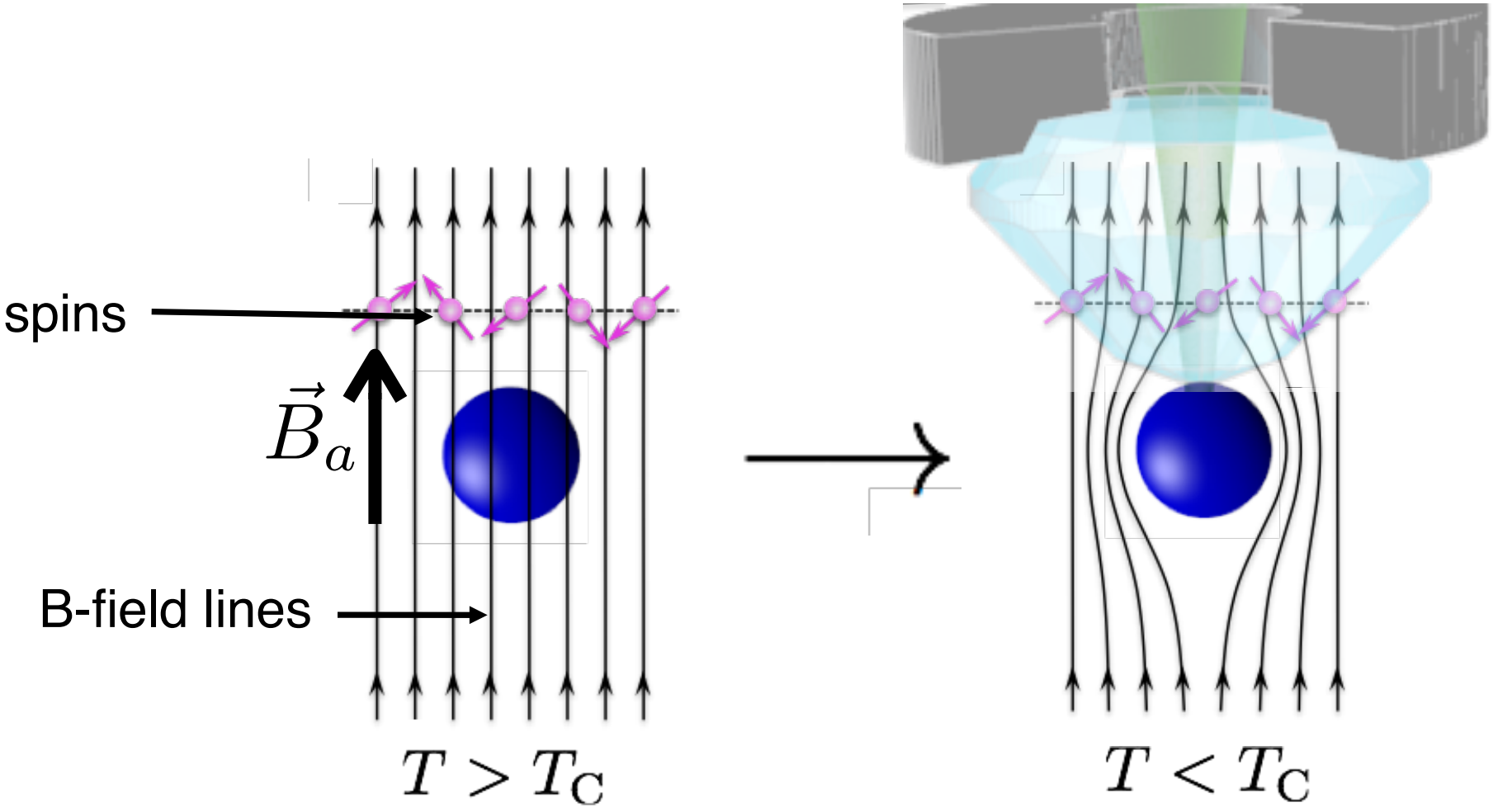

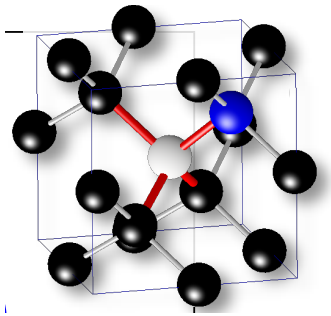

NV color center in diamond: electron spin that can be optically detected and manipulated by combining optical and microwave excitations

NV center: optically detected magnetic resonance

- Spin structure S=1 in the ground and excited electronic states
- NV axis as z quantization axis + C_{3v} symmetry
- No spin–orbit coupling: transitions with $\Delta m_S = 0$ rule

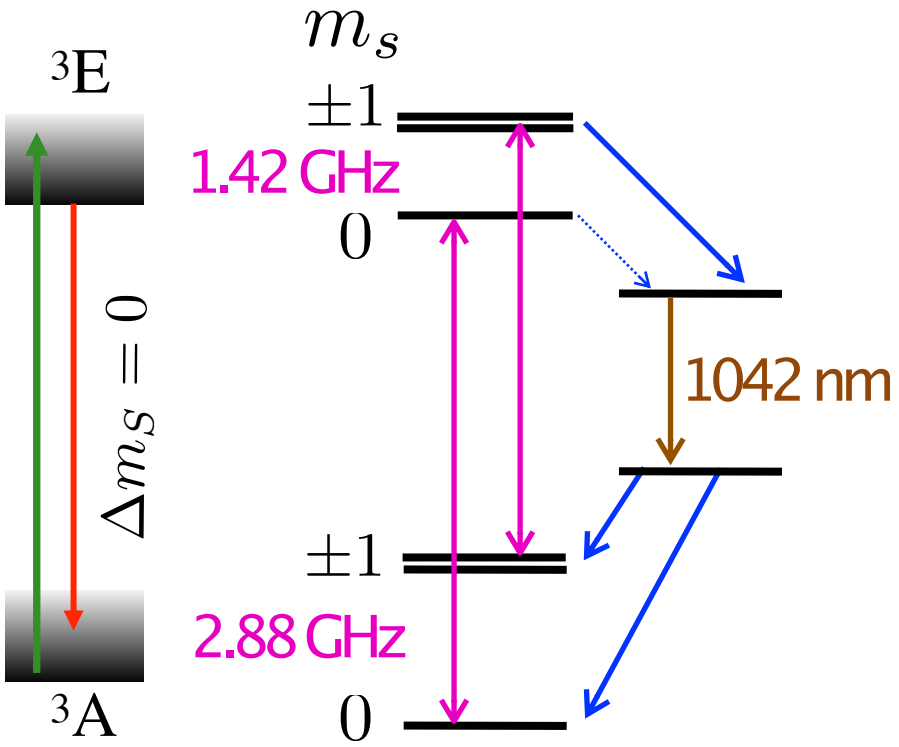

NV center: optically detected magnetic resonance

- Spin structure S=1 in the ground and excited electronic states
- NV axis as z quantization axis + C_{3v} symmetry
- No spin–orbit coupling: transitions with $\Delta m_S = 0$ rule

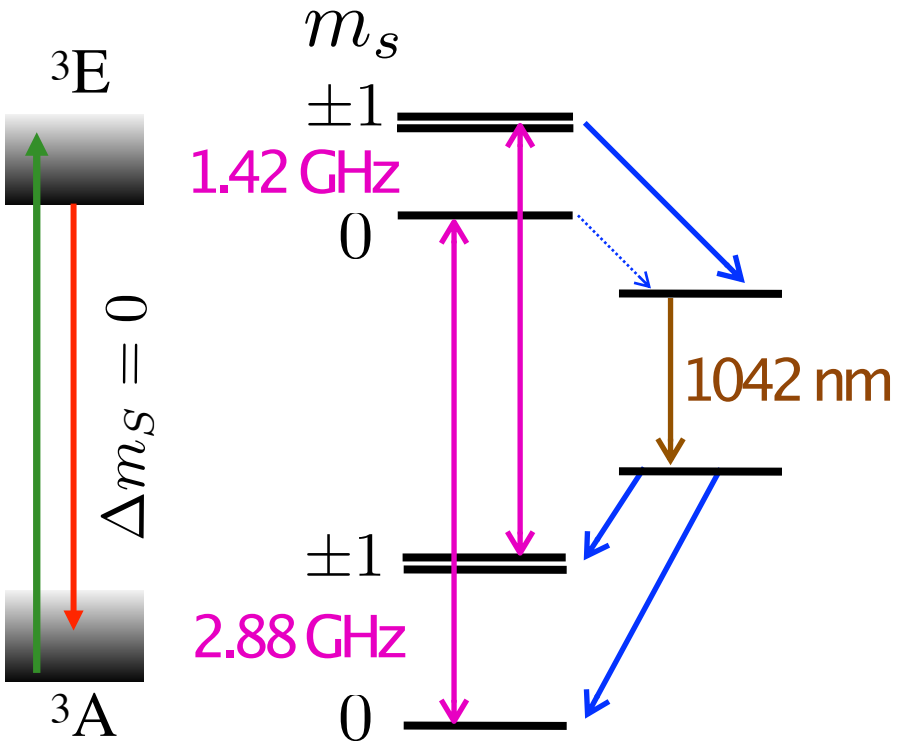

- Optical pumping into $m_S = 0$ induced by green excitation
- The intensity level of the photoluminescence discriminates $m_S = 0$ (high brightness) from $m_S = \pm 1$ (low brightness)

NV center: optically detected magnetic resonance

- Spin structure S=1 in the ground and excited electronic states
- NV axis as z quantization axis + C_{3v} symmetry
- No spin–orbit coupling: transitions with $\Delta m_S = 0$ rule

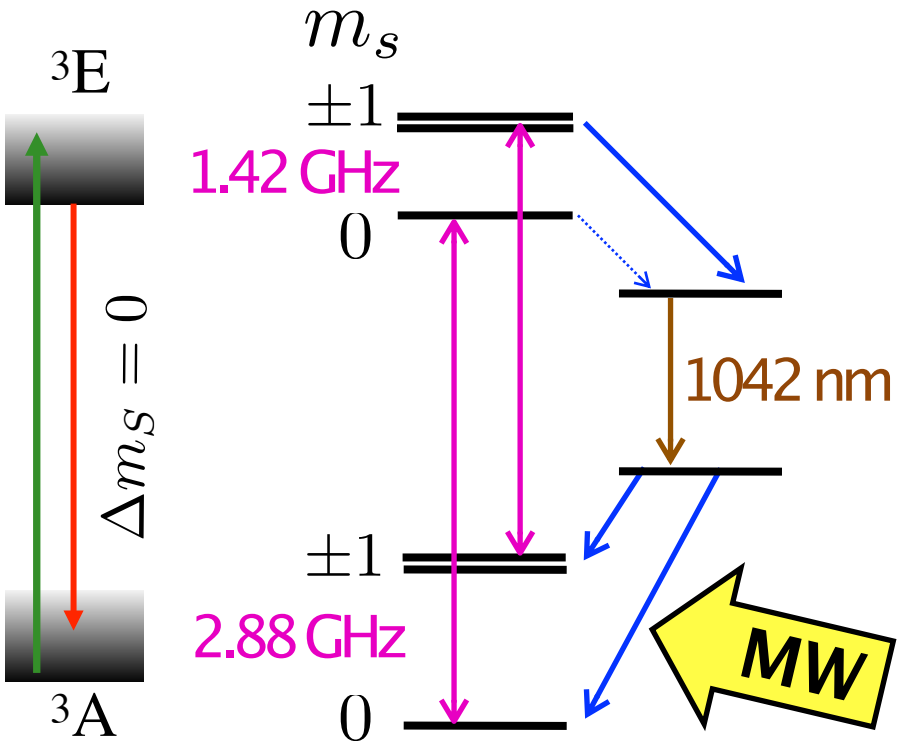

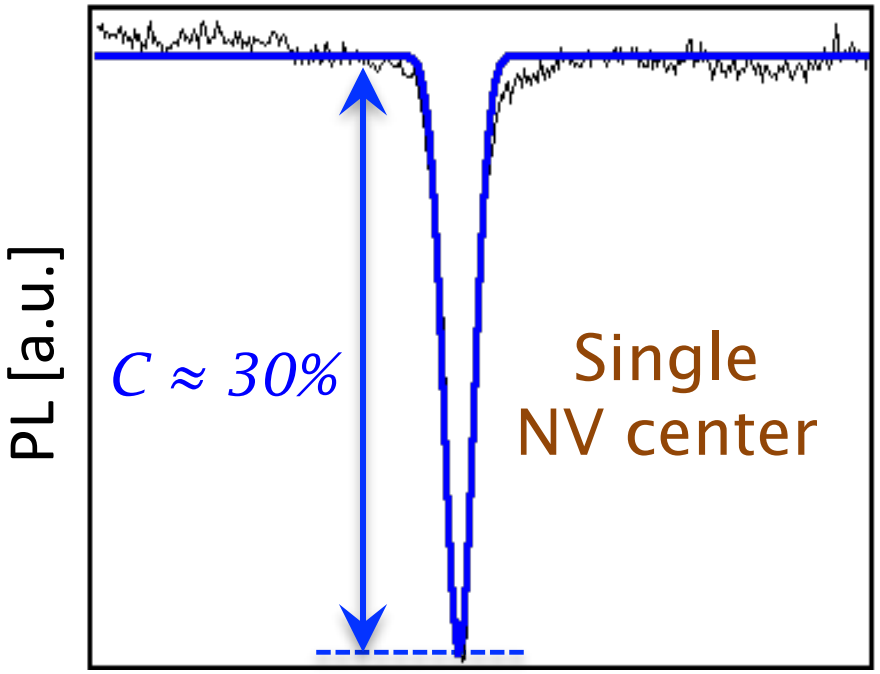

- Optical pumping into $m_S = 0$ induced by green excitation
- The intensity level of the photoluminescence discriminates $m_S = 0$ (high brightness) from $m_S = \pm 1$ (low brightness)

Magnetic field sensing

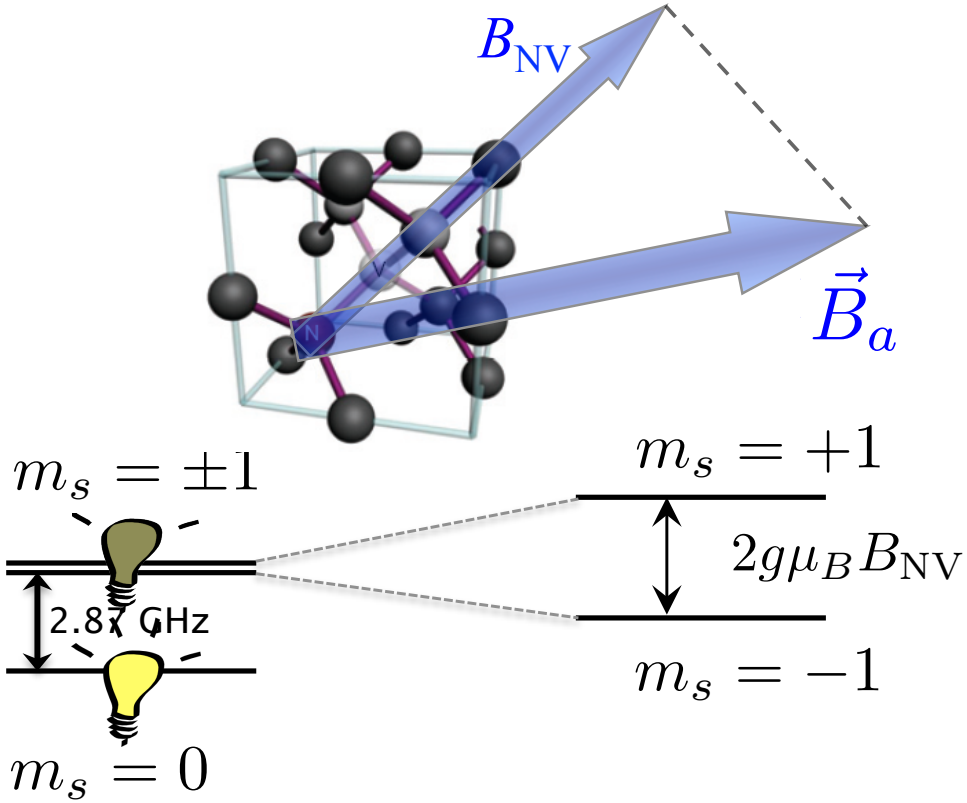

Magnetic field sensing

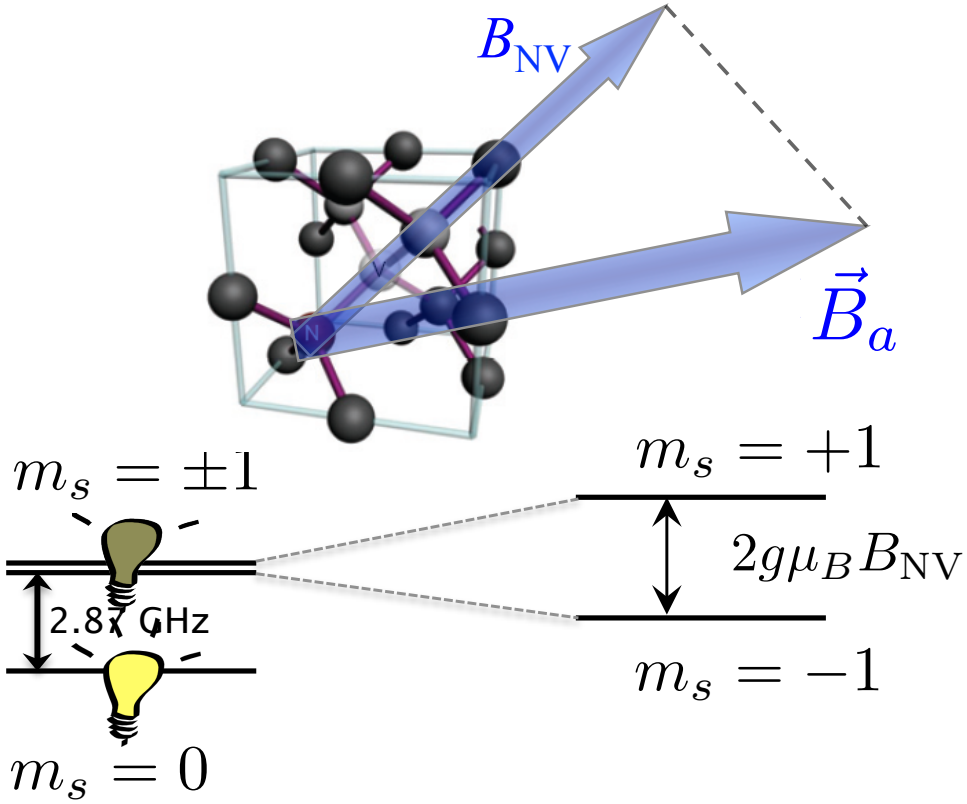

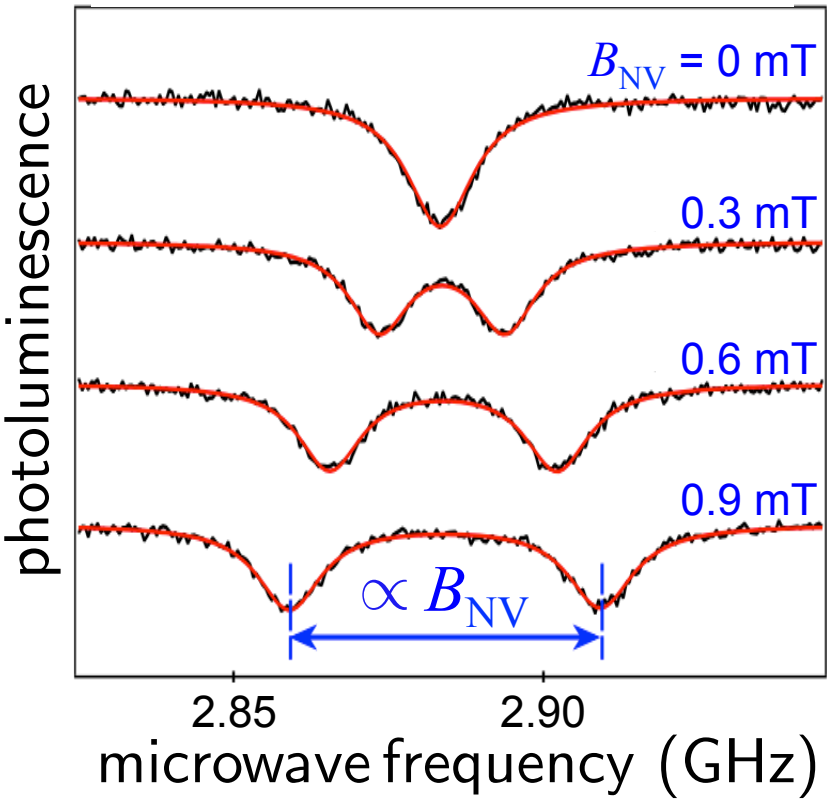

Magnetic field sensing

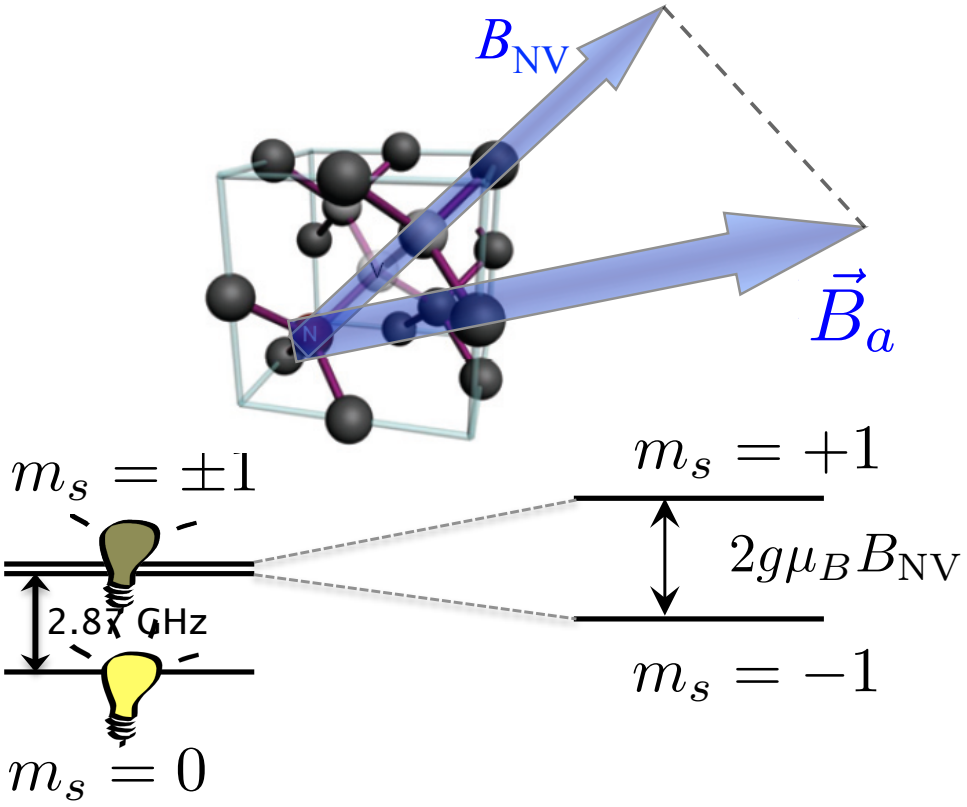

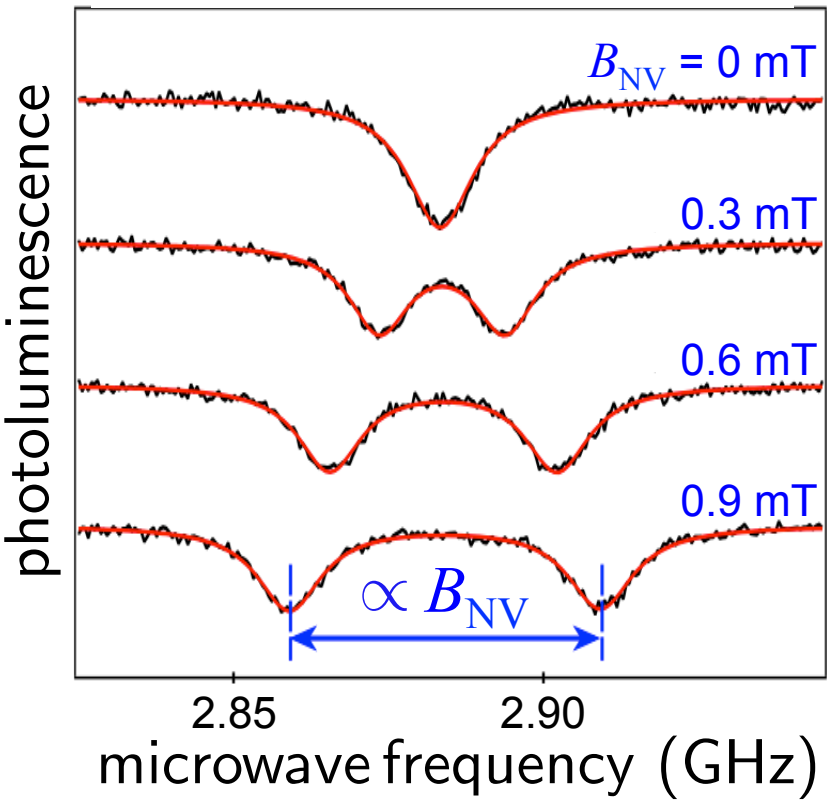

$g_{\mathrm{NV}} = 2.0030 \longrightarrow$ Zeeman shift $\approx 28\,\mathrm{MHz/mT}$

NV center $\equiv$ magnetometer of atomic size
with sensitivity to DC magnetic field $\approx \mu$T

Review: L. Rondin et al., Rep. Prog. Phys. **77**, 056503 (2014)

Creation of NV centers using ion implantation

ultrapure single-crystal diamond

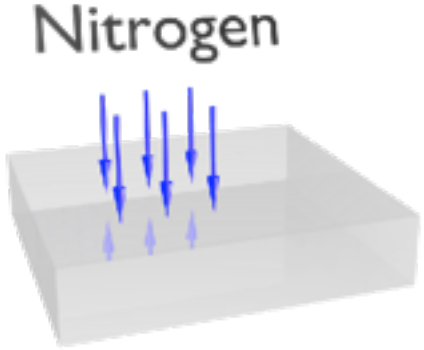

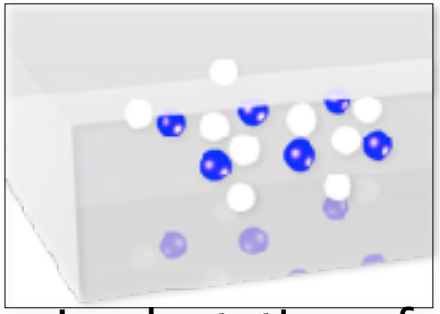

Implantation of nitrogen atoms + creation of vacancies

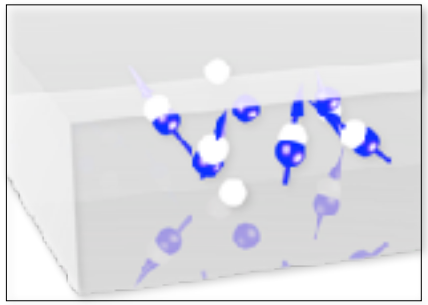

Annealing 800°C – 2h

Creation of NV centers using ion implantation

ultrapure single-crystal diamond

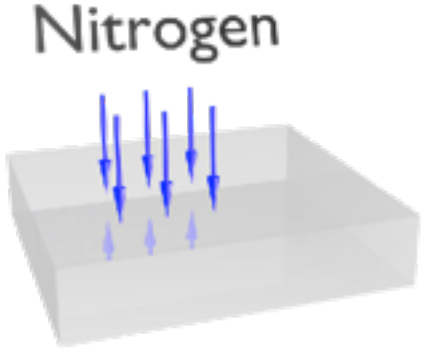

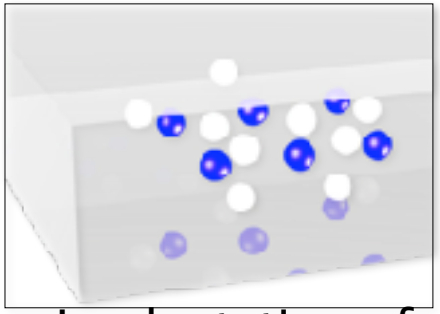

Implantation of nitrogen atoms + creation of vacancies

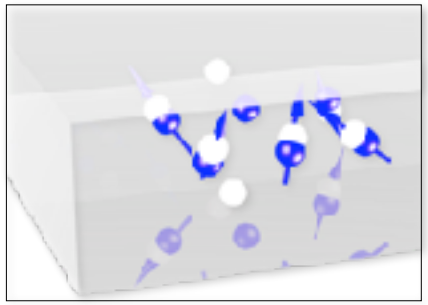

Annealing 800°C – 2h

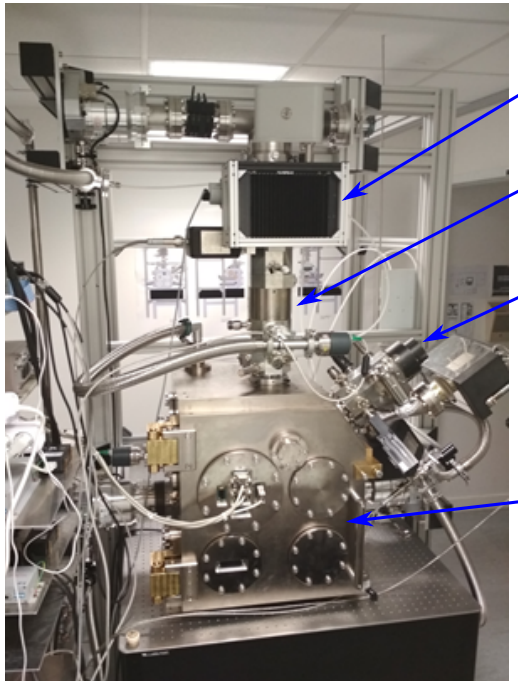

FIB with N_2^+ or Xe^+ beam
~50 nm resolution

M. Lesik et al, *Phys. Stat. Solidi A* **210**, 2055-2059 (2013)

Creation of NV centers using ion implantation

ultrapure single-crystal diamond

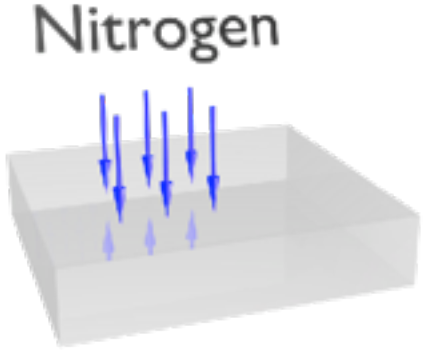

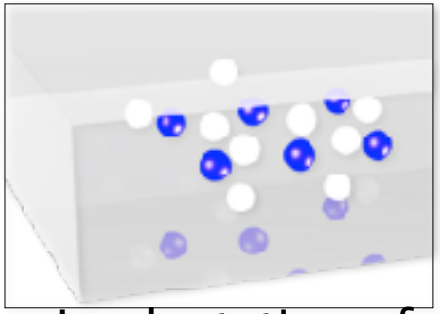

Implantation of nitrogen atoms + creation of vacancies

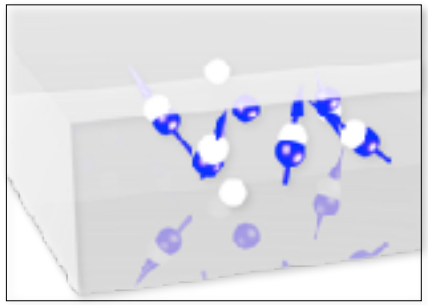

Annealing 800°C – 2h

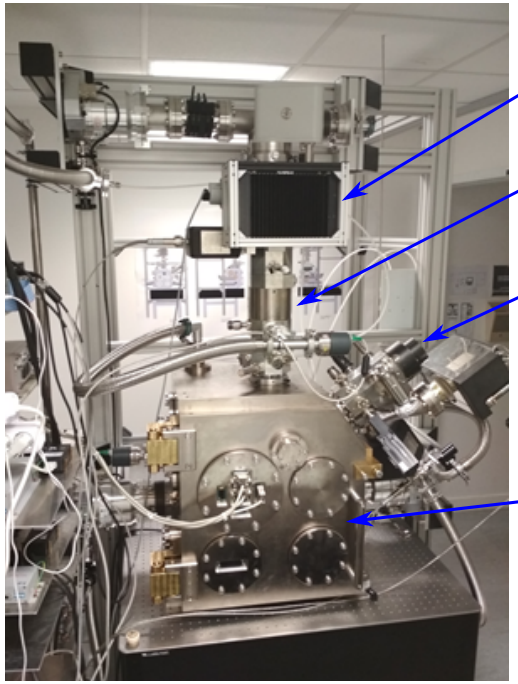

FIB with N_2^+ or Xe^+ beam
~50 nm resolution

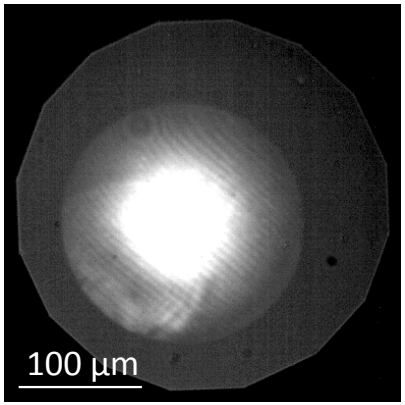

anvil of 300 μm layer of NVs

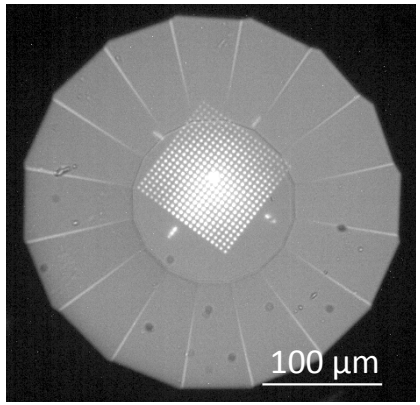

anvil of 150 μm pattern of NVs

M. Lesik et al, *Phys. Stat. Solidi A* **210**, 2055-2059 (2013)

High-pressure NV magnetometry: set-up

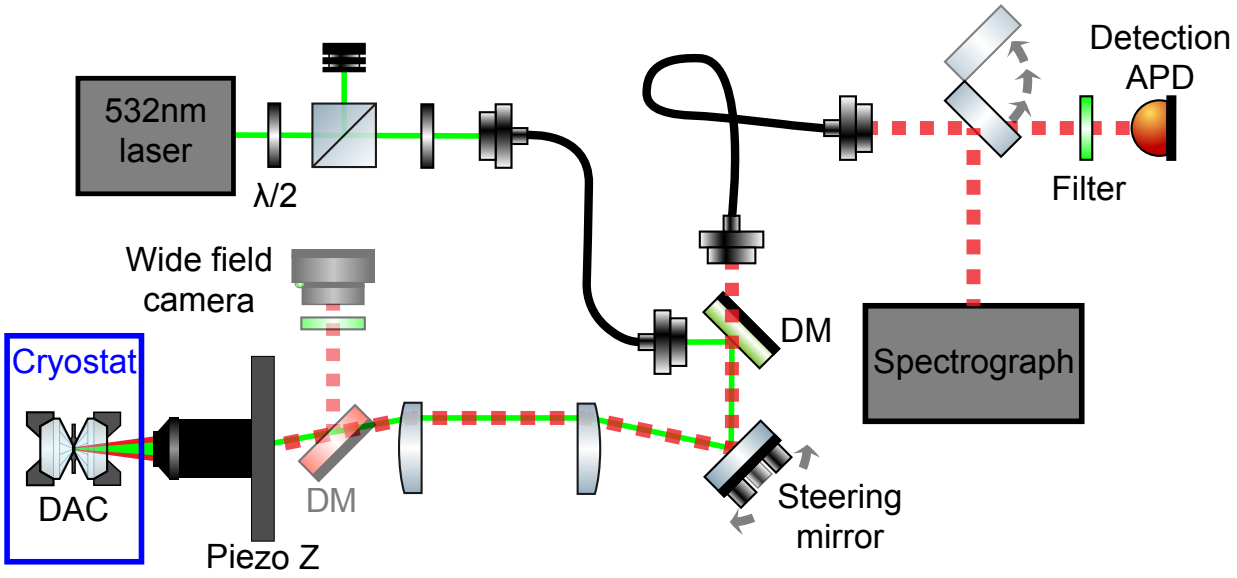

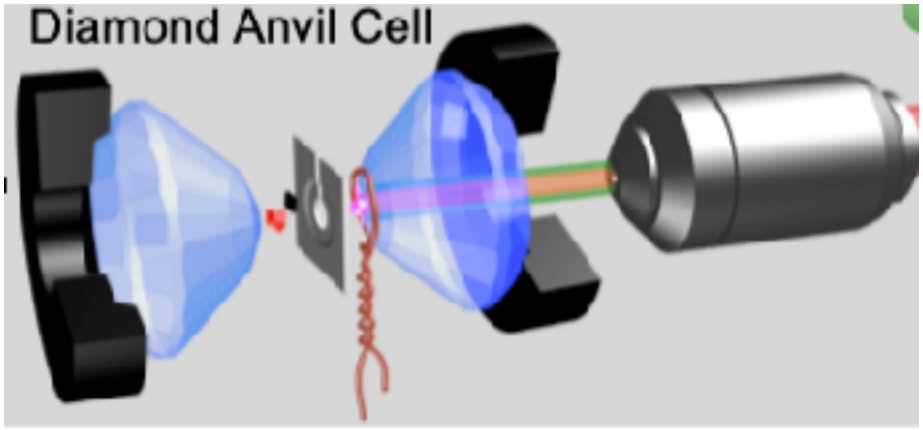

High-pressure NV magnetometry: set-up

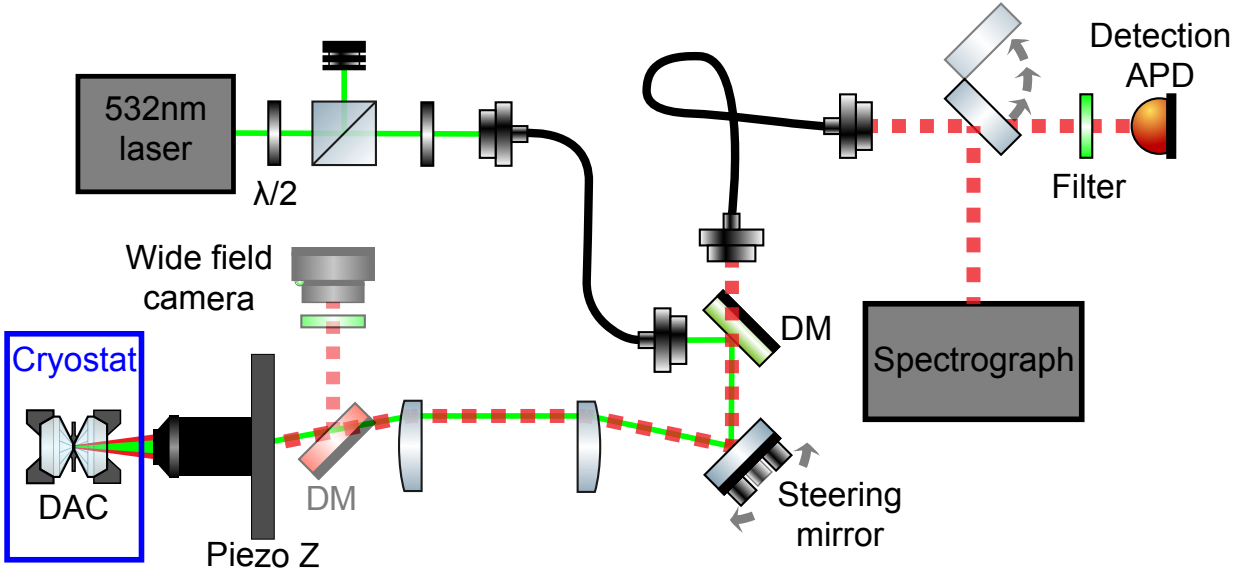

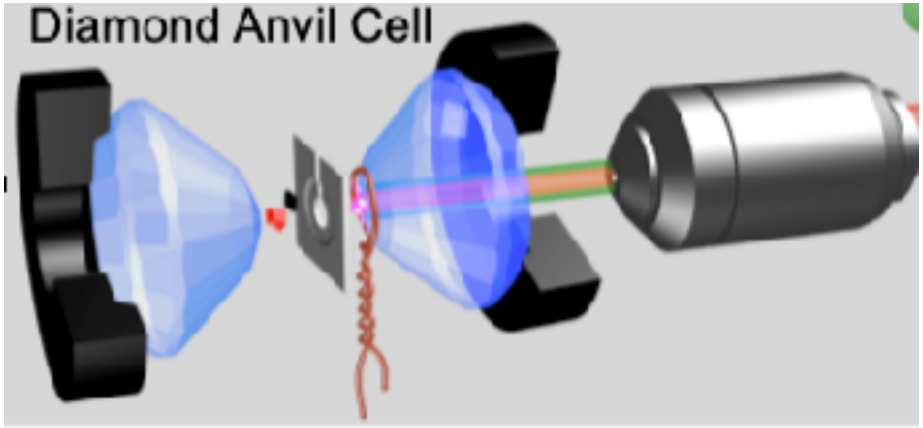

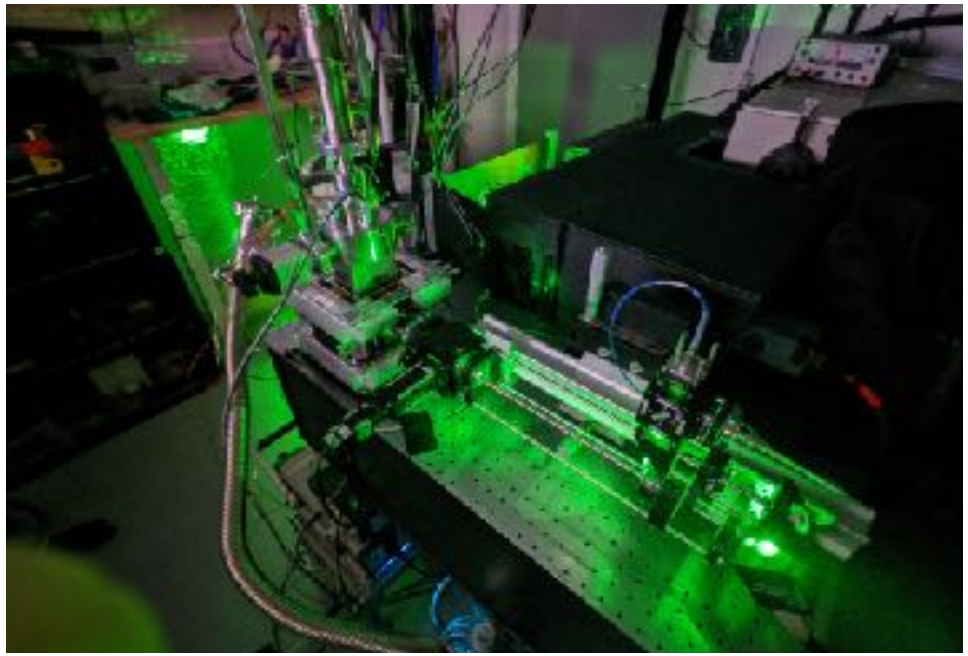

Microwave excitation and metallic gasket

COMSOL simulation of the eddy currents induced in the gasket by the microwave coil

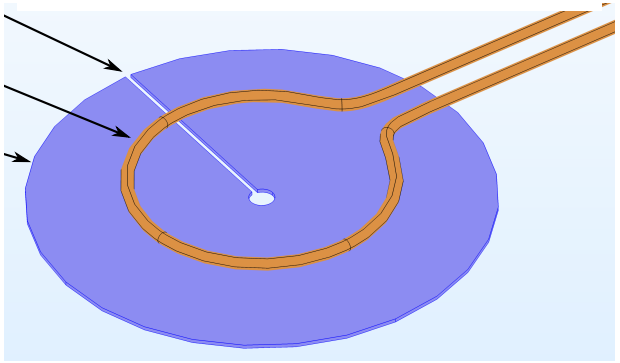

Microwave excitation and metallic gasket

COMSOL simulation of the eddy currents induced in the gasket by the microwave coil

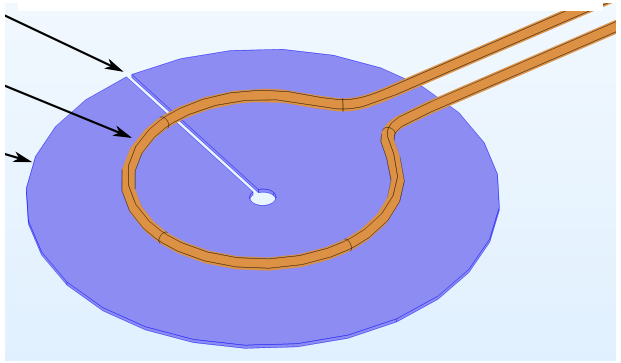

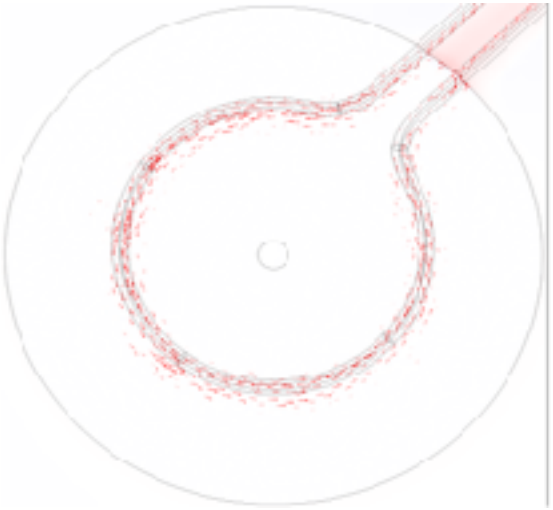

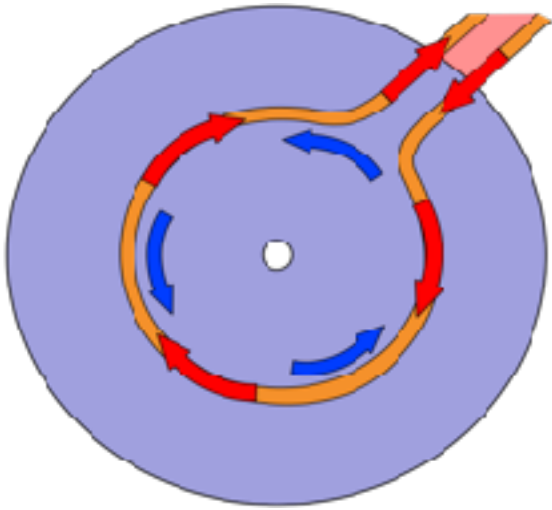

Microwave excitation and metallic gasket

COMSOL simulation of the eddy currents induced in the gasket by the microwave coil

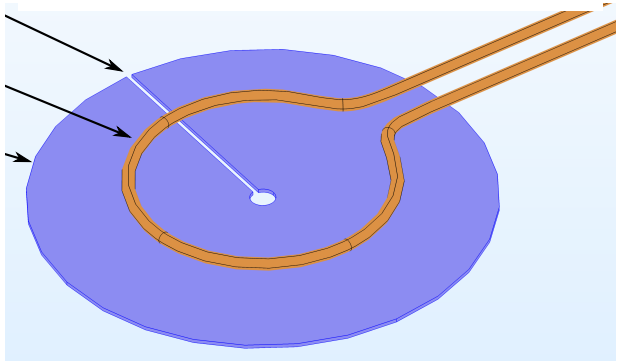

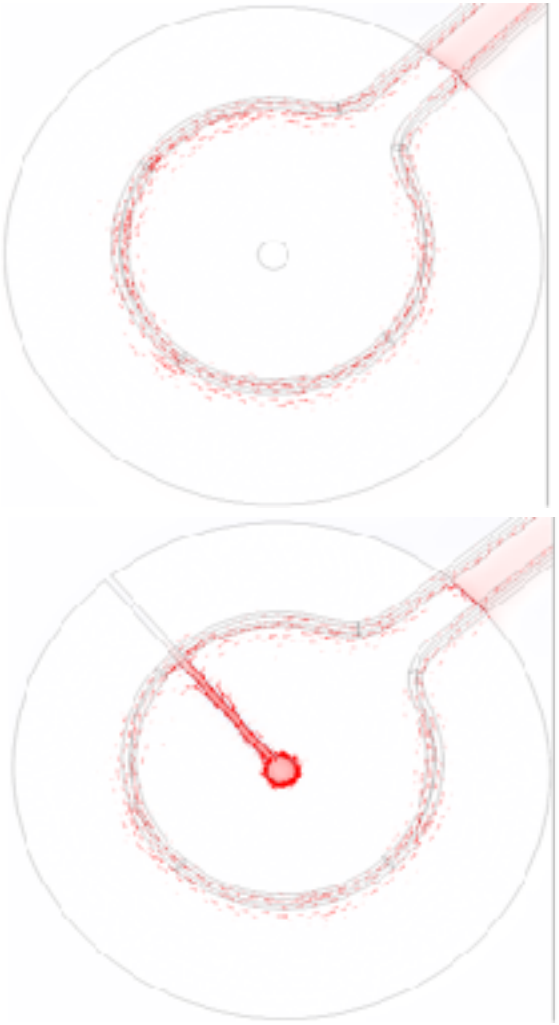

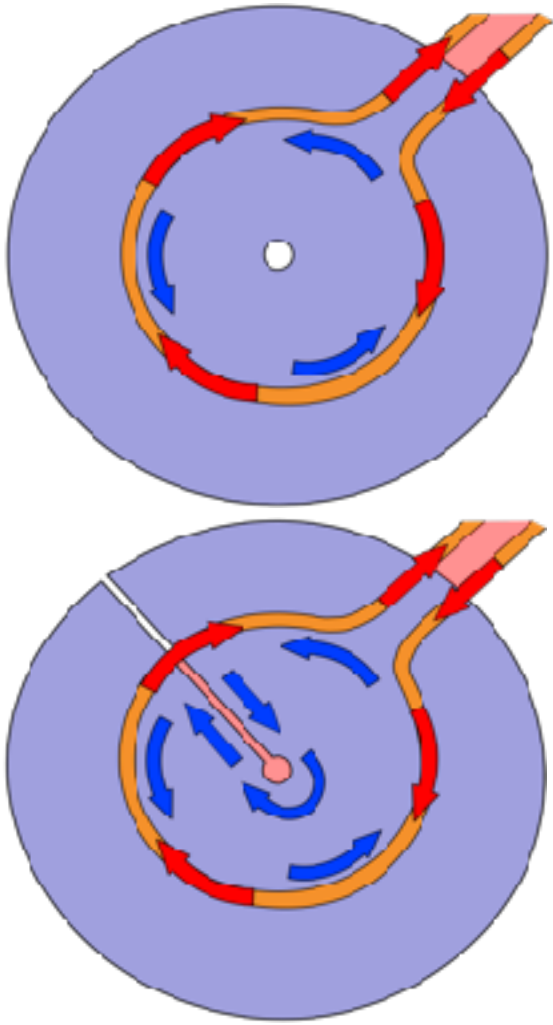

Microwave excitation and metallic gasket

COMSOL simulation of the eddy currents induced in the gasket by the microwave coil

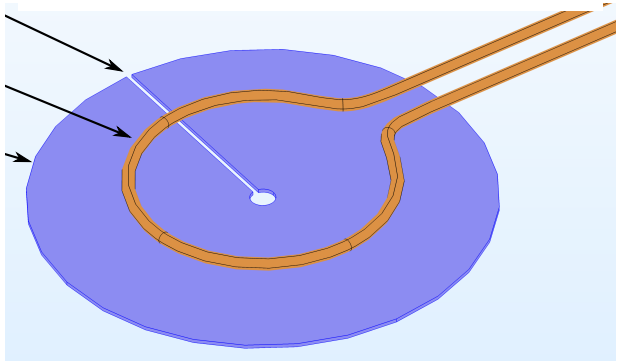

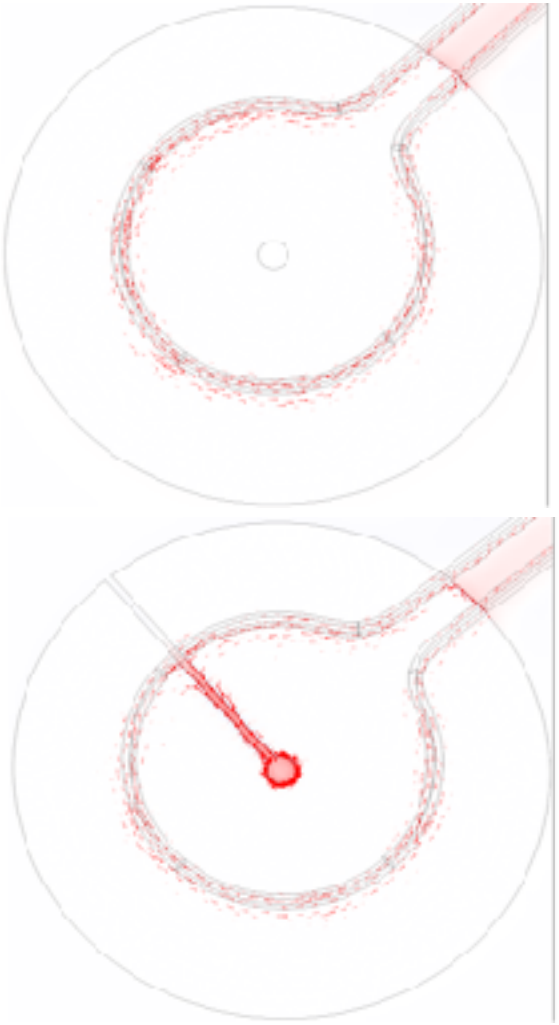

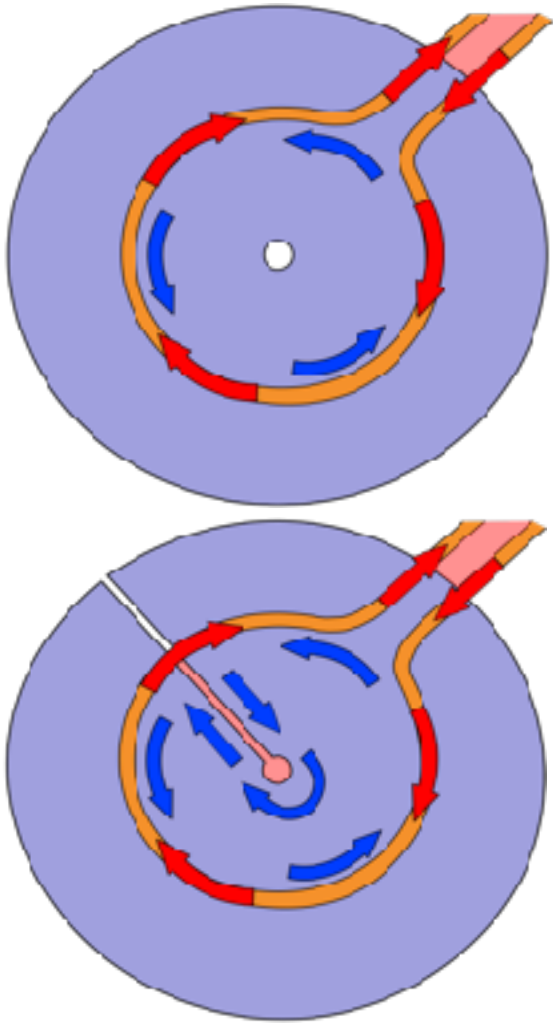

The slit cut in the metallic gasket avoids shielding but also behaves as a **focusing lens** for the microwave excitation

T. Meier et al, Sci. Adv. **3**:eaao5242 (2017)

Microwave excitation and metallic gasket

COMSOL simulation of the eddy currents induced in the gasket by the microwave coil

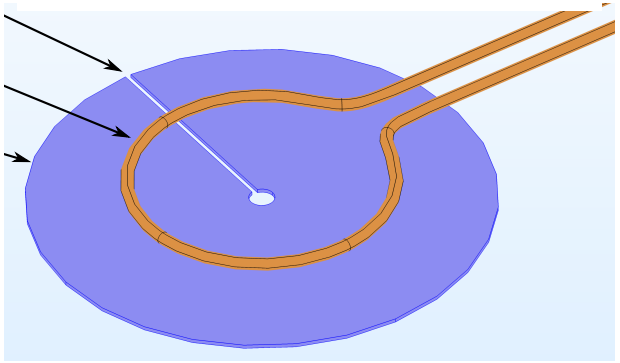

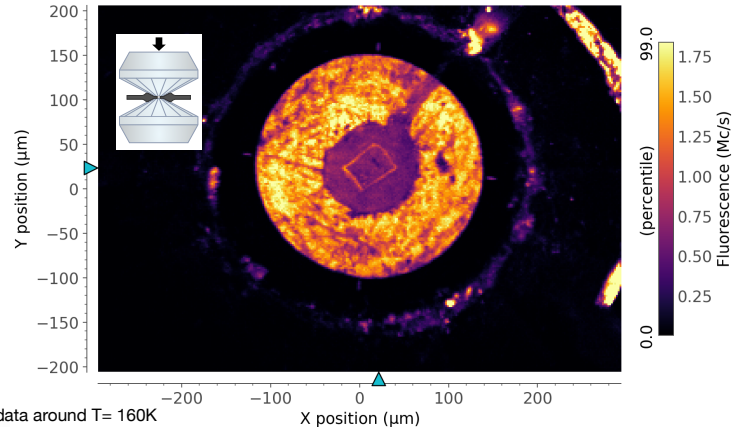

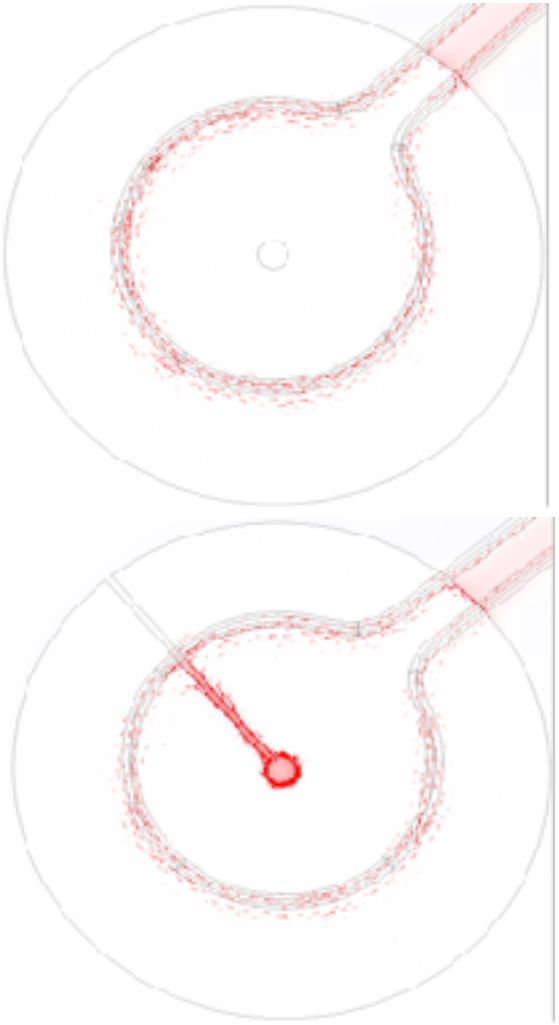

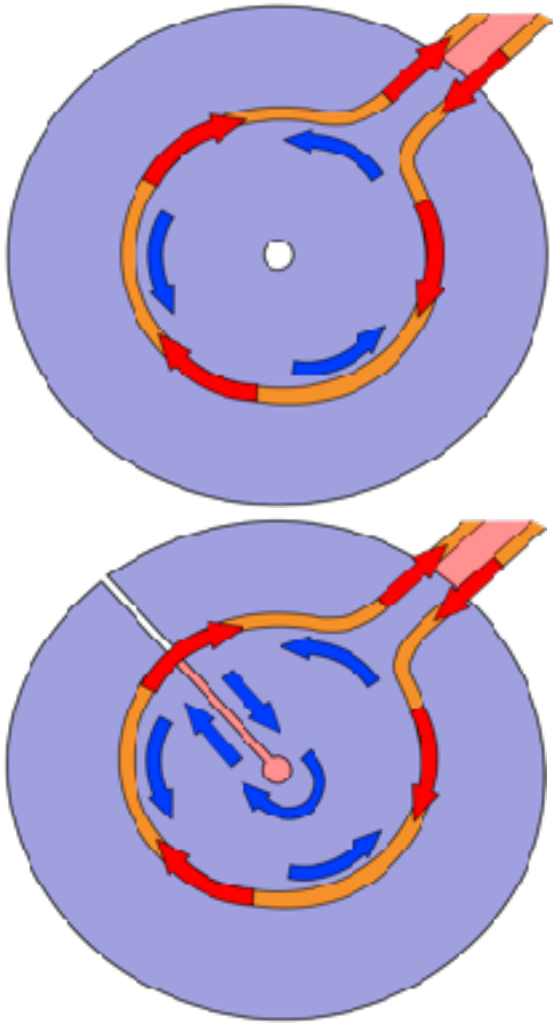

The slit cut in the metallic gasket avoids shielding but also behaves as a **focusing lens** for the microwave excitation

T. Meier et al, Sci. Adv. **3**:eaao5242 (2017)

Superconductivity of MgB_2 at 7 GPa

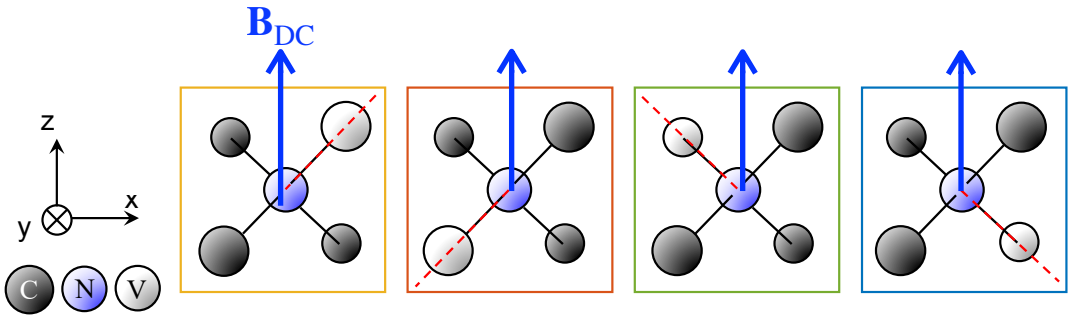

$\mathbf{B}_{DC}$//[100]

same projection B_{NV} for the four NV families along [111] axis

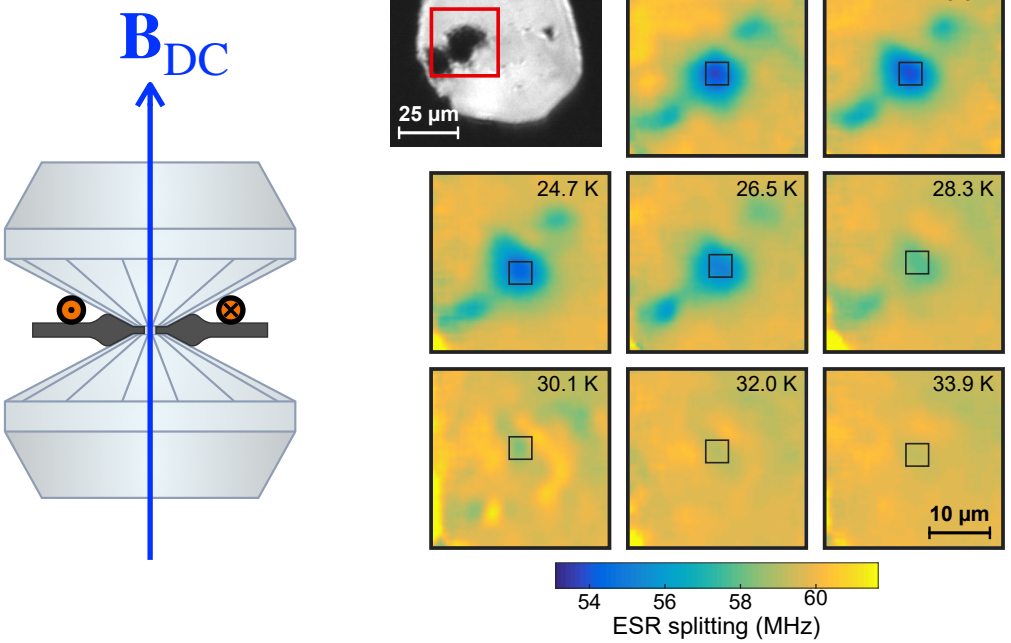

Superconductivity of MgB_2 at 7 GPa

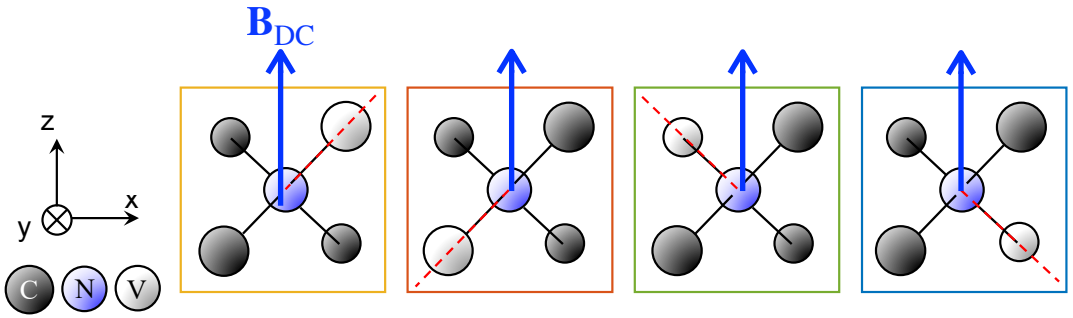

$\mathbf{B}_{DC}$//[100]

same projection B_{NV} for the four NV families along [111] axis

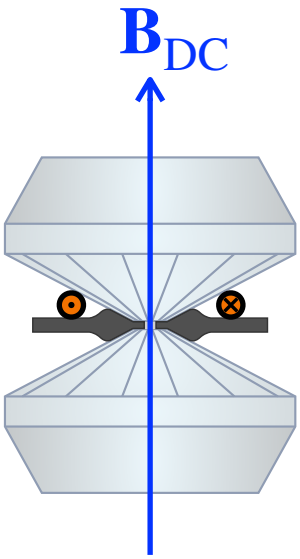

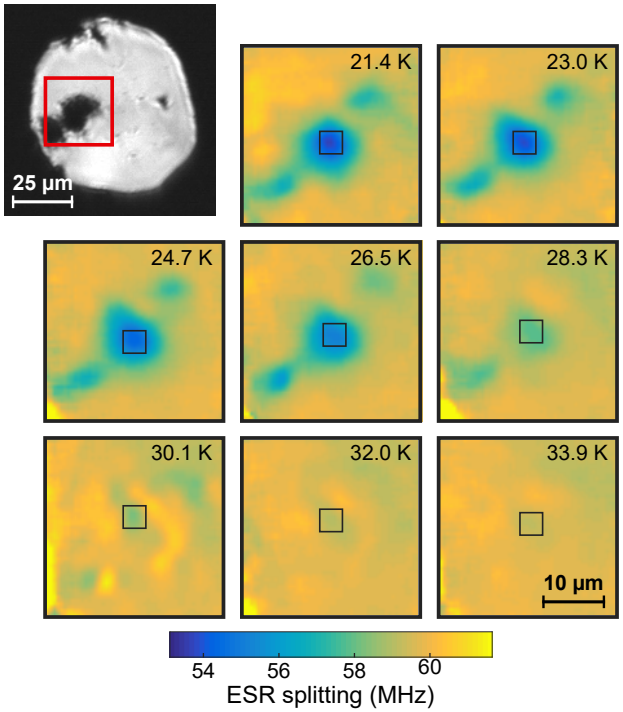

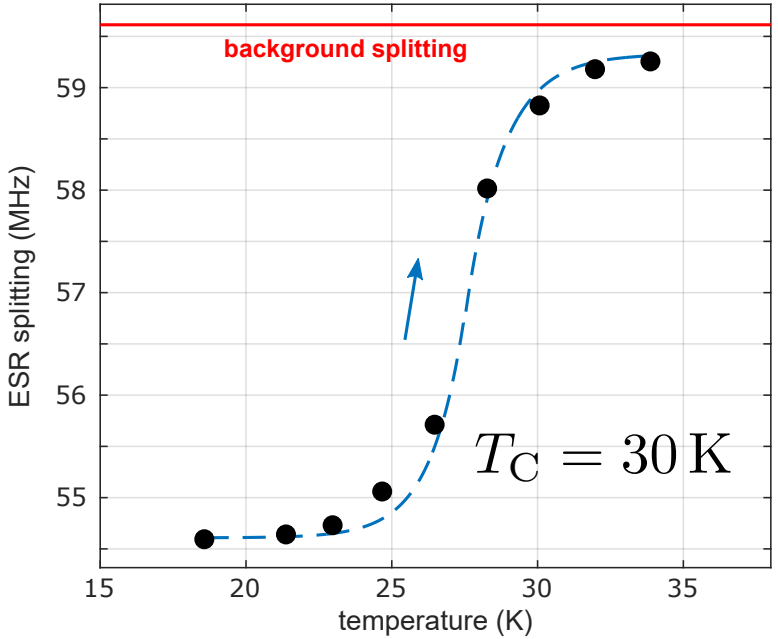

Superconductivity of MgB_2 at 7 GPa

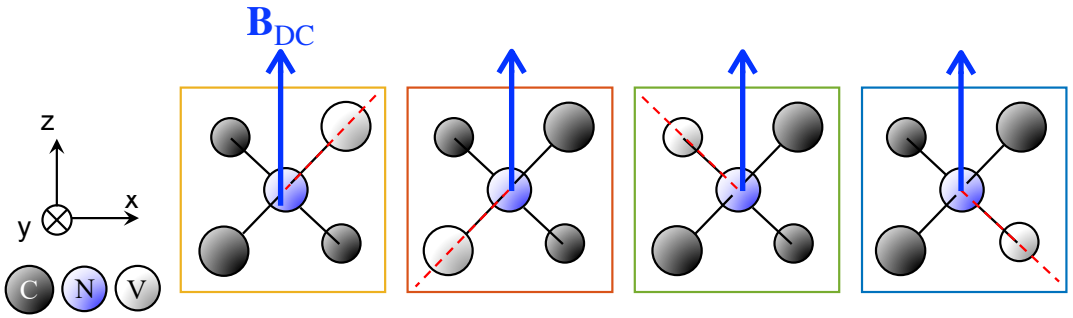

$\mathbf{B}_{DC}$//[100]

same projection B_{NV} for the four NV families along [111] axis

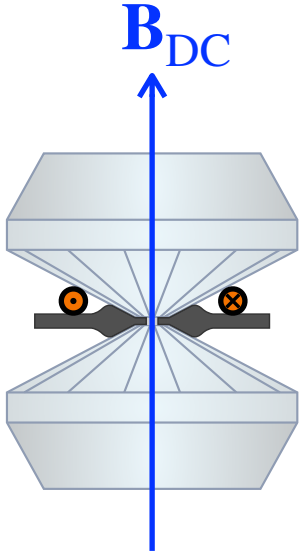

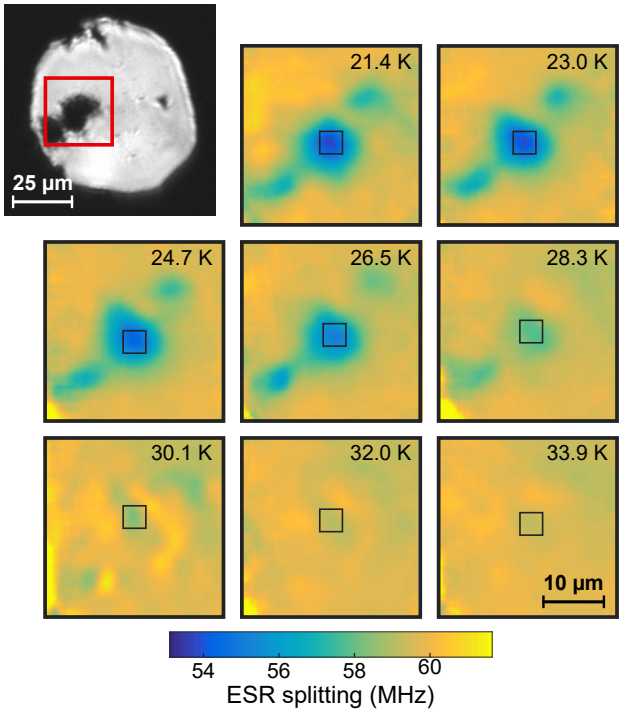

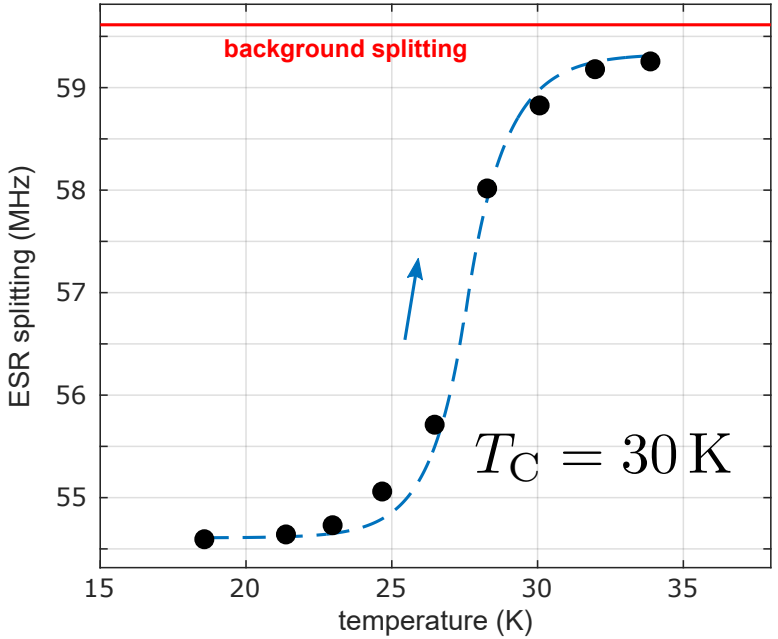

M. Lesik, L. Toraille et al., Science **366**, 1359–1362 (2019)

Hsieh et al., Science **366**, 1349–1354 (Norman Yao's group)

Yip et al., Science **366**, 1355–1359 (Sen Yang's group)

Cuprate Hg-1223 under pressure

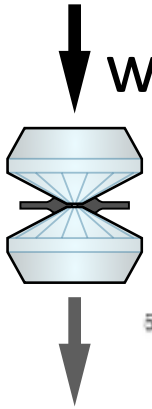

wide-field transmission
with white light

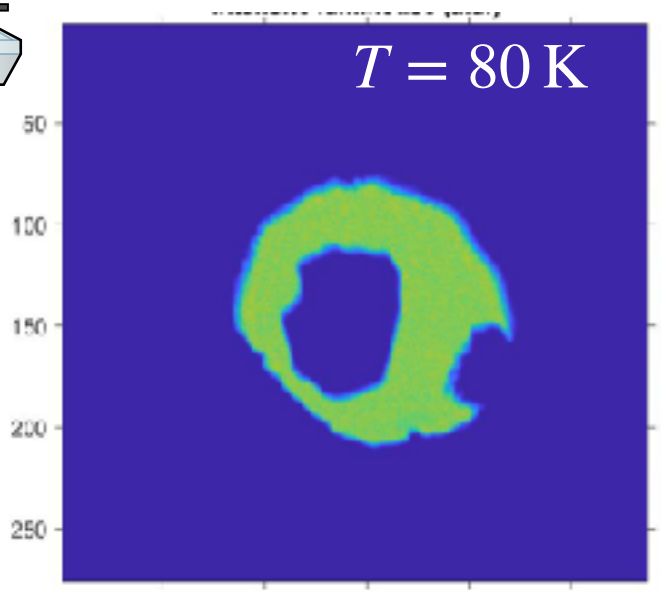

Microcrystal of Hg-1223
in Ar gas as pressure
transmitting medium

Dorothée COLSON
CEA-SPEC

Cuprate Hg-1223 under pressure

wide-field transmission with white light

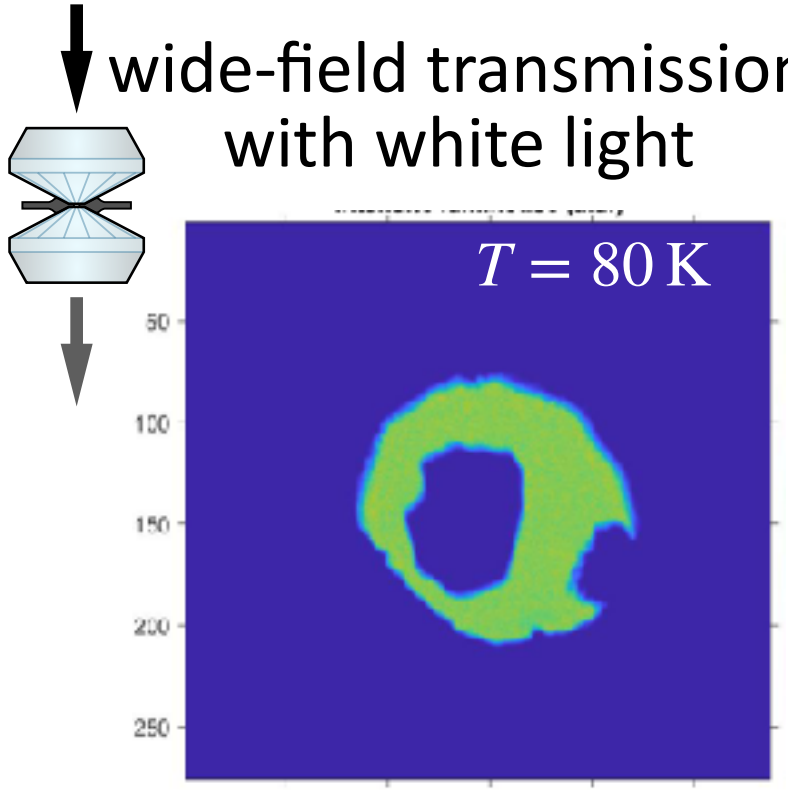

NV luminescence detected by confocal microscopy

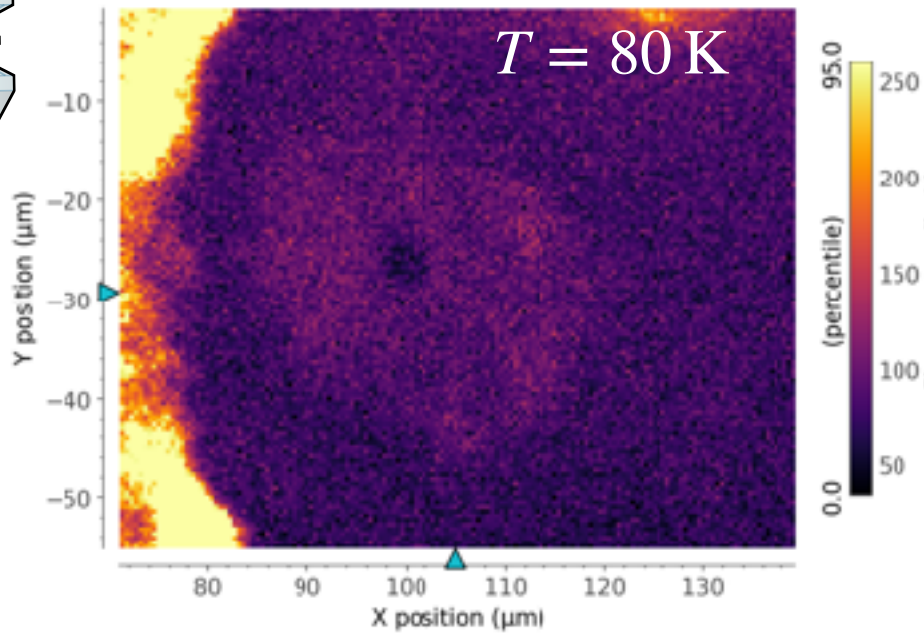

Microcrystal of Hg-1223 in Ar gas as pressure transmitting medium

Dorothée COLSON
CEA-SPEC

Cuprate Hg-1223 under pressure

wide-field transmission with white light

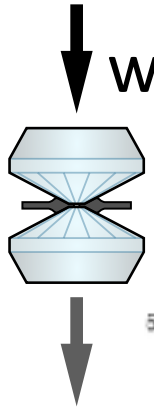

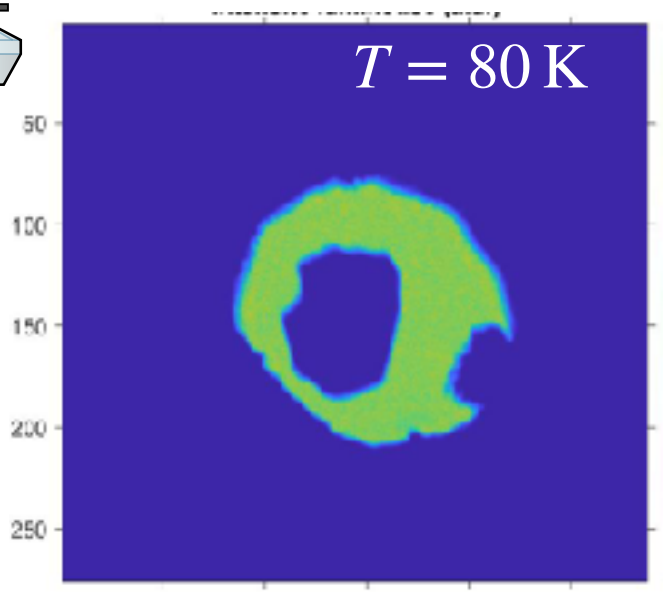

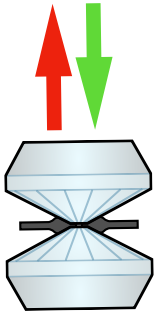

NV luminescence detected by confocal microscopy

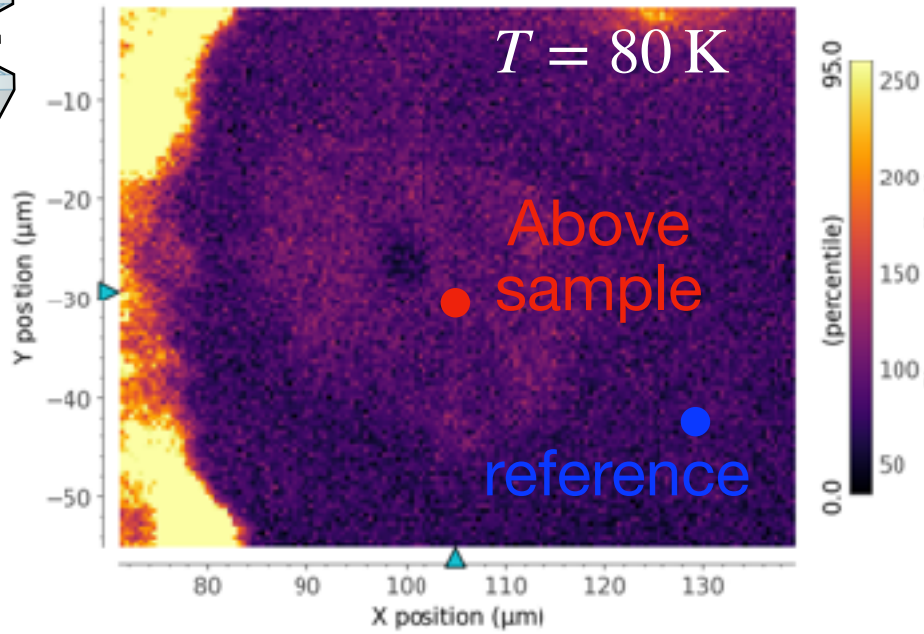

Microcrystal of Hg-1223 in Ar gas as pressure transmitting medium

Dorothée COLSON
CEA-SPEC

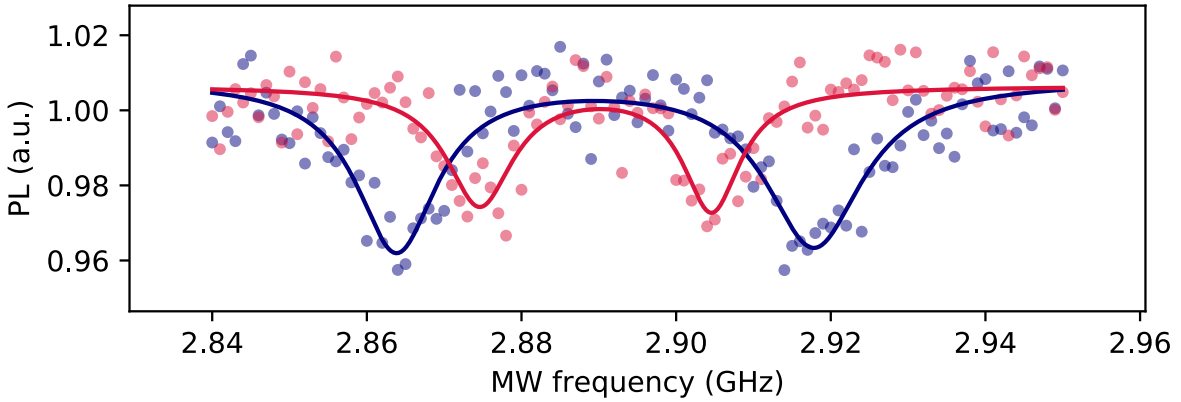

Optimization of the microwave excitation

P ambiant

P = 35 GPa

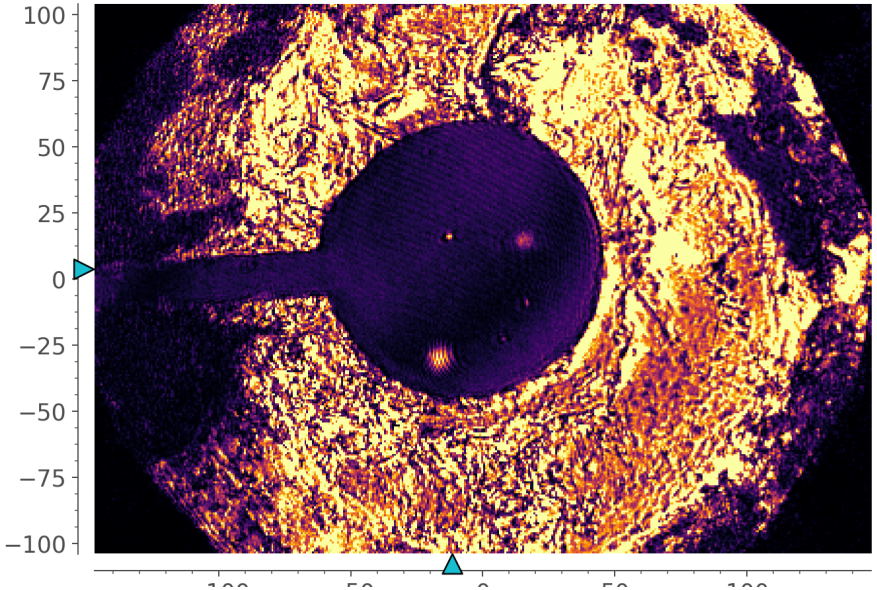

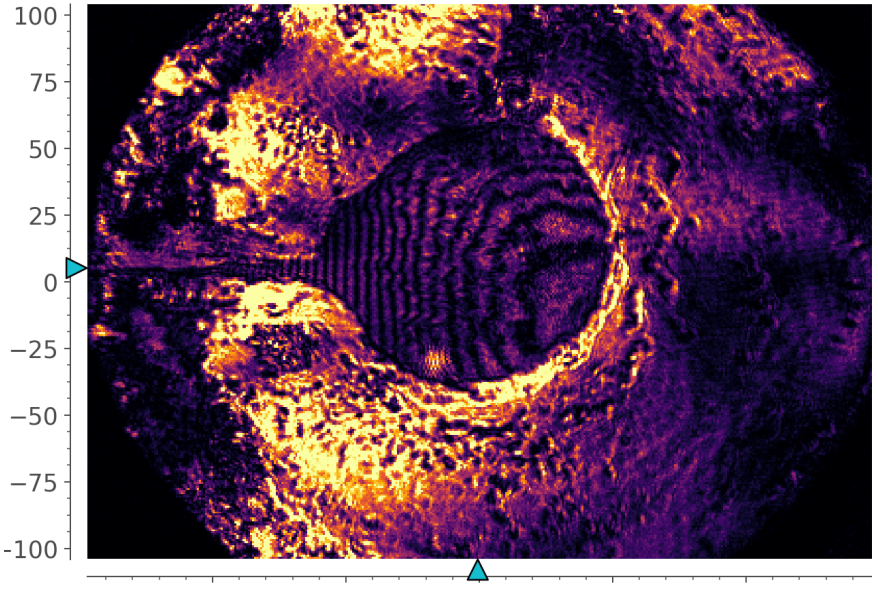

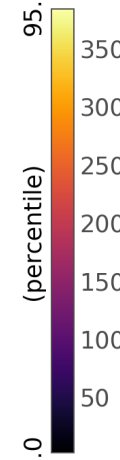

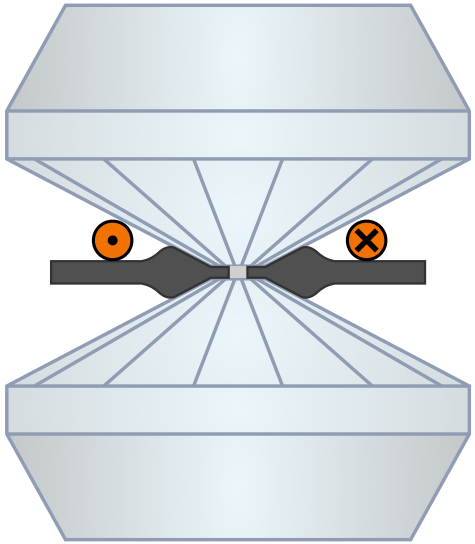

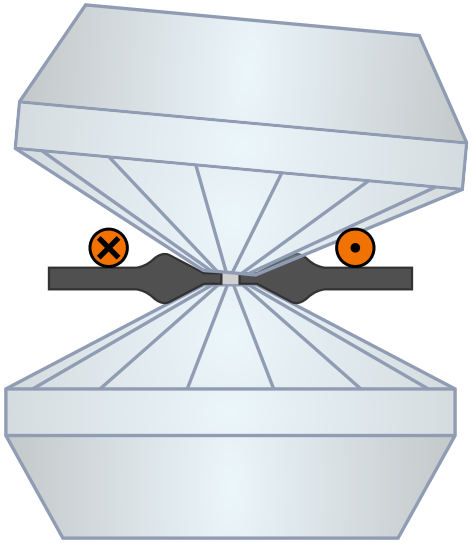

Optimization of the microwave excitation

- Optimization of the slit design: shape and dimensions of the slit, its filling (epoxy glue + boron powder) and heating duration of the filling
- Solid medium (KBr) in the DAC as pressure transmitting medium to improve the stability of the gasket

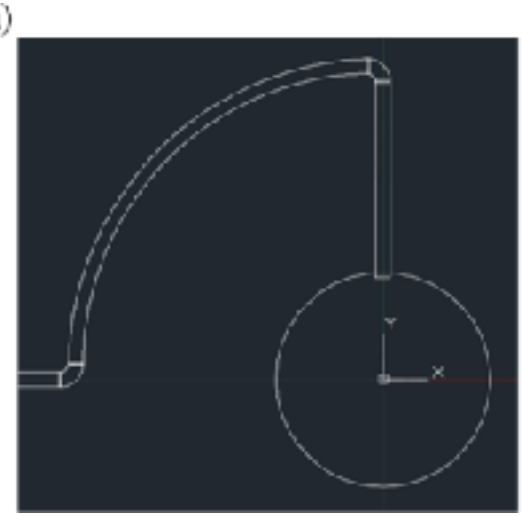

(b)

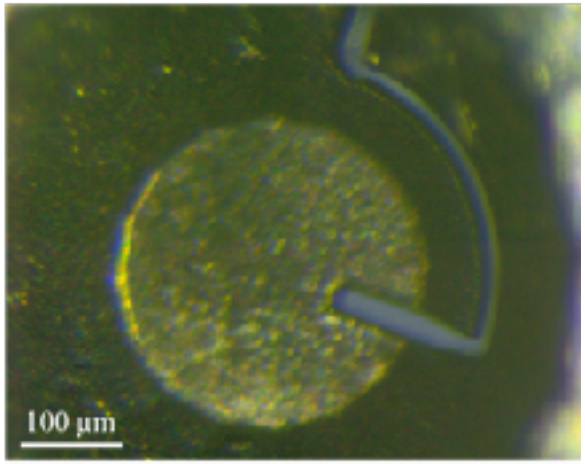

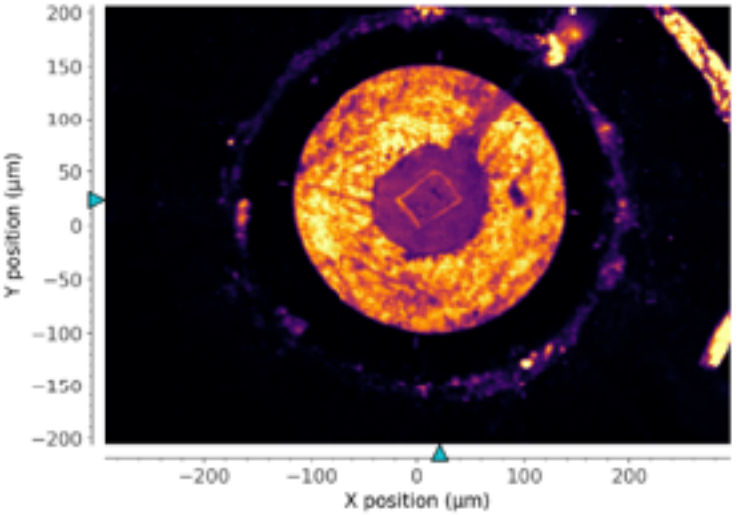

- Record of ODMR signals above 50 GPa
- Reduced distortion of parallelism between the two anvils

Superconductivity of cuprate Hg1223

Superconductivity of cuprate Hg1223

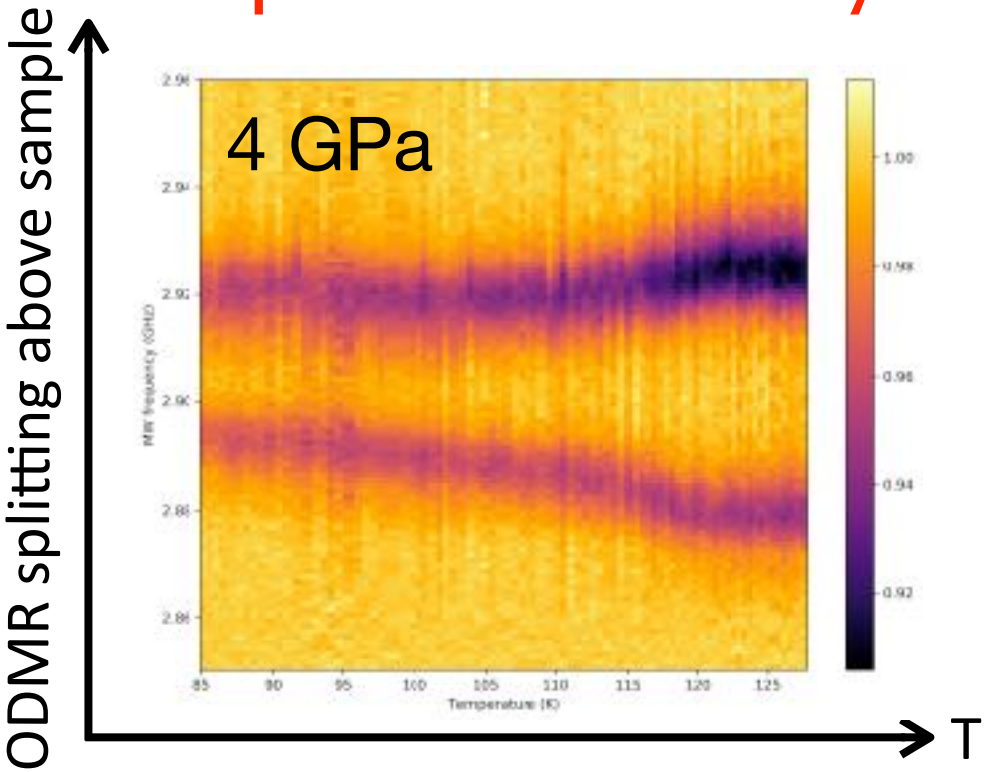

Superconductivity of cuprate Hg1223

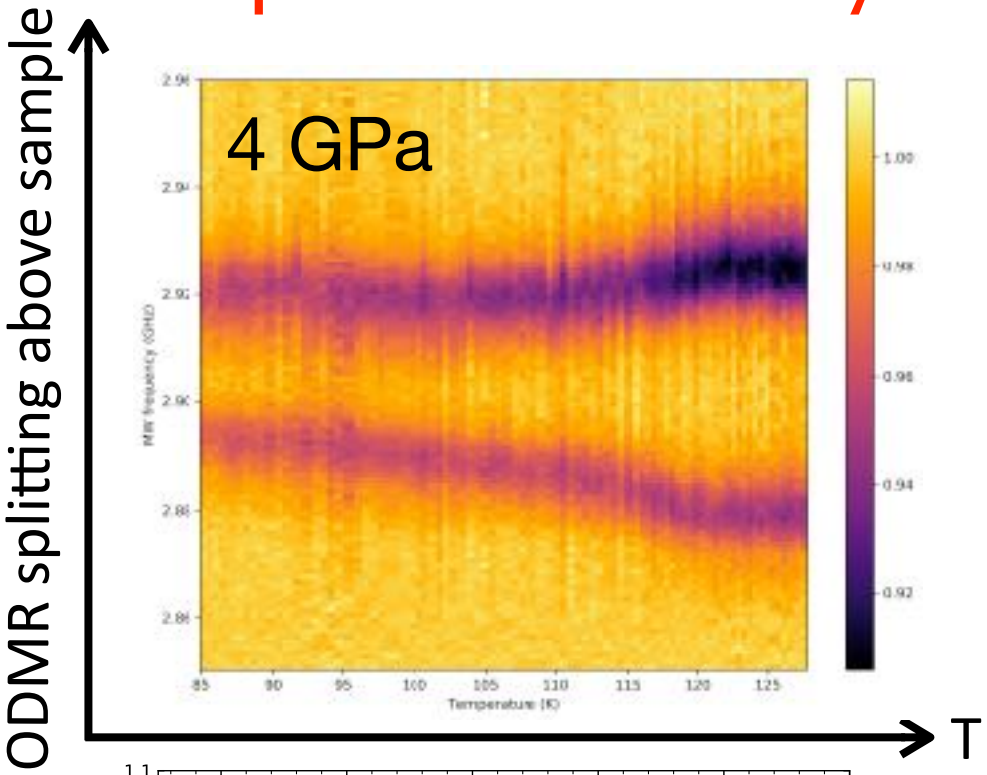

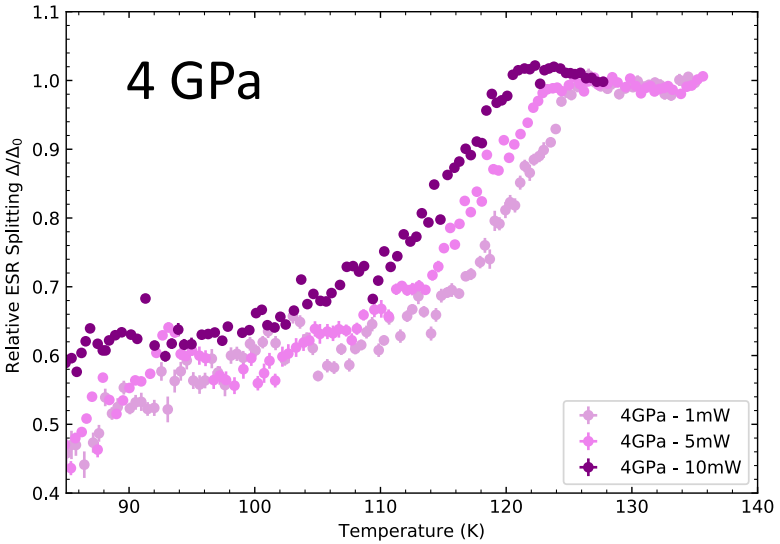

Superconductivity of cuprate Hg1223

ODMR splitting above sample

T

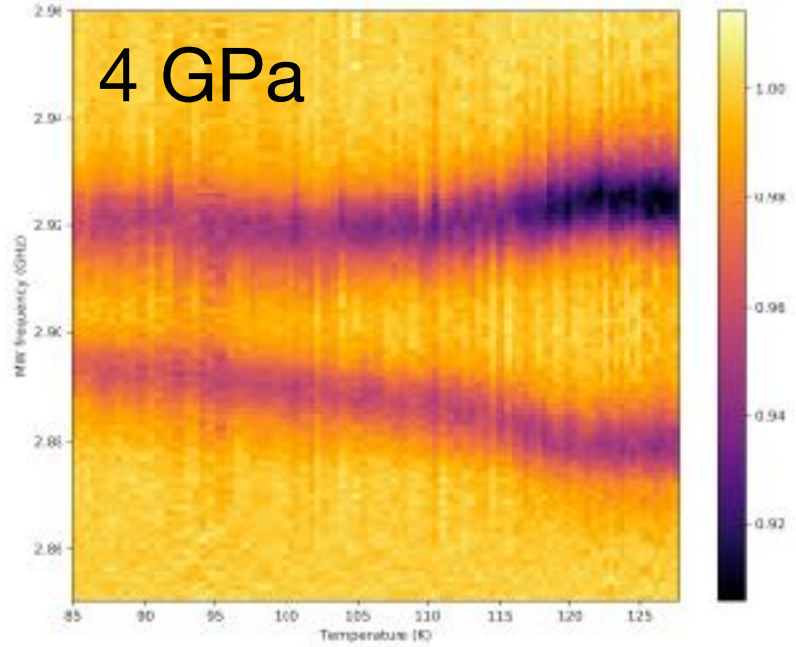

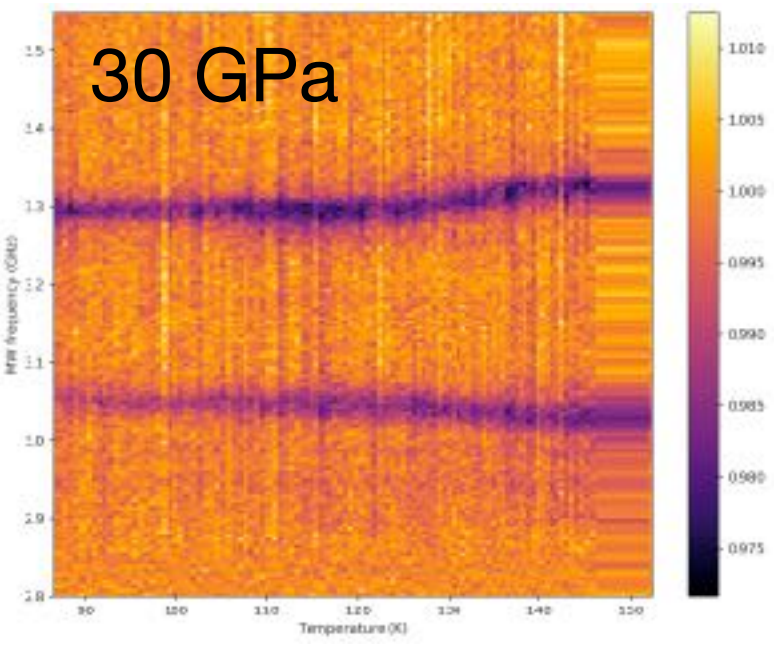

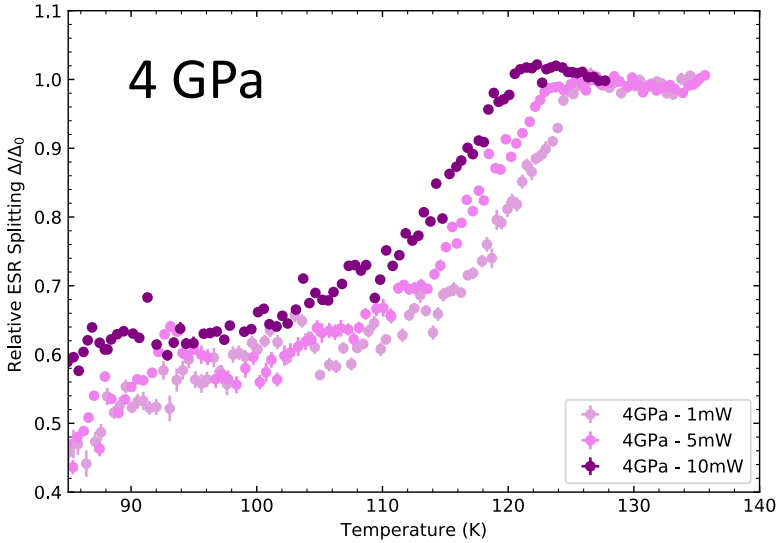

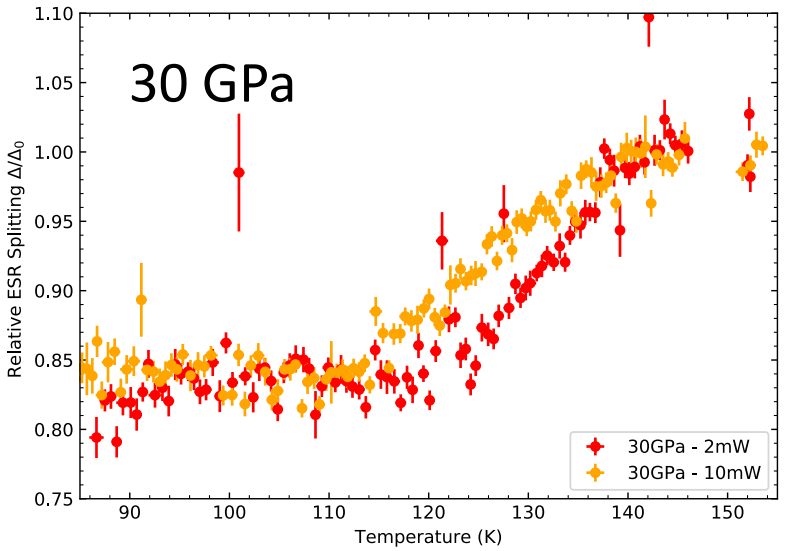

Evolution of T_c for cuprate Hg1223

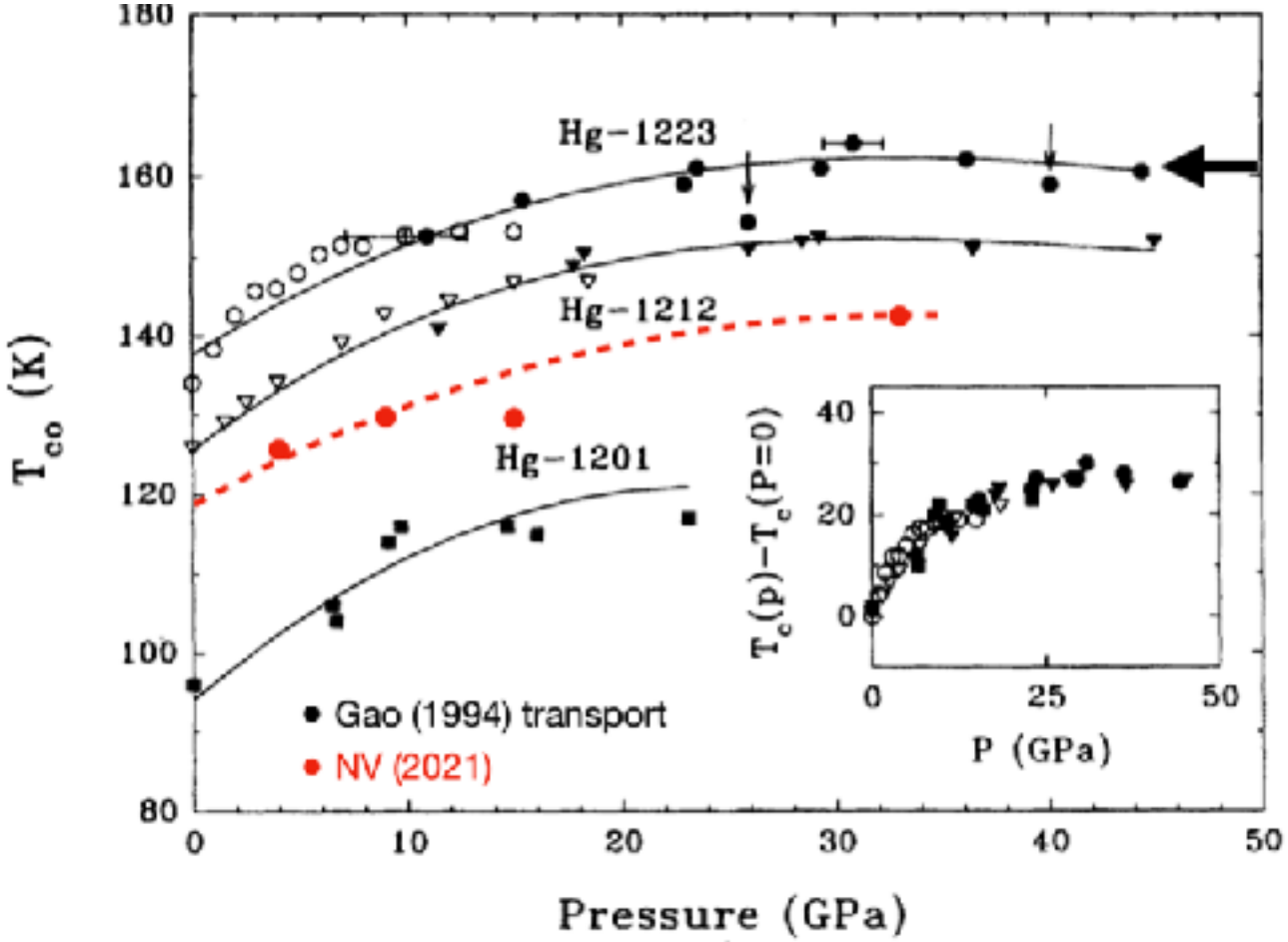

L. Gao et al., Phys. Rev. B 50, 4260 (1994)

Evolution of T_c for cuprate Hg1223

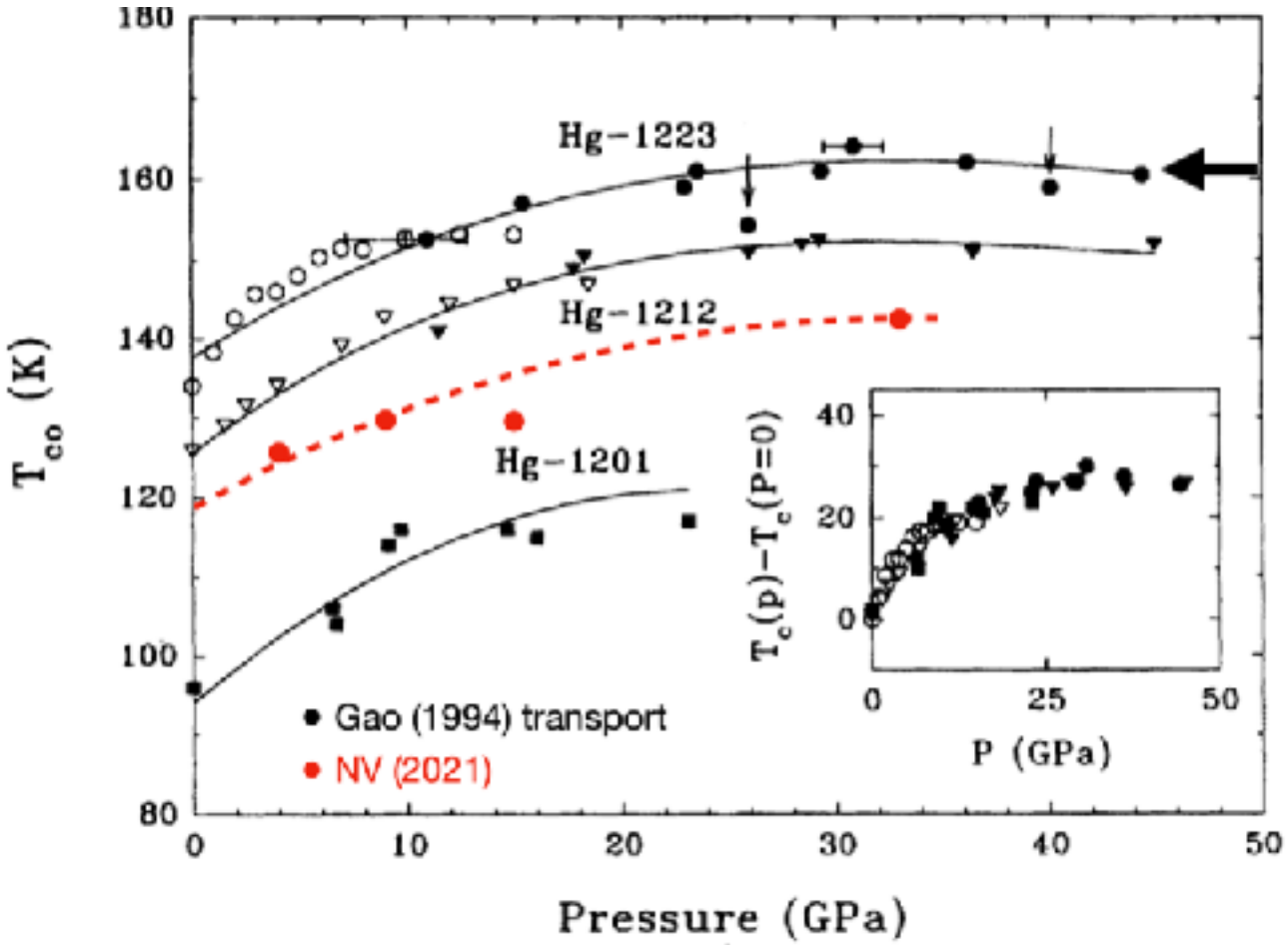

L. Gao et al., Phys. Rev. B 50, 4260 (1994)

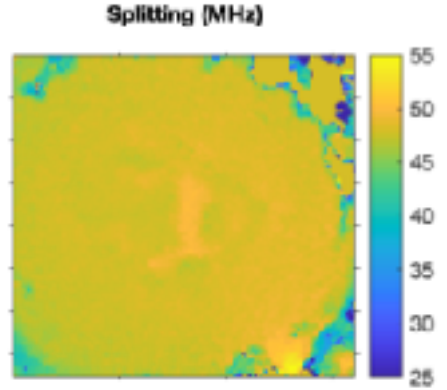

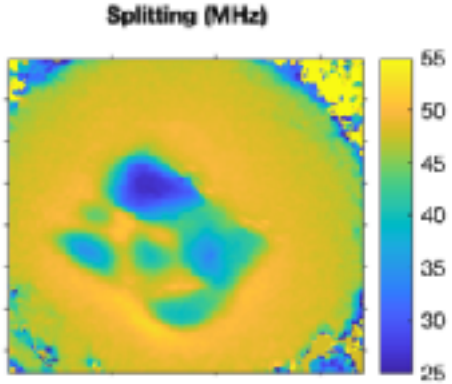

Strong inhomogeneities
Damaged sample

Need new pristine micro-crystals with optimized oxygen doping

Can we investigate the superconductor at pressures > 50 GPa?

ODMR signals for implanted NV centers

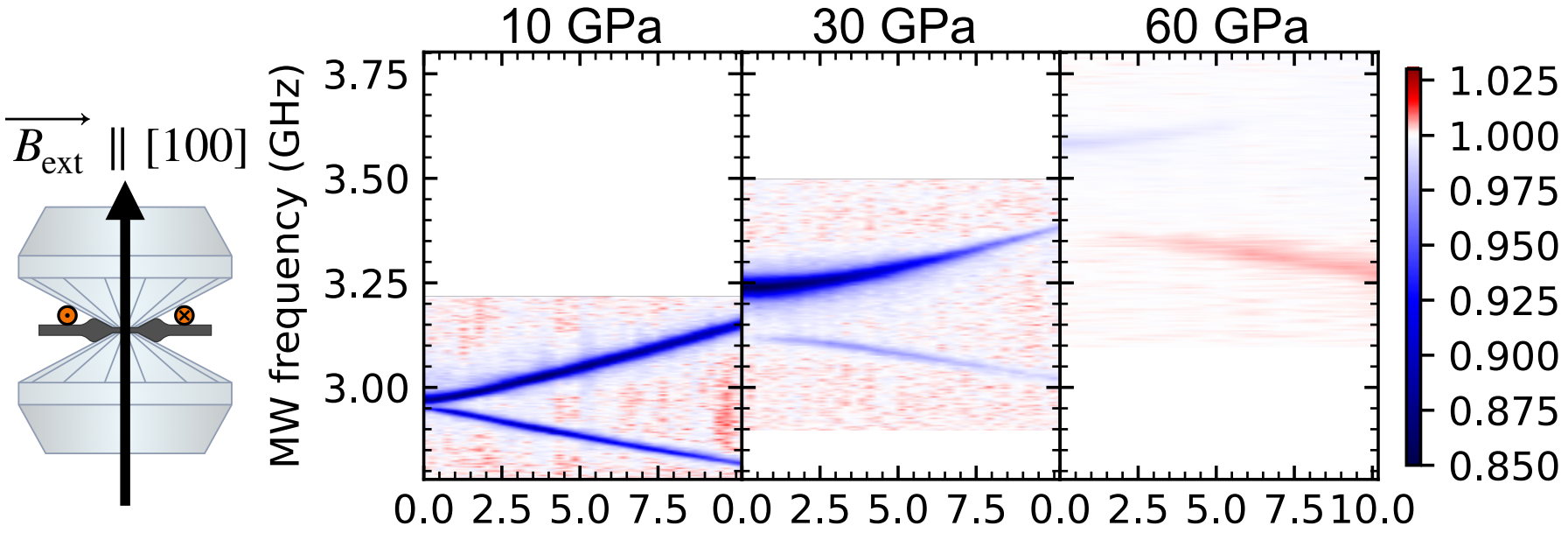

ODMR signals for implanted NV centers

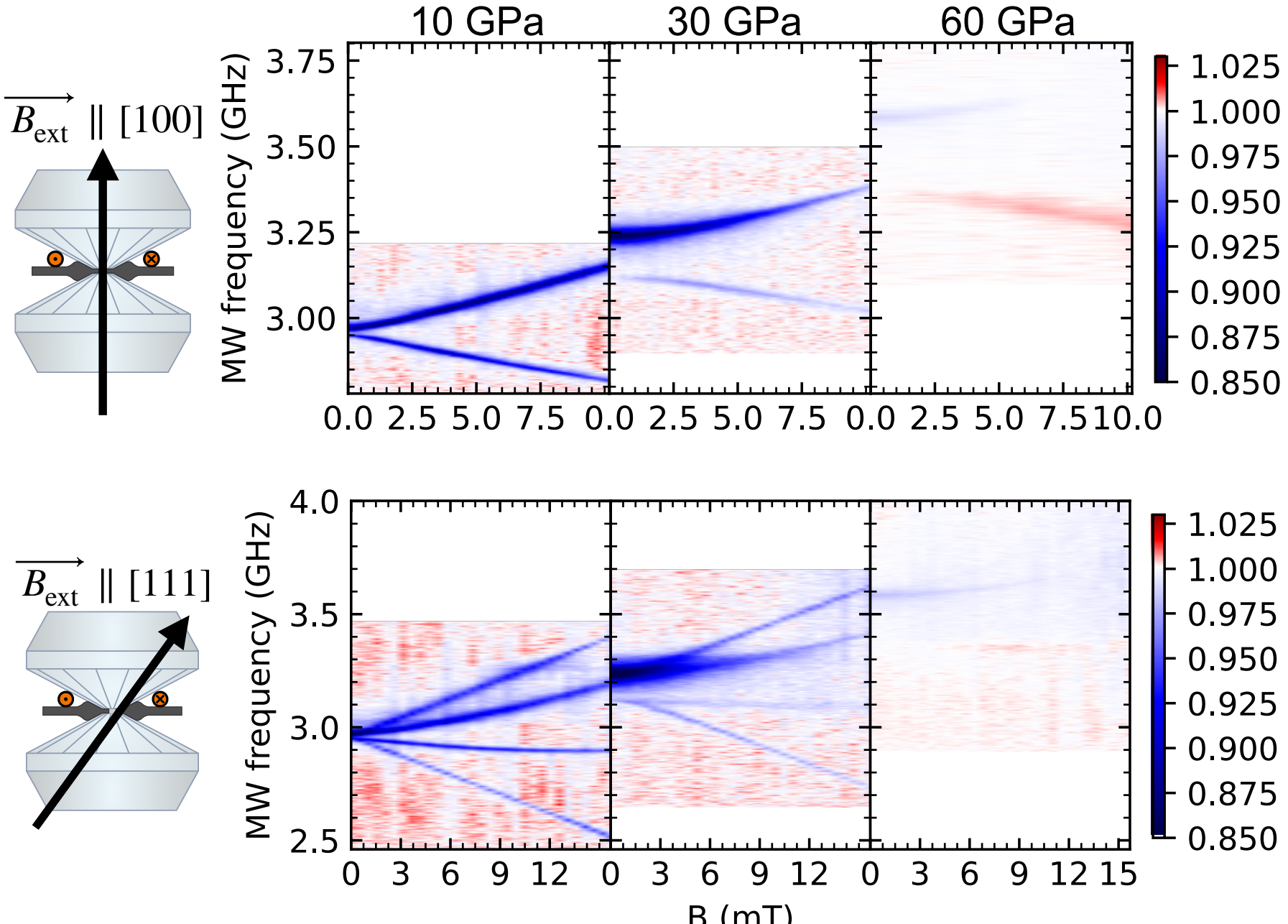

Stress tensor and intrinsic NV symmetry

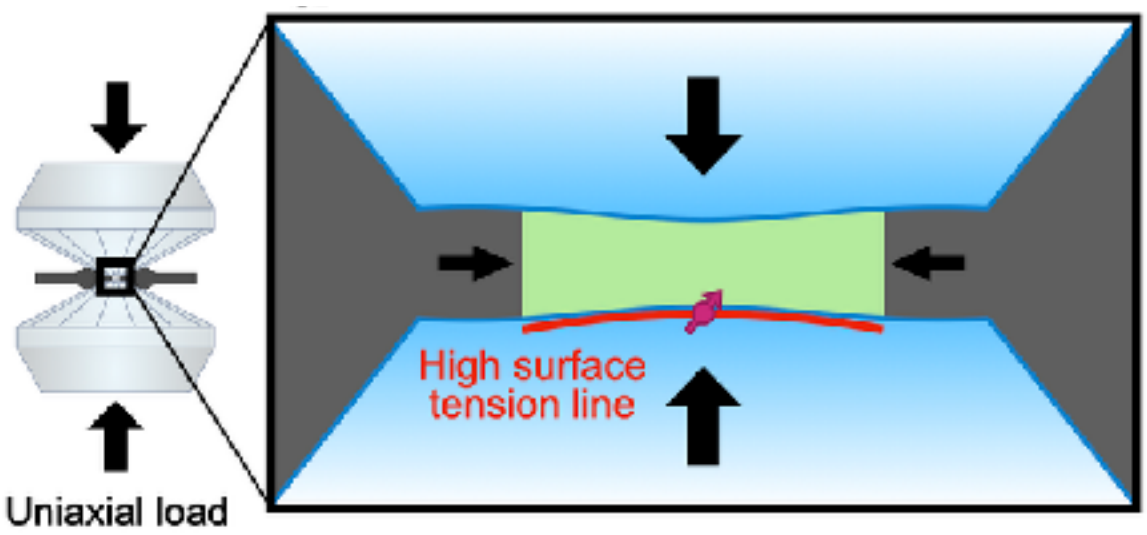

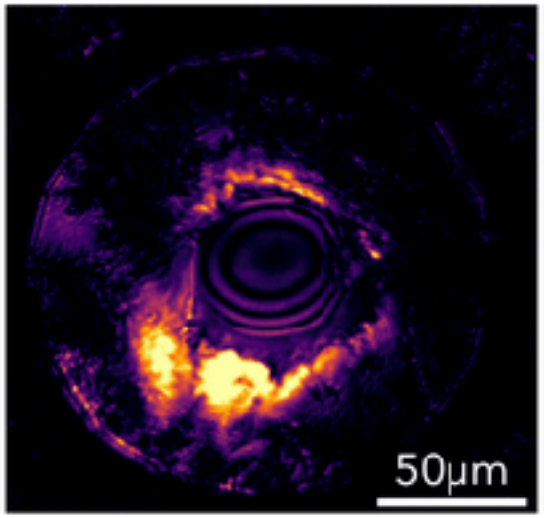

Stress tensor and intrinsic NV symmetry

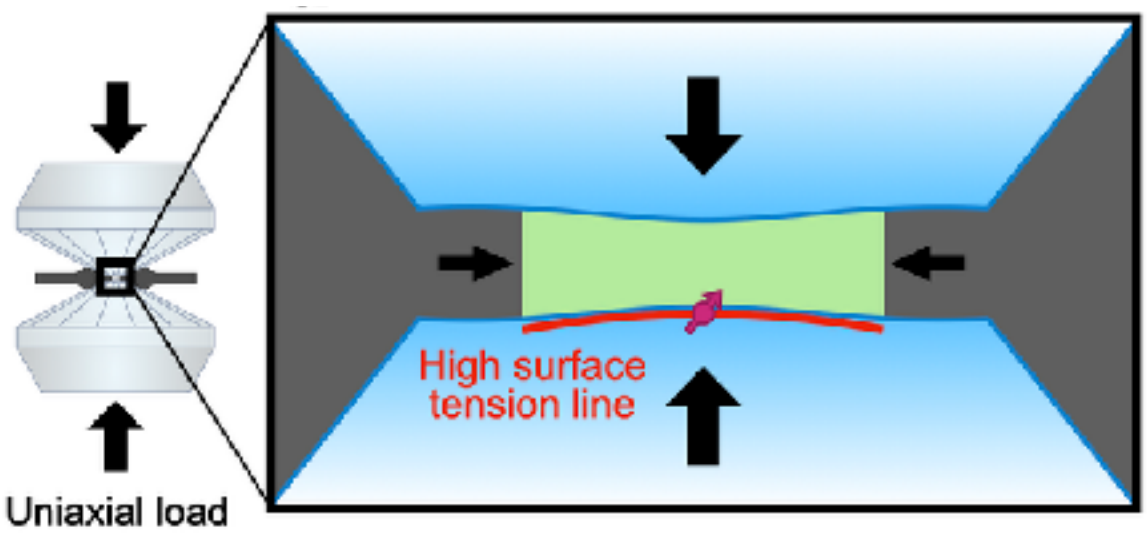

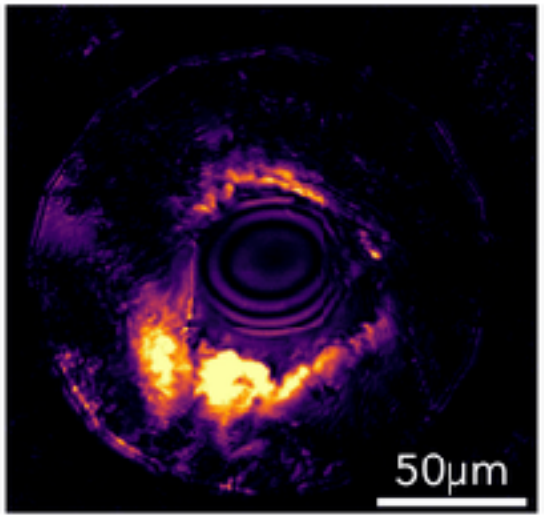

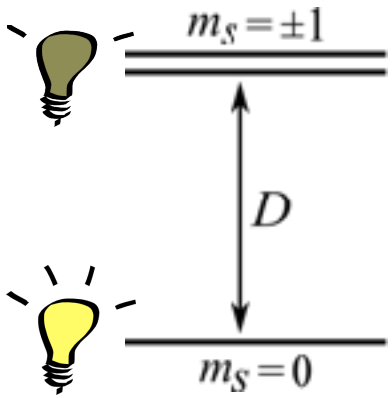

Stress tensor and intrinsic NV symmetry

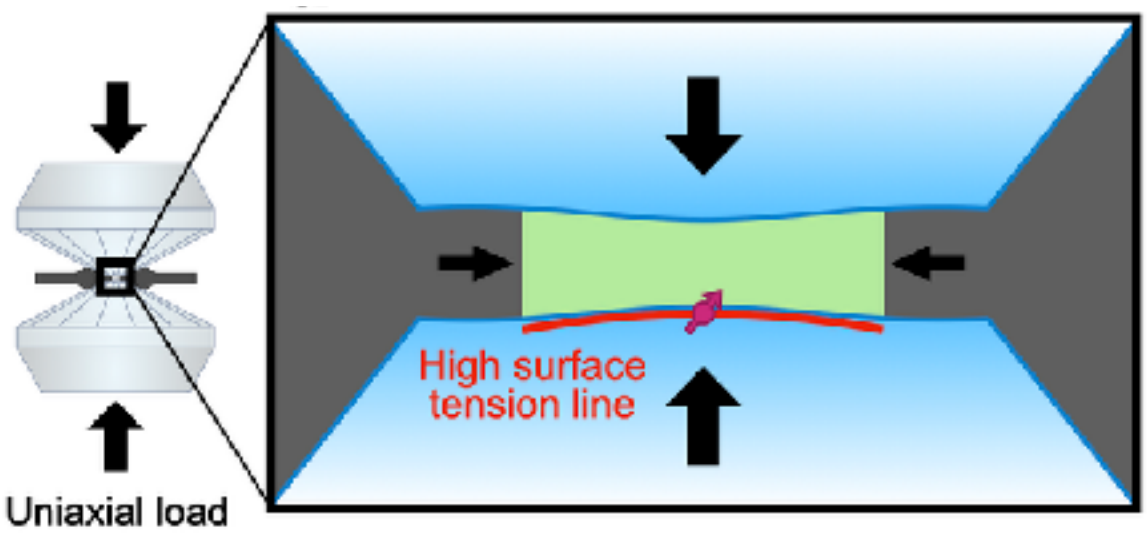

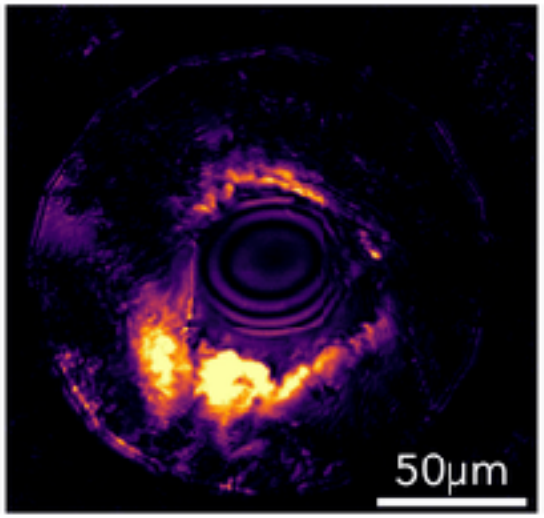

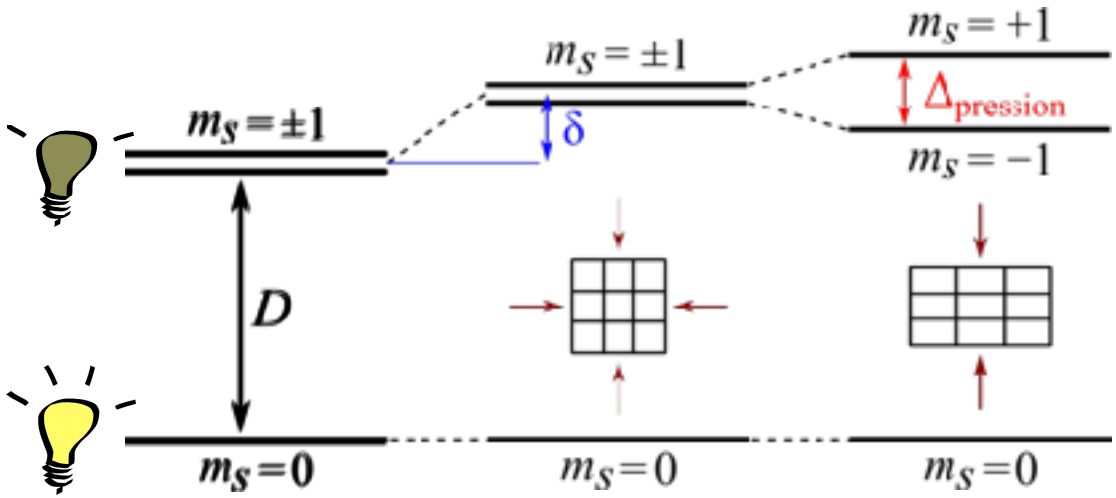

Stress tensor and intrinsic NV symmetry

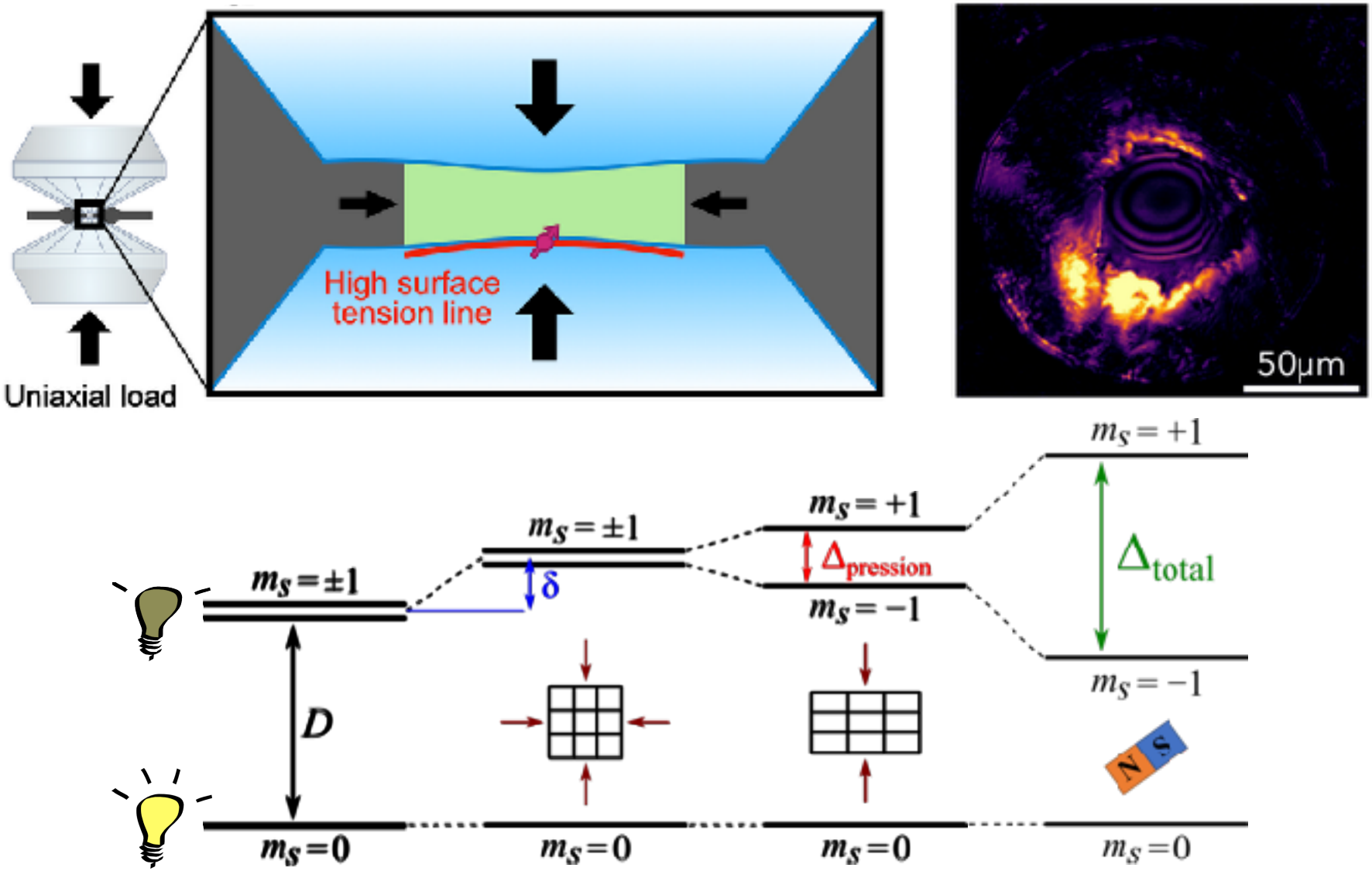

Stress tensor and intrinsic NV symmetry

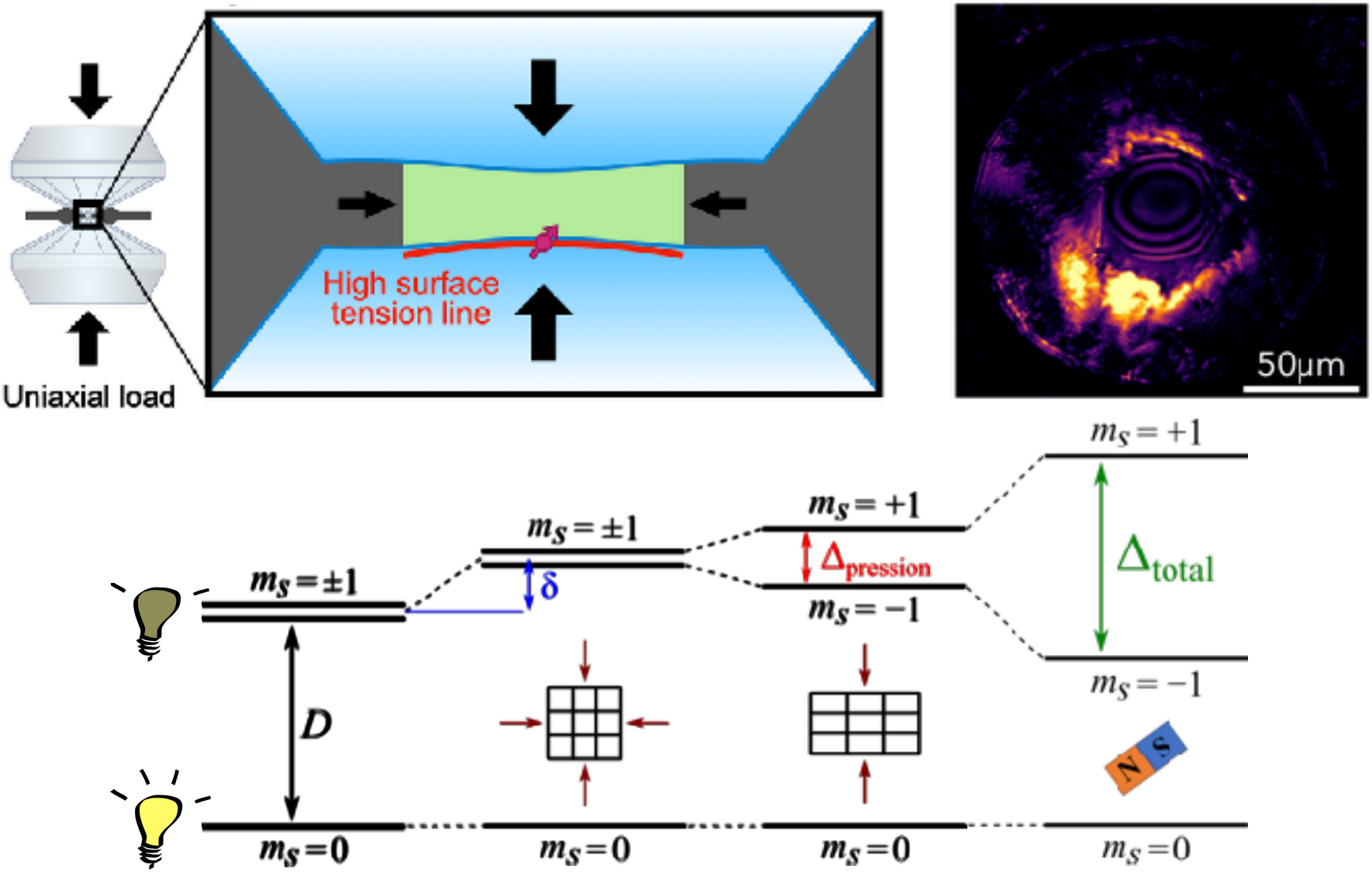

Loss of the ODMR contrast: influence of anisotropic stress on the NV *excited* state on which little is known (contrary to real atoms)

Controlling the NV stress environment

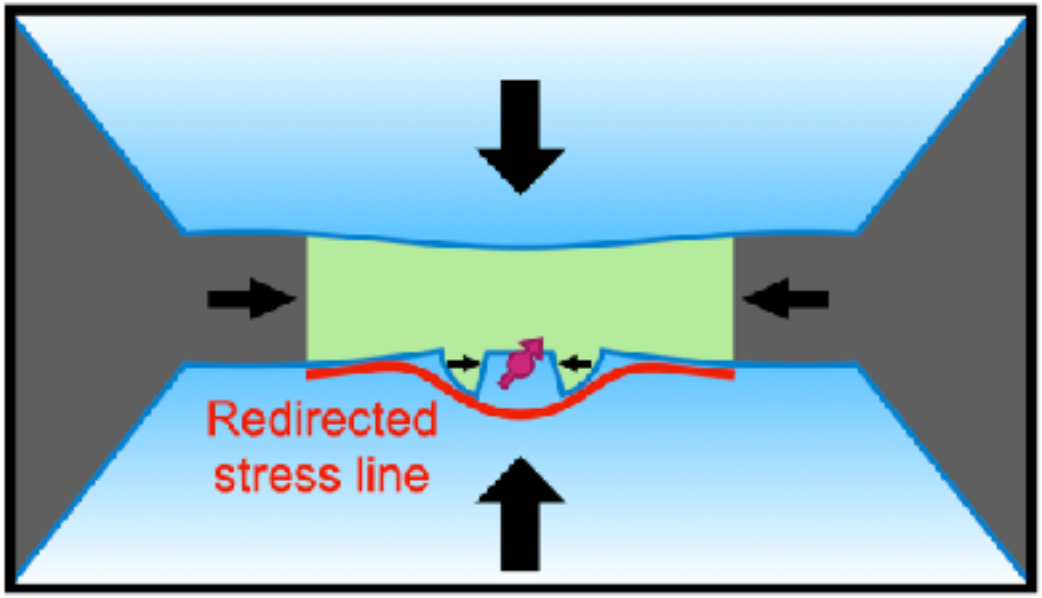

Controlling the NV stress environment

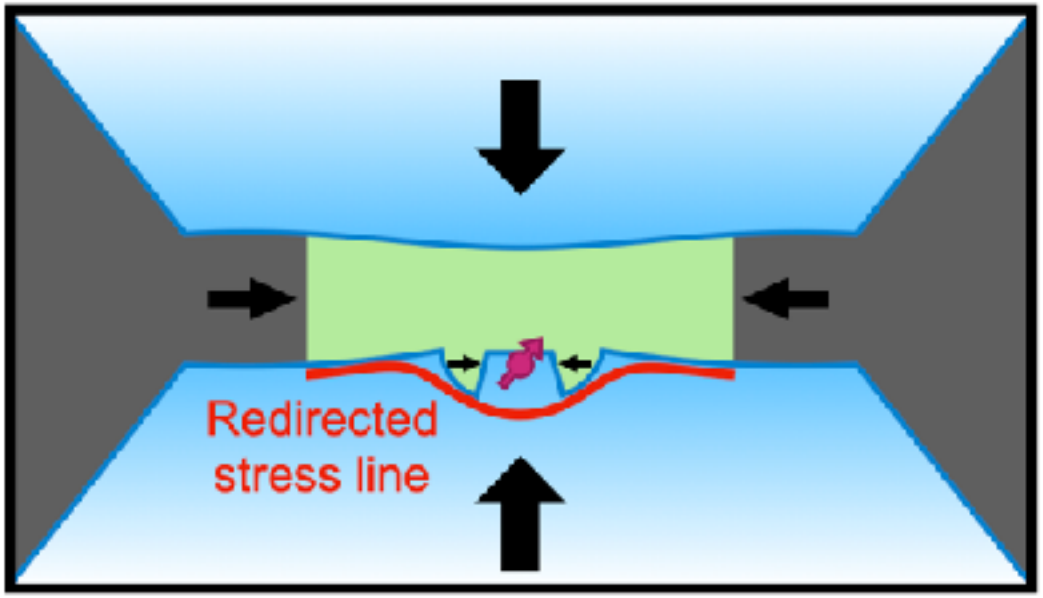

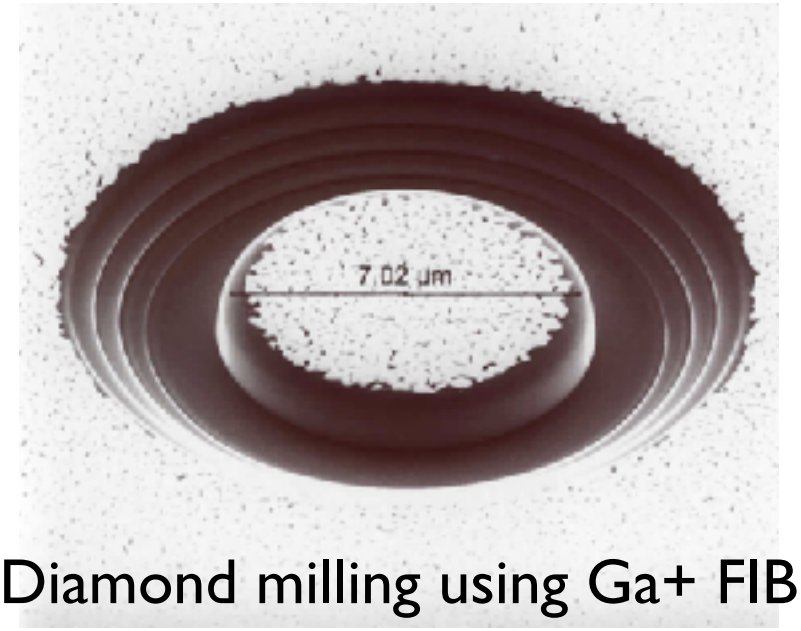

Diamond milling using Ga+ FIB

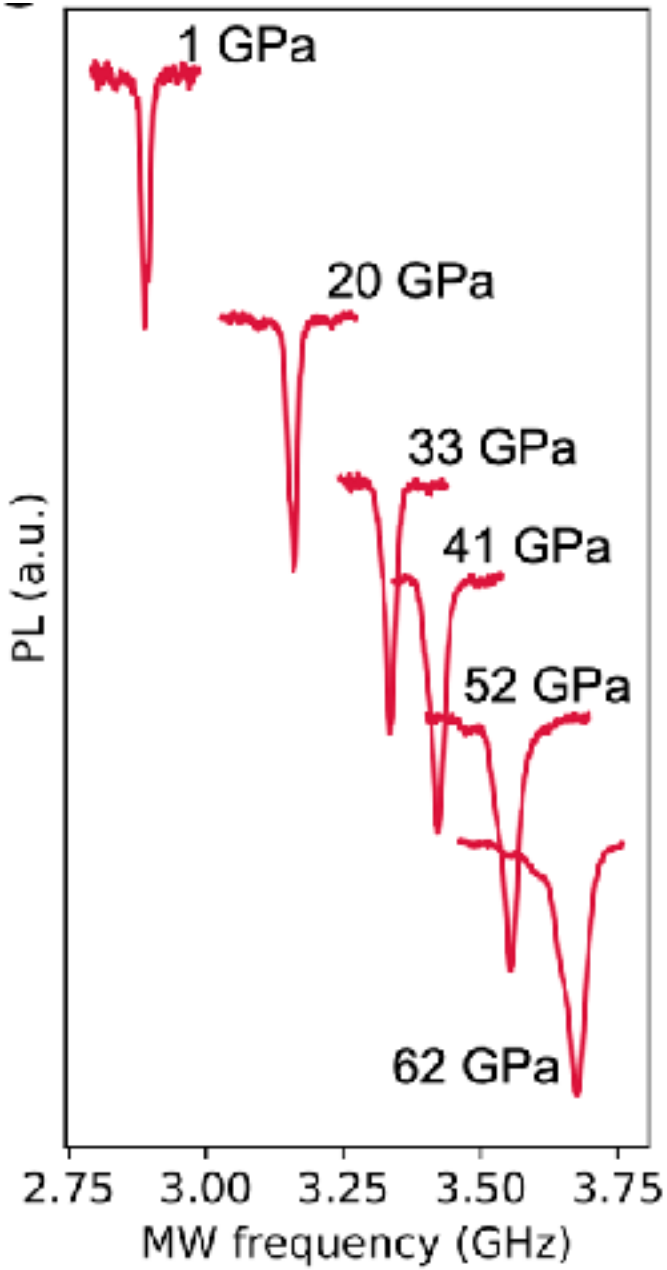

Preliminary comparison of ODMR signals

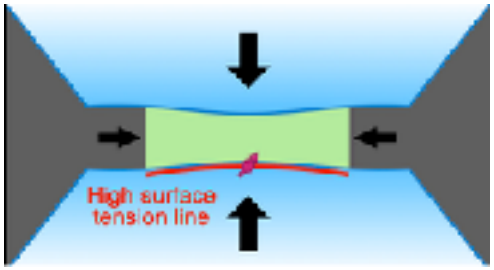

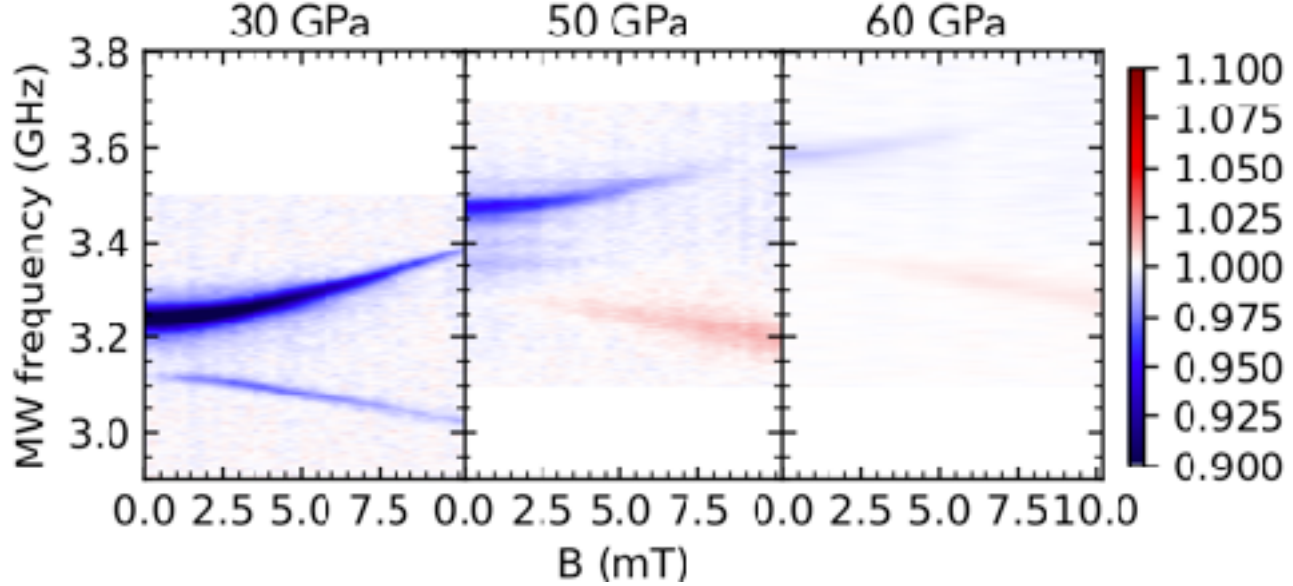

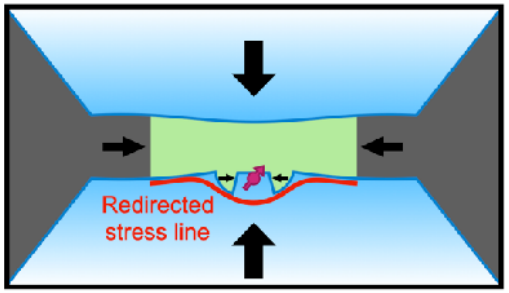

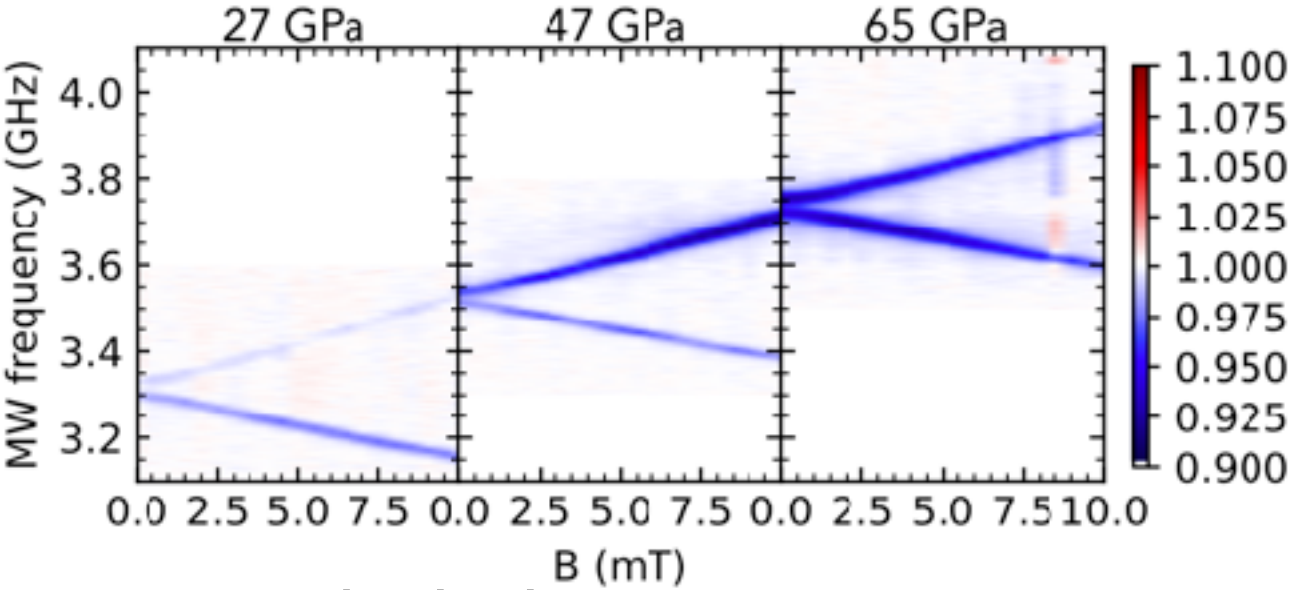

Behavior now similar to the hydrostatic environment that keeps the intrinsic NV symmetry

Stress engineering and enhancement of photon collection efficiency : paraboloids

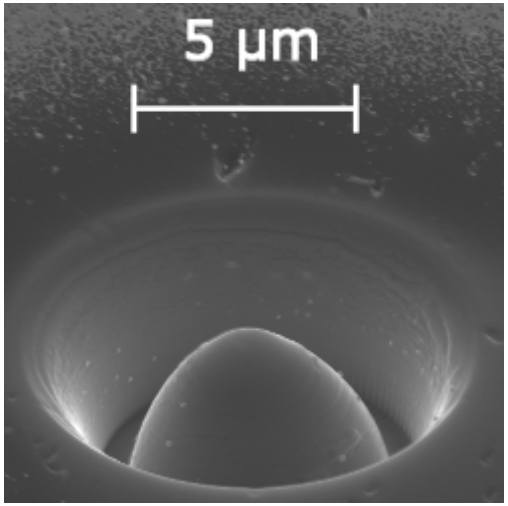

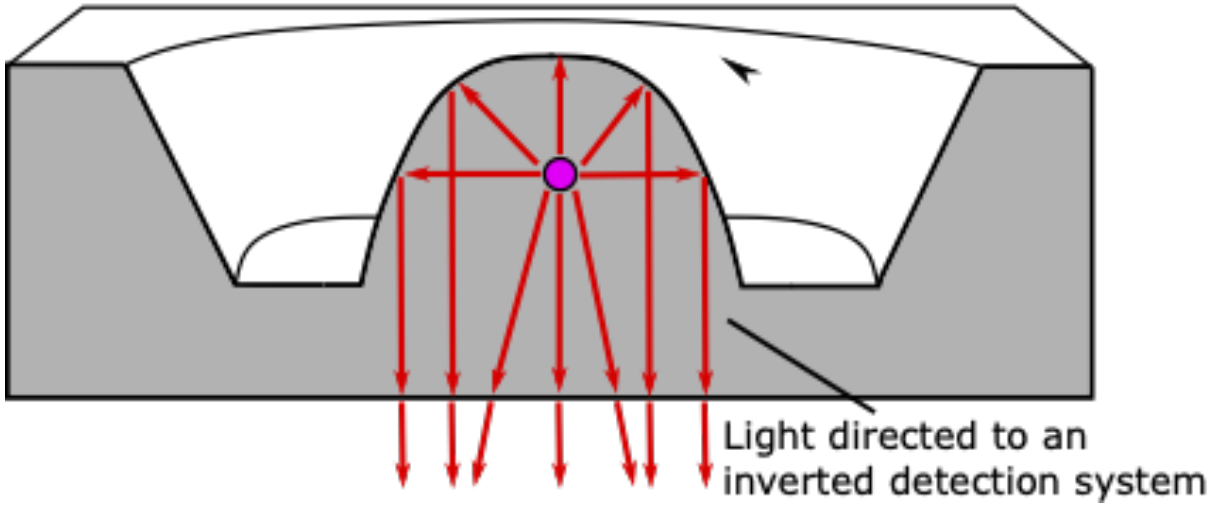

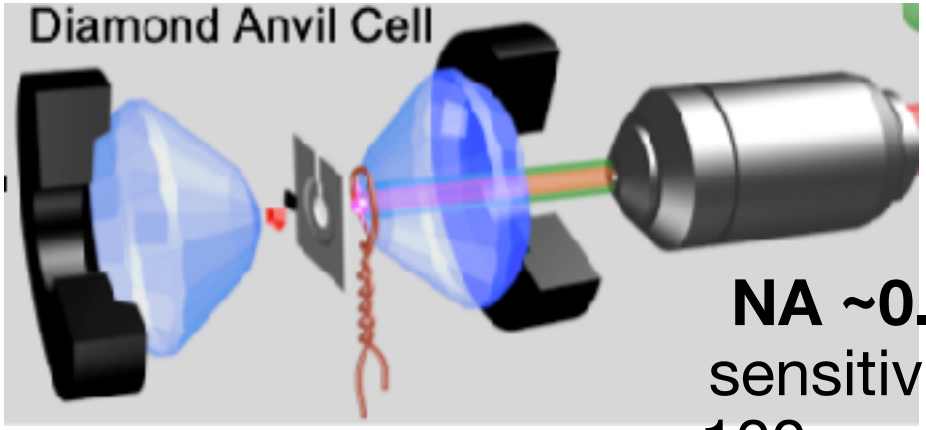

NA ~0.4
sensitivity
>100 centers

→

detection of single NV centers at high pressure?

Dual measurement of magnetic behavior and crystallographic structure

Proof-of-principle test on synchrotron Soleil

see Loic Toraille's talk

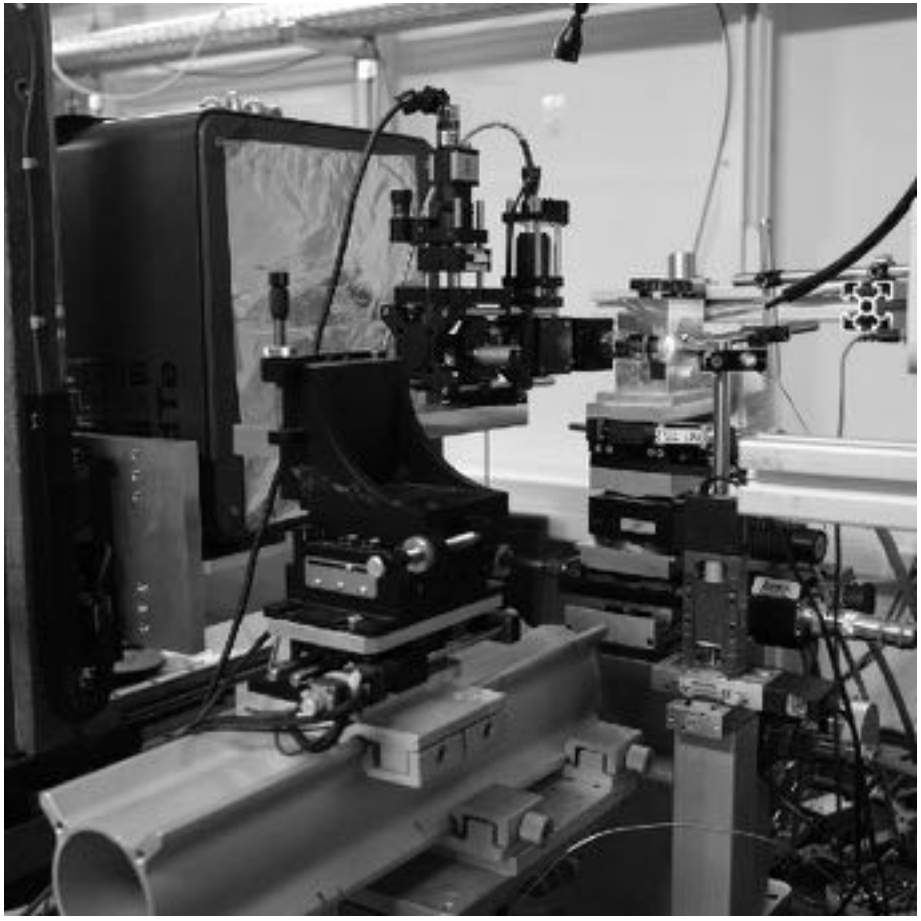

Conclusion

- The NV center is a novel tool to investigate magnetic and superconducting properties of materials at high pressure
  Development of a cryogenic platform with ATTOCUBE
- It is the only technique that can provide a direct and **unbiased** proof of the Meissner effect inside a DAC
- It can be combined with synchrotron-based techniques providing e.g. the crystallographic structure of the sample

Conclusion

- The NV center is a novel tool to investigate magnetic and superconducting properties of materials at high pressure
  Development of a cryogenic platform with ATTOCUBE
- It is the only technique that can provide a direct and **unbiased** proof of the Meissner effect inside a DAC
- It can be combined with synchrotron-based techniques providing e.g. the crystallographic structure of the sample

Some perspectives

- Integration of the microwave excitation in the diamond anvil cell
- Stress engineering for sensing under hydrostatic conditions
- Meissner effet of hydrides (P>100 GPa)

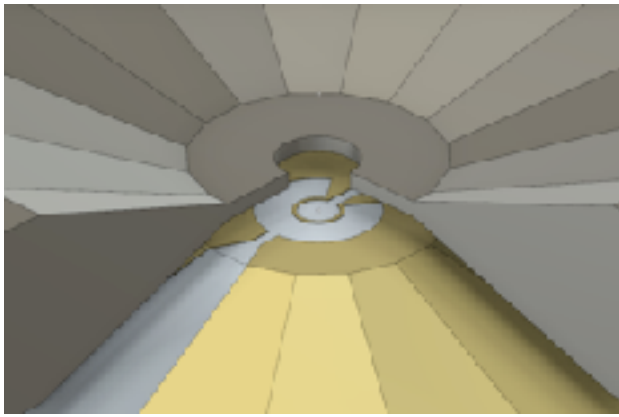

Conclusion

- The NV center is a novel tool to investigate magnetic and superconducting properties of materials at high pressure
  Development of a cryogenic platform with ATTOCUBE
- It is the only technique that can provide a direct and **unbiased** proof of the Meissner effect inside a DAC
- It can be combined with synchrotron-based techniques providing e.g. the crystallographic structure of the sample

Some perspectives

- Integration of the microwave excitation in the diamond anvil cell
- Stress engineering for sensing under hydrostatic conditions
- Meissner effet of hydrides (P>100 GPa)

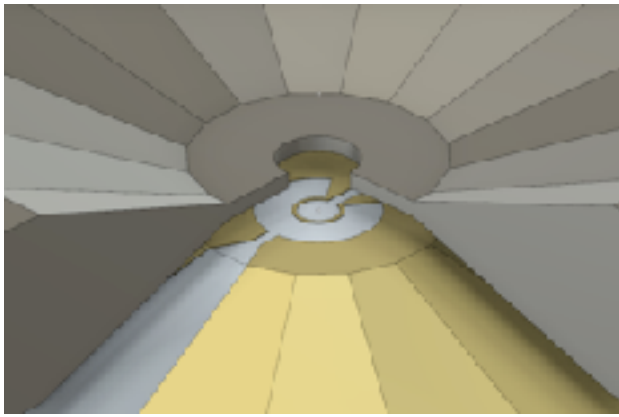

Application to magnetic/superconductivity in 2D Moiré materials

Acknowledgements

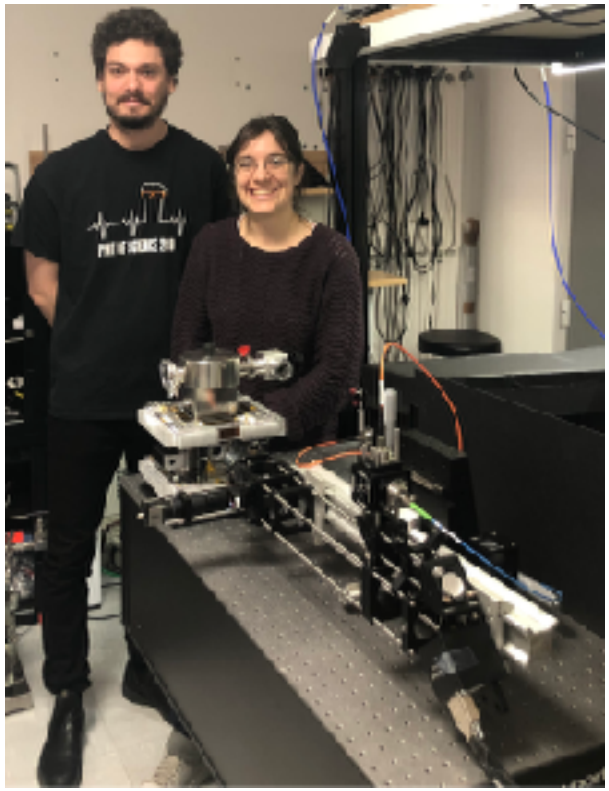

Marie-Pierre Adam
Antoine Hilberer

Margarita Lesik

Loïc Toraille

Martin Schmidt

Cassandra Dailledouze

Thomas Plisson

Paul Loubeyre

THALES

Thierry Debuisschert

Acknowledgements

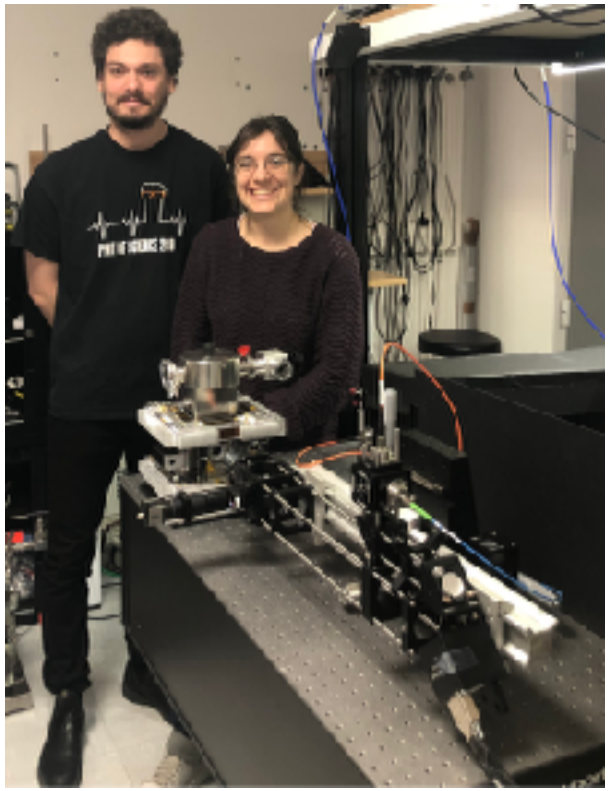

Marie-Pierre Adam
Antoine Hilberer

Margarita Lesik

Loïc Toraille

Thomas Plisson

Martin Schmidt

Cassandra Dailledouze

Paul Loubeyre

THALES

Thierry Debuisschert

ASTERIQS

îledeFrance

SIR TEQ

INVESTIR L'AVENIR

30 IUF ANS

institut universitaire de France

anr agence nationale de la recherche
AU SERVICE DE LA SCIENCE

Ground-state Hamiltonian

Hamiltonian for NV family $i \in (1,2,3,4)$:

$$H_i = \left(D + \mathscr{M}_{Z_i}\right) S_{Z_i}^2 + \gamma_{\mathrm{NV}} \mathbf{B} \cdot \mathbf{S}_i - \mathscr{M}_{X_i}\left(S_{X_i}^2 - S_{Y_i}^2\right) + \mathscr{M}_{Y_i}\left(S_{X_i} S_{Y_i} + S_{Y_i} S_{X_i}\right)$$

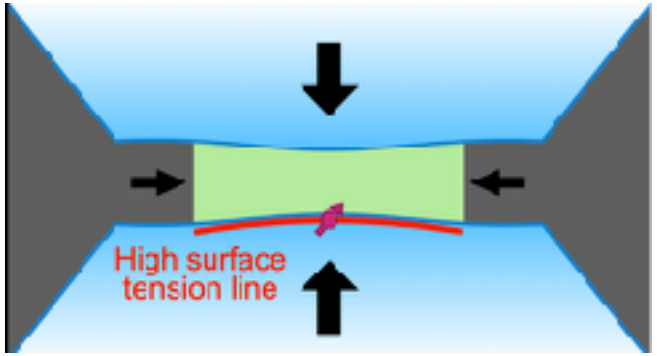

Coupling $C_{3\mathrm{v}}$ symmetry to stress tensor:

$$\begin{aligned}
\mathscr{M}_X &= b(2\sigma_{zz} - \sigma_{xx} - \sigma_{yy}) + c(2\sigma_{xy} - \sigma_{yz} - \sigma_{zx}) \\
\mathscr{M}_Y &= \sqrt{3}[b(\sigma_{xx} - \sigma_{yy}) + c(\sigma_{yz} - \sigma_{zx})] \\
\mathscr{M}_Z &= a_1(\sigma_{xx} + \sigma_{yy} + \sigma_{zz}) + 2a_2(\sigma_{yz} + \sigma_{zx} + \sigma_{xy})
\end{aligned}$$

$$\bar{\bar{\sigma}} = \begin{pmatrix} \sigma_{xx} & \sigma_{xy} & \sigma_{xz} \\ \sigma_{yx} & \sigma_{yy} & \sigma_{yz} \\ \sigma_{zx} & \sigma_{zy} & \sigma_{zz} \end{pmatrix} \downarrow \bar{\bar{\sigma}} = \begin{pmatrix} \alpha P & 0 & 0 \\ 0 & \alpha P & 0 \\ 0 & 0 & P \end{pmatrix}$$

First-order perturbation theory :

$$\nu_{\pm} = D + \delta \pm \frac{\Delta}{2}$$

$$\delta = \mathscr{M}_z = a(1 + 2\alpha)P$$

$$\Delta = 2\sqrt{b^2(1-\alpha)^2P^2 + \left(\frac{g\mu_{\mathrm{B}}}{\hbar} B_{\mathrm{NV}}\right)^2}$$

ODMR contrast and stress

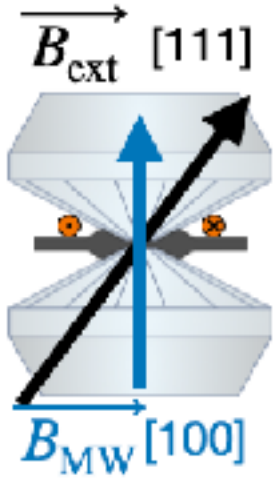

Hamiltonian for NV family $i \in (1,2,3,4)$:

$$H_i = \left(D + \mathcal{M}_{Z_i}\right) S_{Z_i}^2 + \gamma_{\text{NV}} \mathbf{B} \cdot \mathbf{S}_i - \mathcal{M}_{X_i}\left(S_{X_i}^2 - S_{Y_i}^2\right)$$

Pressure + Zeeman:

eigenstates $|0\rangle, |1\rangle, |-1\rangle$

$$|0\rangle \xrightarrow[\text{circular}]{\text{transitions } \sigma_+, \sigma_-} \begin{matrix} |1\rangle \\ |-1\rangle \end{matrix}$$

Anisotropic stress:

eigenstates $|0\rangle, |+\rangle, |-\rangle$

$$|0\rangle \xrightarrow[\text{linear}]{\text{transitions } x, y} \begin{matrix} |+\rangle \\ |-\rangle \end{matrix}$$

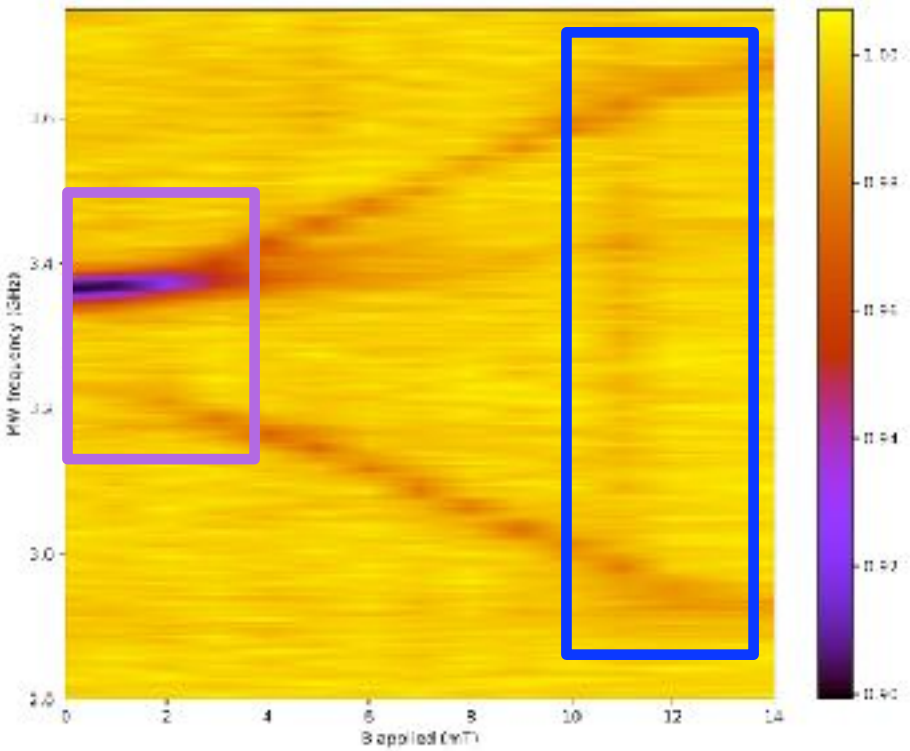

linearly polarized B_{MW}

→ selection rules